The identification of STAT2 as a pervasive negative regulator of STAT1 activity and cytokine signalling

Johnathan Ho

Student ID: 4182046

Thesis submitted to the University of Nottingham for the degree of

Doctor of Philosophy

September 2017

Abstract

Interferons (IFNs) are cytokines which play a crucial role in the host defence against pathogens through the upregulation of hundreds of target genes. The binding of an IFN molecule to its specific receptor, results in the tyrosine phosphorylation of a member of the Signal Transducer and Activator of Transcription (STAT) protein family, a process often termed 'STAT activation'. The first observation of this mechanism was the discovery of STAT1 and STAT2, which are both activated in response to type-I interferon and form a DNA-binding heterodimer which acts as a transcription factor. In the 25 years since this breakthrough, the establishment of these proteins as partners in signal transduction has been shown repeatedly.

Whilst STAT1 has since be found to act as a signal transducer for many different cytokines, STAT2 appears to be almost exclusively driven by type-I IFN. Nonetheless, STAT2-deficient phenotypes suggest a broader and IFN-independent role for this protein. This thesis focused on the role of the STAT N-domain, which has been recently identified as an important site for cytokine-independent interactions. Using a variety of methods, including fluorescence microscopy as well as biochemical and biological assays, STAT2 was shown to be constitutively bound to STAT1 via their N-domains. The consequence of this binding was a strong inhibitory effect on the activity of STAT1. This was attributed to the formation of semi-phosphorylated dimers which were excluded from entering the cell nucleus. Furthermore, a single residue was found to abrogate this interaction and resulted in a hyper-responsive STAT1 phenotype in several immune responses such as parasitic immunity, antigen presentation and senescence. Therefore, STAT2 should now be considered an innate negative regulator of STAT1 activity in all cytokine signalling pathways with the exception of type-I interferon.

Acknowledgments

I would like to thank the host of friends and colleagues, whom all contributed to the success of this work immensely. The pursuit of great scientific work cannot be undertaken alone and I feel very fortunate to have met many exceptionally talented and helpful people along the way.

Firstly, I must thank my supervisor Prof. Uwe Vinkemeier who has continually ensured that my research was carried out in a nurturing environment whilst also teaching me the value of robustly challenging the established canon. This work was performed safe in the knowledge that his advice, experience and insight were always on the other side of an open door.

Further thanks go to Mrs Maureen Mee, who took me under her wing from the start and showed a level of patience and modesty that I will never forget. Kind support and mentorship was also provided by Dr Andreas Begitt and Ms. Christin Pelzel. These three special people all trained me in many of the laboratory techniques used in this thesis and were always available for advice once I was developing new assays of my own.

Publications

HO, J., PELZEL, C., BEGITT, A., MEE, M., ELSHEIKHA, H. M., SCOTT, D. J. & VINKEMEIER, U. 2016. STAT2 Is a Pervasive Cytokine Regulator due to Its Inhibition of STAT1 in Multiple Signaling Pathways. PLoS Biol, 14, e2000117.

Declaration

I confirm that all of the work contained within this thesis is my own, and I take full responsibility for it, with the following exceptions:

1. The generation of the stably reconstituted U6A STAT2 and STAT2 L82A cell lines was carried out in collaboration with Mrs Maureen Mee and Dr Andreas Begitt.
2. Biochemical analysis of the U6A cell lines shown in **Figure 4.4** and the gene expression analysis in **Figure 4.5** are courtesy of Dr Andreas Begitt.

Signed,

Johnathan Ho

Table of Contents

1. Introduction

This thesis details work that focuses on the interaction of two members of the Signal Transducer and Activator of Transcription (STAT) family of proteins; namely STAT1 and STAT2. Briefly, the presented data reveals a heretofore undescribed interaction motif and its consequences on the function of these proteins. This work therefore relates to two major aspects of biological science: the immune response (particularly interferon signalling) and signal transduction by the JAK-STAT pathway.

This introduction aims to set out the current scientific understanding of these research areas, with a view to highlighting their impact within medical care and disease pathologies as well as describing the established canon to which this thesis adds novel insight. At the conclusion of this chapter the hypotheses and aims of this work are stated.

1.1. The Immune Response

1.1.1. The role of interferons in the immune system

The host immune response is an integral mechanism for survival of an organism in an environment co-inhabited by millions of other species. There is a tendency in nature to have many species that parasitise others, which puts enormous selective pressure on species to develop a means to survive and neutralise an invasive organism. Even simple prokaryotes are targets of yet smaller organisms (Weinbauer, 2004).

Larger complex multicellular beings, such as humans, act as excellent hosts to a huge range of species including small invertebrates as well as fungi, bacteria and viruses. Therefore, it is unsurprising that the human body has developed a vast and complex immune system with which to counter invasive organisms. This complexity requires an intricate system of regulation involving many distinct cell types and signalling mechanisms. Amongst the largest families of immune-related signalling molecules are the cytokines. This family consists of

over 50 molecules that bind to specific cell surface receptors and elicit a response that directs the behaviour of the target cell (Dinarello, 2007).

The first cytokines discovered were the interferons (IFNs); so named because they interfered with the reproduction of viral particles when added to a host culture (Isaacs and Lindemann, 1957). The next half century saw advances in our understanding of interferons, revealing a crucial role not only in host anti-viral defence but also in several autoimmune disorders, tumour detection and killing (Borden et al, 2007). Consequently, interferon therapy has a variety of applications extending beyond the treatment of infections and into autoimmunity and cancer also. The interferon family is currently divided into three types: I, II and III. These each bind to different type-specific receptors; which subsequently elicit overlapping but distinct responses by the target cell (Zhang et al, 2008).

Type I IFNs are the archetypal class of IFN; insofar as they appear essential for the normal anti-viral response by the host. Primarily, this class of IFN is considered a major part of the innate immune system. Recently, however, a significant amount of research focus is now being directed towards other immunomodulatory functions of these IFNs. This includes their role in intestinal homeostasis (Cho and Kelsall, 2014) and lipid metabolism (Wu et al, 2016). Amongst this group, IFN-α and IFN-β are the most well-known and understood, however nine subtypes of this family of proteins have been identified within mammals such as IFN-Ω, IFN-ε and limitin as well as 13 subtypes of the aforementioned IFN- α (Pestka et al, 2004). Almost all cell types are capable of both producing and responding to type I IFNs, conferring the essential ability to defend against a viral infection anywhere within the body. Surprisingly, the response to all of the myriad type I IFNs is mediated through one common heterodimeric receptor composed of IFNAR1 and IFNAR2 (Pestka et al, 2004). Patients and transgenic animals with a deficiency in type I IFN signalling (via an inability to either produce or respond to type I IFN) are often highly susceptible to viral infections and require substantial medical care in order to survive (Zhang et al, 2008).

The production of type I interferons is induced following the detection of viral or other pathogens by the cell. Detection is achieved via activation of the pathogen recognition receptors (PRRs) such as the Toll-like receptors (TLRs). These are a group of both cell surface and cytosolic proteins that can recognise the foreign nucleotides of viruses or the cell wall

glycoproteins of bacteria (Uematsu and Akira, 2007). This causes the rapid production of IFN-α/β that is released into the extracellular matrix. Type-1 IFN drives cells into an anti-viral state through the upregulation of hundreds of genes. Some, such as protein kinase R (PKR) and 2'5'-oligoadenylate synthase (OAS), inhibit viral protein synthesis whilst others attract resident immune cells to the site of infection and initiate the presentation of foreign antigens to the adaptive immune system (Randall and Goodbourn, 2008).

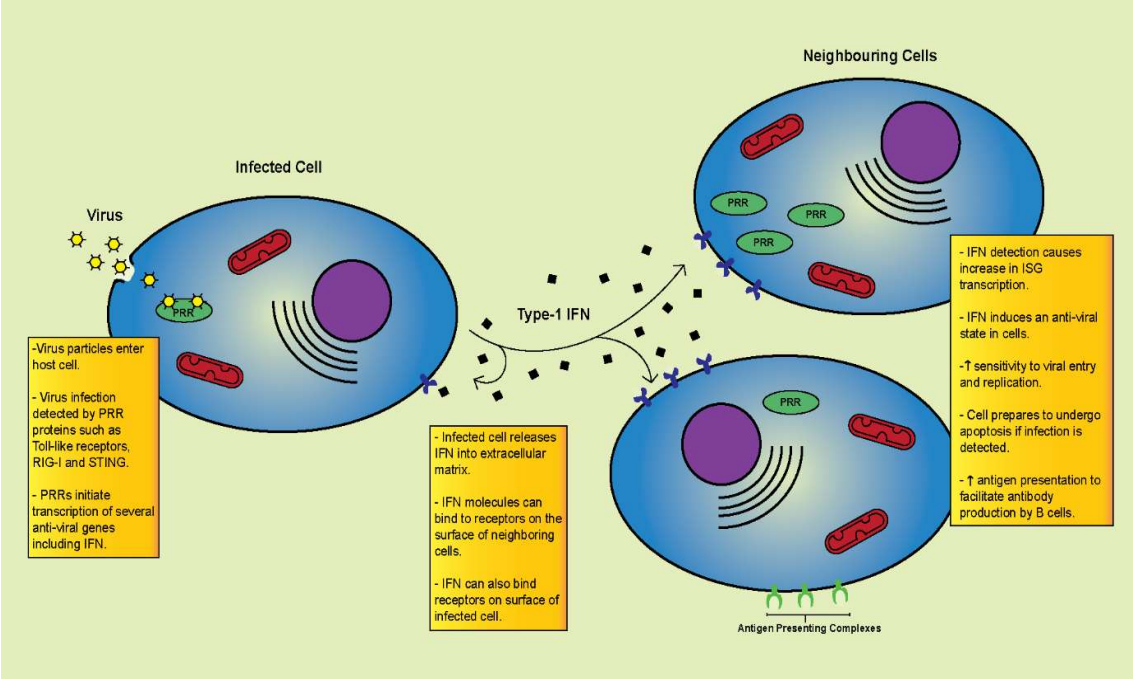

Figure 1.1: *Role of type-1 IFN in the immune response to viral infection. Viral entry into the cell is detected by pathogen recognition receptors (PRRs), which induces interferon stimulated genes (ISGs) including the production and secretion of IFN itself. Type-1 IFN then confers an anti-viral state in neighbouring cells, resulting in upregulation of PRRs and antigen presentation mechanisms to facilitate activation of the adaptive immune response.*

In contrast to the numerous type I IFN members, the type II IFN family is comprised solely of IFN-γ. This unique cytokine is secreted by a smaller cohort of cells; specifically thymus-derived T-cells and natural killer cells (**Figure 1.2**). Like the other IFNs it can confer anti-viral protection to target cells however, it also has a key role in organising the host defence against bacteria and other intracellular parasites such as protozoa and fungi (Schroder et al, 2004) and is an essential signal molecule for cell-mediated immunity. IFN-γ promotes the

accumulation and maturation of T cells into T helper 1 (T_h1) cells whilst antagonising the maturation of T helper 2 (T_h2) cells, which are dependent on IL-4 (Billiau, 1996). This antagonism defines whether a cell-mediated or humoral (involving antibody generation by B-cells with the assistance of T_h2) response is invoked. In cell-mediated immunity, IFN-γ driven T_h1 cells in turn release IFN-γ to activate any infected antigen presenting cells (APCs) they encounter, facilitating the destruction of internalised pathogens and subsequent presentation of foreign antigens to cytotoxic CD8+ T-cells (Boehm et al, 1997). Dendritic cells and phagocytes, such as macrophages, are key examples of APCs in this response and IFN-γ induces them to kill ingested pathogens via the inducible nitric oxide synthase (iNOS) production of free radicals (Blanchette et al, 2003) as wells as present antigens to CD8+ T-cells. The cytotoxic T-cells themselves also release IFN-γ, which not only facilitates positive feedback loops with T helper cells and APCs, but also restricts viral replication in infected cells prior to induction of apoptosis thus preventing inadvertent spread of viral particles.

The transition from innate to adaptive immunity is also begun by this cytokine, in combination with IL-12 (Schroder et al, 2004). Dendritic cells and macrophages respond to IFN-γ by upregulating the cell surface expression of the major histocompatibility complex (MHC) class I and II proteins (Chan et al, 2006). It is these complexes that facilitate the presentation of extracellular proteins, such as those of bacteria to CD8+ T cells, of which some remain as dormant memory T cells that can be rapidly activated in the case of a second infection (Boehm et al, 1997).

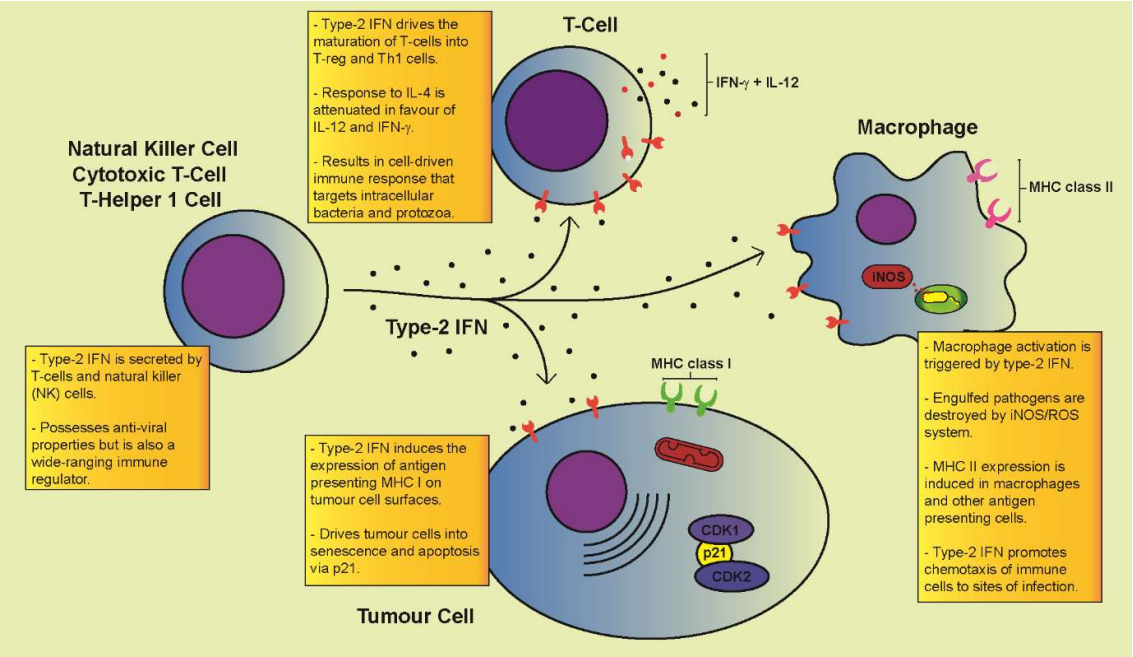

Figure 1.2: *Role of type-2 IFN in the regulation of the immune system. Like type I IFN, IFN-γ can also confer anti-bacterial protection however has a wide range of functions within the immune system. IFN-γ promotes the maturation of T cells into Th1 cells which drive cell-mediated immune responses. It also has anti-tumorigenic role by increasing tumour cell detection via MHC class I expression and arresting cell growth via inhibition of CDK1/2 by p21. Finally, IFN-γ triggers the destruction of pathogens by macrophages through iNOS production of free radicals as well as the presentation of pathogenic antigens by MHC class II upregulation.*

Type-II IFN also plays a vital role in the detection and killing of tumorigenic cells (Dighe et al, 1994; Kaplan et al, 1998). The mechanisms underlying this are believed to include direct effects on tumour cell growth, enhanced activity of tumour sensing cells such as cytotoxic T-cells and inhibition of local angiogenesis to prevent tumour blood supply (Ikeda et al, 2002). IFN-γ can mediate growth arrest in tumour cells through multiple pathways including expression of p21, also known as cyclin-dependent kinase inhibitor 1, which inhibits the complexes of cyclin-dependent kinase (CDK) 1 and 2 thus blocking G_1/S phase transition (Harvat and Jetten, 1996; Hobeika et al, 1999). Th1 cells, in particular, have been identified as forcing tumour cells into growth arrest through IFN-γ release (Braumüller et al, 2013).

The final class of IFN, type III, includes the IFN-λ1, IFN-λ2 and IFN-λ3 molecules. The response to type III IFNs is very similar to that of type I IFNs, so much so that they share the same signal transduction mechanism and a high degree of overlap in target genes (Levy et al, 2011). However, the expression of the type III IFN receptors is limited to cells of epithelial

lineage. This has been highlighted as a critical distinction; allowing for an effective immune response to be mounted by the cells most exposed to external pathogens, whilst avoiding a potentially damaging systemic immune response (Zhou et al, 2007; Okabayashi et al, 2011).

1.1.2. Lessons learned from immune disorders

Interferons, along with the other cytokines, are constantly being released in the body at various intervals and their roles likely extend beyond what they are currently understood to do. One example of an emerging interferon role is in cellular ageing, also known as senescence. Yu et al. (2015) observed that DNA damage (which accumulates over a lifetime) can trigger IFN-β, which in turn inhibits stem cell function and promotes the ageing process. Braumüller et al. (2013) demonstrated that IFN-γ, amongst other cytokines, can trigger senescence in cells. These observations build upon research into age-related immune dysfunction which ranges from widely seen increased susceptibility to pneumonia and influenza in elderly populations (Falsey and Walsh, 2006; Schanzer et al, 2008) to the onset of specific auto-immune conditions such as rheumatoid arthritis in old age (Pawlowska et al, 2011).

Furthermore, we now understand that cytokines work both synergistically and antagonistically so as to maintain a balance within the host that can shift depending on external factors i.e. pathogen recognition or physical traumas (Delgoffe et al, 2011). This balance can be upset by other factors such as stress, chronic injury or infection giving rise to immune system disorders such as lupus and rheumatic disease (Chizzolini et al, 2009; Yao et al, 2016). Understanding the molecular mechanisms behind such 'cross-talk' is a fundamental step towards being able to manipulate this balance in the immune system, yet it is initially through the investigation of these conditions that our understanding of this cross-talk has increased.

The clinical importance of this cannot be understated as one of the current major causes of death, septic shock, is a result of a loss of cytokine homeostasis (Deutchsmann and Tracy, 2014). The role of interferon in the onset and treatment of sepsis patients is subject of much research and debate (Rackov et al, 2017) with some research even suggesting a role for IFN-β in the protection against sepsis by inhibition of NF-κB (Yoo et al, 2014). Another example of the therapeutic effect of IFN is in the treatment of multiple sclerosis, an auto-immune

disorder that affects the central nervous system (Reder and Feng, 2014). This seemingly paradoxical effect of IFN in controlling an auto-immune disorder highlights how much more we have to learn about the function of these molecules.

Interferons, and all other cytokines, converge on the Janus Kinase – Signal Transducer and Activator of Transcription (JAK-STAT) pathway in order to initiate the gene expression required to alter the target cell's behaviour. This work focuses on this signal transduction pathway and how it regulates cell responsiveness to IFNs. In this regard, the following sections will focus on the molecular consequences of IFN signalling; primarily the activation and translocation of STAT proteins.

1.1.3. STATs and the JAK-STAT pathway

The JAK-STAT pathway was first described as the signal transduction mechanism of interferons in the early 1990's (Shuai et al, 1992; Shuai et al, 1994). The last quarter century of research has fundamentally enhanced our understanding of this pathway, which is the principle mechanism used by cytokines (Stark and Darnell, 2012). Subsequently, this has led to several treatments that manipulate the pathway; most prominently the JAK3 inhibitor tofacitinib, used in rheumatoid arthritis patients (Boyle et al, 2015).

The canonical model of JAK-STAT signalling involves the recognition of cytokines by their respective cell surface receptors (**Figure 1.3**). IFN-α/β binds to two receptor proteins, interferon alpha receptor (IFNAR) 1 and 2, whilst IFN-γ is recognised by interferon receptor gamma (IFNGR) 1 and 2.

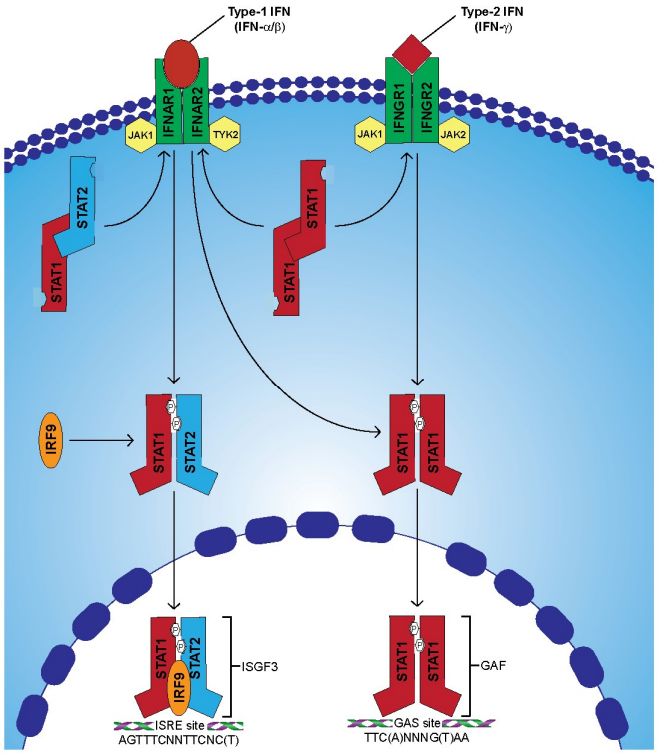

Figure 1.3: *The canonical JAK-STAT pathway in response to IFN. IFN binding to the receptor results in STAT recruitment and activation via phosphorylation of a highly conserved tyrosine residue within the STAT by JAK. Type-1 IFN results in the activation of both STAT1 and STAT2 producing heterodimers which incorporate IRF9 to form the ISGF3 complex. Activated STAT1 may also form a homodimer (GAF), which is produced during both type-1 and type-2 IFN signalling. The activated STAT dimer translocates to the nucleus and binds specific DNA sequences within the promoter regions of target genes.*

Whilst cytokine receptors have no intrinsic kinase activity, they are all associated with a member of the Janus kinase (JAK) protein family. There are a total of 4 members of the JAK family: JAK1, JAK2 JAk3 and TYK2. In the cases of IFNAR1 and IFNAR2, they are associated with JAK1 and Tyk2 respectively. Both IFNGR1 and IFNGR2 are associated with JAK1 and JAK2. The receptor proteins are brought together in close proximity by the presence of interferon, which allows JAK auto-phosphorylation reactions to occur. The JAKs subsequently catalyse the phosphorylation of tyrosine residues at the intracellular surface of the receptors. These phosphorylated sites act as docking points for latent STAT proteins; of which there are 7 members STATs 1-4, 5a, 5b and 6. STAT1 and STAT2 are both recruited to the IFNAR complex and two STAT1 molecules associate with the IFNGRs. Once the STAT proteins are in position specific tyrosine residues are phosphorylated by the JAKs in a

process that is termed STAT activation (Shuai et al, 1993). The active STAT proteins form dimers through mutual interactions between the phospho-tyrosine of each STAT with a highly conserved Src Homology 2 (SH2) domain on the other (Shaui et al, 1994). They subsequently translocate to nucleus where they bind to specific DNA sequences within the promoter regions of target genes.

In response to interferon, STAT1 and STAT2 are the primary signal transducers. Type-1 IFN signalling results in an activated heterodimer of STAT1 and STAT2 which forms a trimeric complex known as ISGF3 with another protein, interferon regulated factor 9 (IRF9) (Qureshi et al, 1995). This activated complex then accumulates in the nucleus where it can bind to specific DNA sequences known as interferon stimulated response element (ISRE). The sequence 5'-AGTTTCNNTTTCNC/T-3', is considered the canonical ISRE and is found in the promoter regions of type I IFN target genes. STAT1 and IRF9 drive the binding to DNA of this complex, whilst STAT2 supports the recruitment of the transcriptional machinery to the target gene (Au-Yeung et al, 2013). ISGF3 is not formed in response to IFNGR1/2 activation which instead produces a homodimer of activated STAT1, also known as gamma activated factor (GAF). In this case, the target site is known as the gamma activated sequence (GAS), a palindromic region with the sequence 5'-TTCNNNNGAA-3' (Kahn et al, 1993). This provides a means of distinguishing between type-1 and 2 target genes, although there is a significant overlap in these sets of genes, highlighting the fact that the separate requirements of anti-viral and anti-bacterial immunity share many similar mechanisms. Furthermore, activated STAT1 homodimers are also produced in response to type-1 IFN, although the ISGF3 complex is the primary signal transducer. The influences of these genes in each type of interferon signalling, as well as the role of STATs in providing routes of cross-talk, are discussed in the following sections.

1.1.4. Target genes

The interferons are a closely related family of cytokines and subsequently show substantial overlap in their target genes, with the promoters of many containing both GAS and ISRE sites. However, there are some unique target genes that are crucial in driving the distinct phenotypes of different interferon responses. Accordingly, it should be noted that the

responses to various immune stimuli can be differentiated not only by the type of interferon produced but also the quantity of interferon released, thus allowing for the appropriate response to be dictated by these circumstances. This section will describe some of the classic interferon target genes and genes specific to either type I or type II IFNs. The role of STATs and other conditions that further accentuate variation between the two IFN families will also be discussed.

Interferons can instigate the upregulation of over 300 genes and, as previously mentioned, drive cells into an anti-viral state (Randall and Goodbourn, 2008). This anti-viral state is a major component of the innate immune response and results in increased expression of several proteins that inhibit viral replication. PRRs which detect pathogens are highly upregulated in response to interferon and thus result in a highly sensitised cell. These include Toll-like receptors (TLRs), an important family of transmembrane glycoproteins found on both the cell surface and endosomal membranes that can induce the production and release of cytokines (including interferon) in infected cells (Uematsu and Akira, 2007), and also retinoic-inducible gene 1 (RIG1)-like receptors, helicase enzymes that detect double stranded or 5'-triphosphorylated RNA and subsequently activate downstream pathways to induce further anti-viral genes (Thompson and Locarnini, 2007; Szabo et al, 2014). Another group of effector proteins upregulated are the IFN-induced protein with tetratricopeptide repeats (IFIT) family. These proteins directly interact with eIF3, an important initiator of translation, and subsequently reduce new protein synthesis in an infected cell (Fensterl and Sen, 2015). These effector proteins result in a cell that has significantly increased pathogen sensing, reduced protein synthesis and rapid destruction of RNA via the activity of RNase L (Tam and Jacques, 2014); greatly reducing the capacity of the host cell to allow viral replication. These classic interferon response genes are upregulated by both IFN-α/β and IFN-γ, and serve as the basis for the innate immune defence in cells.

There are only a few genes characterised as specifically activated by type-1 IFN. MxA has been identified as being upregulated by type-1 IFN but not type-2 (Sanda et al, 2006). This gene encodes a GTPase that is well known as a potent defence against influenza viruses. Oligoadenylate synthase (OAS) genes are another family that is preferentially targeted by ISGF3, which works in tandem with latent endoribonuclease (RNaseL) to detect and cleave the RNA of both host and virus. Due to its wider immunomodulatory function, type-2 IFN

has a wider range of target genes not induced by type-1. Genes that are specifically upregulated by IFN-γ include the components of the MHC class II system (Celeda and Maki, 1991; Sanda et al, 2006). This expands type II IFN signalling to drive the presentation of pathogen-derived antigens to specialised lymphocytes, initiating a pathogen-specific response that is characteristic of the adaptive immune system. Another type II specific response is the expression of the inducible nitric oxide synthetase (iNOS), an enzyme that is vital to the destruction of intracellular pathogens such as phagocytosed bacteria (Lorsbach et al, 1993; Schroder et al, 2004). One special case that should also be considered is that type II IFN causes the upregulation of the interferon regulatory factor 1 (IRF1). IRF1 is a transcription factor that promotes expression of a subset of ISGs that overlap with those triggered by type I interferon, thus indirectly linking type II to type I IFN target genes (Schroder et al, 2004).

1.1.5. STAT1 and STAT2 in Interferon Signalling

STAT1 is crucial for the normal response to IFN. It is a component of both GAF and ISGF3, with neither forming in its absence. STAT1 -/- mice, whilst viable, show severe immune deficiencies in combating both viral and bacterial infections (Meraz et al, 1996). Complete STAT1 deficiency in humans is a rare recessive disorder that results in disseminated bacillus Calmete-Guérin (BCG), increased susceptibility to viral infection and ultimately leads to early mortality (Chapgier et al, 2006). This vulnerability is somewhat unsurprising as the patients lose the ability to respond to all types of IFN and thus are significantly immunocompromised. Nonetheless, studies using STAT1 -/- mice reveal STAT1-independent mechanisms that; in opposition to the more traditional anti-proliferative effects of IFN-γ, appear to enhance cell growth. Further evidence for a STAT1-independent IFN response is drawn from the significantly better anti-viral response in STAT1 -/- mice compared to double IFNAR1/IFNGR1 knock out mice (Meraz et al, 1996). STAT1 homodimers are also a signal transducer of many other cytokines such as IL-6 and IL-27, often in conjunction with STAT3 homodimers. How the response to different cytokines is so varied, whilst converging on a few signal transducers, is still poorly understood and is the subject of much research. STAT1 is unique amongst the STAT family in that it may be bound to the protein SUMO (small ubiquitin-like modifier), which modulates its transcriptional duration in response to both type I and II IFN signalling (Droescher et al, 2011; Maarifi et al, 2015).

As a component of the ISGF3 complex, STAT2 is an essential signal transducer in type I and III IFN signalling. Its contribution to DNA binding is limited; however, it has a large transactivation domain at the C-terminus that provides docking sites for the transcriptional machinery. STAT2 is also believed to play an important role in type I IFN-induced activation of STAT1. Studies show that some cell lines lacking STAT2 have a reduced ability to phosphorylate STAT1; leading to a model of type I IFN signalling that involves STAT2 recruitment to the IFN receptor facilitating subsequent recruitment of STAT1 (Leung et al, 1995). STAT2 is also quite unique amongst the STAT family in that it has a small group of cytokines which activate it; to date it is best known to be activated in response to type I and III IFN, with some activation by IL-4. In contrast, STAT1 is activated in response to a large cohort of cytokines. STAT2 appears to have limited influence beyond type I IFN. In fact, one area of STAT2 research focuses on how STAT2 can influence cell behaviour outside of the ISGF3 complex. A STAT2-IRF9 complex is reported to exist prior to IFN signalling and contribute to tonic ISG expression in cells (Lou et al, 2009). Likewise an inactive (lacking STAT tyrosine phosphorylation) ISGF3 complex has recently been reported to contribute to the upregulation of a specific set of ISGs in melanoma cells (Cheon et al, 2013). These reports of non-canonical functions of STAT2 are part of a growing drive to uncover the more subtle functions of this protein.

During the conclusion of IFN signalling both STAT1 and STAT2 are returned to their latent inactive state by TC45 phosphatase enzymes (ten Hoeve et al, 2002). Subsequently, ISG expression is tempered by a host of negative feedback mechanisms. Several of these mechanisms involve proteins that influence the STAT proteins, with two protein families in particular: suppressors of cytokine signalling (SOCS) and protein inhibitors of activated STATs (PIAS). PIAS proteins are thought to inhibit STATs through interactions involving their function as a SUMO E3 ligase (Shuai and Liu, 2005), thus targeting the STATs for degradation. The SOCS proteins target the JAK-STAT pathway at the receptor associated kinases. SOCS1 inhibits the activity of JAK2 and to a lesser extent TYK2 and JAK1, ending further activation of STAT proteins thus effectively allowing the phosphatases to facilitate the shift from active to inactive STAT dimers in the cell (Yoshimura et al, 2007). A particular target of SOCS1 is IFN-γ; knockout mice show many defects attributed to uncontrolled IFN signalling. Yet another IFN target gene, ISG15, encodes an ubiquitin-like molecule that

specifically targets the JAK-STAT pathway as a stabalising protein that prolongs IFN-induced protein activity (Zhang and Zhang, 2011). STAT1 and STAT2 are therefore the targets of both the initiating and resolving mechanisms of IFN signalling.

As previously stated, many cytokines converge upon the limited number of STAT proteins thus providing the ideal circumstances for signal crosstalk. This is a common occurrence among cytokines and involves several mechanisms including altered protein expression and post-translational modifications. Cells rarely receive cytokines in isolation but rather as a part of an ever changing blend. Several examples where this balance impacts upon STATs exist. Low doses of IFN are known to cause a large upregulation of both STAT1 and STAT2 but not STAT3, thus sensitising cells for further stimuli and also affecting the response to cytokines other than IFN that converge on STAT1 (Hu et al, 2002). In the case of IL-6 and IL-27, these two cytokines drive many antagonistic phenotypes, with IL-6 promoting Th2 and Th17 differentiation and IL-27 driving Th1 maturation, yet both signal through STAT1 and STAT3. Gene analysis of STAT knockout mice have revealed that one key difference is the role of STAT1; which is better activated and essential for the transcription of significantly more IL-27 specific genes compared to IL-6 (Hirahara et al, 2015). IFN stimulation also triggers a large global increase in SUMO and ubiquitin conjugation, with STAT1 a noteworthy target of SUMO, therefore affecting subsequent STAT1 activity in response to IFN or another cytokine (Droescher et al, 2011; Begitt et al, 2011). It is clear that via a myriad of ways, STAT1 and STAT2 are the conduits for manipulation of cytokine responses by each other.

1.2. The Structure of STATs

The STAT proteins share a similar structure with six conserved domains that contribute to the function and behaviour of members of this family (**Figure 1.4**). Since the successful determination of the crystal structure of STAT1 bound to DNA, many of the classical functions attributed to each domain have been well characterised. Despite this, recent research has focused on exploring non-canonical and STAT-specific functions in an effort to fully understand how a myriad of cytokine responses can be initiated by the 7 STAT proteins.

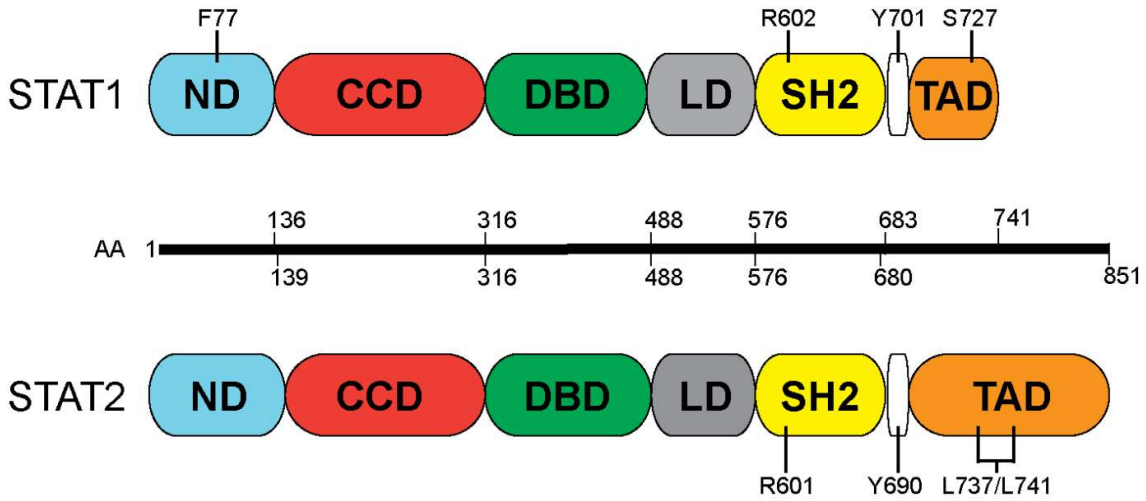

Figure 1.4: *Domain structure of STAT1 and STAT2. STATs have 6 domains, amino terminal (ND), coil-coil (CCD), DNA-binding (DBD), Linker (LD), Src-homology 2 (SH2) and C-terminal or transactivation (TAD). Highlighted are residues critical for certain characteristics of each STAT including dimer formation and polymerisation(F77A), activation (R602/Y701 and R601/Y690) and nuclear export (L737/L741).*

1.2.1. The Amino-Terminal Domain

The amino terminal, or N-Domain, is one of the most conserved domains within the STAT protein family and comprises around 130 amino acids. Since the crystal structure of STAT4 amino-terminal domain, or N-domain, was determined, much research has focused on the role of this domain in the polymerisation of activated STAT dimers on DNA (Chen et al, 1998; Levy and Marie, 2012). This has culminated in the discovery that this polymerisation is a key distinguishing feature between type 1 and type 2 interferon gene induction; being dispensable in the former whilst essential for the latter, demonstrated by the inability of the non-polymerising STAT1 F77A mutant to induce IFN-γ response (Begitt et al, 2014). However, our understanding of the role of the N-domain has expanded significantly in recent years.

With the exception of STAT4, the N-domain is not necessary for activation of STATs at the receptor (Murphy et al, 2000). However, it is required for efficient deactivation (Mertens et al, 2006) of STATs. This is due to two distinct orientations of STAT dimers; termed parallel and anti-parallel. Parallel dimers are the classic transcription factor, with mutual interactions between the SH2 domains of the STATs, and will be discussed later. The less understood conformation is the anti-parallel dimer, which relies on interactions between

STAT N-domains. With regards to the inactivation, this conformation is important as it exposes the conserved tyrosine that is phosphorylated to phosphatases. As such, STAT proteins that cannot transition to the anti-parallel dimer remain activated for a much longer duration than the wild type. The N-domain is also essential for the nuclear translocation of STATs, as truncated STAT1 cannot accumulate in the nucleus despite normal activation at the receptor. This is apparently not due to direct contact with the nuclear import machinery (Nardozzi et al, 2010) nor can the N-domain for one STAT recapitulate import for another as N-domain STAT chimeras are also unable to translocate to the nucleus despite adequate activation (Strehlow and Schindler, 1998).

The N-domain is not only important in STAT polymerisation on DNA, but also in the polymerisation of activated STATs into paracrystalline structures in the nucleus. This phenomenon is considered an important mechanism in extending the nuclear presence of activated STAT proteins, particularly in acute immune responses (Droescher et al, 2011). In the case of STAT1 during interferon signalling, the formation of these paracrystals is inhibited by the small ubiquitin-like modifier (SUMO) providing a further platform for modification of the cytokine response. Knock-in mice which express a STAT1 that cannot be SUMO-modified exhibit an increase in the formation of STAT1 paracrystals after IFN-γ; which coincides with hypersensitivity to this cytokine (Begitt et al, 2011). STAT1 paracrystals can be abrogated by the same point mutation within the N-domain, Phe77Ala, which precludes STAT1 polymerisation on DNA (Droescher et al, 2011).

Studies show that the N-domain interactions of the STAT families are not consistent (Ota et al, 2004, Wenta et al, 2008). Their results reveal that affinities for self-association of STAT1, STAT3 and STAT4 N-domains differ considerably, suggesting that their role in the signalling pathway may be STAT-specific, and by that measure also cytokine-specific.

1.2.2. The Coiled-coil Domain

As the name suggests, the coiled-coil domain (CCD) is composed of several alpha helices that arrange themselves into a coil structure. This domain is important for several critical STAT protein interactions, including receptor docking and subsequent STAT activation. Indeed, several gain-of-function mutations in the STAT1 CCD have been identified and are characterised by STAT1 hyperactivity, IFN-γ hypersensitivity and the development of the

chronic mucocutaneous candidiasis (Martinez-Martinez et al, 2015). Furthermore, this domain is also vital for the formation of IFN-induced ISGF3 complex formation, by acting as an interface for binding of STAT2 and IRF9.

1.2.3. The DNA-binding Domain

The DNA-binding domain (DBD) of STAT proteins is essential to their function as activators of transcription, both in terms of providing a protein-DNA interface but also in recognising the specific target DNA sequence for the STAT (Horvath et al, 1995). The domain adopts an immunoglobulin fold-structure, similar to the DNA-binding domains of fellow transcription factors, NF-κ3 and p53 tumour suppressor protein. The crystal structure of a STAT1 dimer bound to DNA has been resolved, with four segments of this domain making contact with DNA. The segment at the C-terminal end of this domain is the most crucial, containing an asparagine at position 460 in STAT1 that makes contact with base pairs at the centre of the GAS element (Chen et al, 1998).

The affinity of the activated STAT proteins to DNA is determined by residues within this domain. The DNA-binding of STAT1 can be dramatically increased by the introduction of positively charged amino acids at positions 327, 426 and 427, all within the DBD. Conversely, genetic knock-in of negatively charged amino acids at positions 426 and 427 significantly impairs STAT1 ability to bind DNA. The importance of the DBD in STAT protein function can be observed clinically in the case of an immunodeficiency known as hyper-IgE syndrome, which is attributed to point mutations within the STAT3 DBD (Minegishi et al, 2007).

Due to only the parallel conformation of STAT dimers being capable of DNA-binding, this domain also has a role in maintaining STAT dimers within this arrangement. Additionally this conformation is also essential to STAT interaction with the importin proteins, which facilitate the nuclear translocation of activated STAT dimers, therefore the STAT DBD is also involved in both nuclear import and retention.

1.2.4. The Linker Domain

At around 100 amino acids in length, the linker domain is believed to have a predominantly structural role in STAT proteins and remains one of the least studied STAT domains.

Nonetheless several mutations have been characterised, with a cysteine residue at position 543 found to be integral to STAT1 nuclear import (Marg et al, 2004). Additionally, a highly conserved motif of 10 amino acids within the linker domain has been identified, containing a lysine residue crucial for GAS element recognition in STAT1 (Lys567) and two glutamic acid residues important for the dissociation of activated STAT1 dimers from DNA (Hüntelmann, 2014).

1.2.5. The Src Homology 2 Domain

Src homology 2 (SH2) domains are found within many proteins associated with intracellular signalling; often in pathways that utilise tyrosine kinases, such as JAKs. Consequently, this domain is of fundamental importance to STAT protein function and as such shows the most conservation within the family. The SH2 domain is responsible for facilitating the recruitment of the STAT protein to the receptor following phosphorylation of specific tyrosine residues that act as docking points. Despite substantial similarity between the STATs in this domain, interchange of SH2 domains between STAT1 and STAT2 has been shown to alter the receptor specificity (Heim et al, 1995).

Along with receptor binding, the SH2 plays an essential role in STAT hetero- or homo-dimerisation in the parallel conformation which is required for STAT DNA-binding and subsequent target gene activation. In STAT1 SH2-phosphotyrosine interactions, a highly conserved arginine residue within the SH2 domain of one STAT recognises the phosphorylated tyrosine residue on the other STAT (Chen et al, 1998). As both STAT proteins in the dimer contain the phosphorylated tyrosine residue, the parallel dimer is stabilised by mutual SH2-phopshotyrosine interactions. This places the SH2 domain alongside the amino-terminal domain as the primary contributors to STAT dimerisation, with the SH2 stabilising parallel-orientated dimers and the N-domain supporting anti-parallel dimerisation.

1.2.6. The Transactivation Domain

STAT transactivation domains (TADs) show the most variation between the family members, in line with their function in facilitating STAT-specific transcriptional effects. Despite this the

TAD is not associated with target gene selection, at least in interferon signalling, as any STAT TAD may substitute for STAT1 in eliciting an anti-viral response (Shen and Darnell Jr., 2001).

STAT2 has a much larger TAD than STAT1, which supports the view that its main contribution to the interferon-induced ISGF3 complex is to provide contact points for transcriptional co-regulators. STAT2 contains a potent nuclear export signal (NES) within the TAD that promotes its largely cytoplasmic distribution within the cell prior to receptor activation, which must subsequently be overcome in order to facilitate nuclear accumulation observed during type-1 IFN signalling.

STAT1, STAT3, STAT4 and STAT5 all contain a serine residue within the TAD that requires phosphorylation in order for full transcriptional potency to be achieved. This allows two independent activating signals to converge on STAT signalling as serine and tyrosine phosphorylation can be induced independently.

1.3. STAT Behaviour and Regulation

Whilst the canonical behaviour of STATs during cytokine signalling is well understood, many aspects of their function and regulation are still emerging. The expression of each STAT can vary greatly amongst cell types, whilst several post-translational modifications can dramatically alter their function or activity. Moreover, whilst STAT activation and nuclear accumulation is a classic result of cytokine signalling, the duration of this accumulation, degree of activation and, ultimately, the transcriptional response are all affected by the cells internal and external environment. This section will highlight some important features in STAT regulation beyond activation and inactivation that have a large role in determining the response to a cytokine, with particular focus given to STAT1 and STAT2.

1.3.1. STAT Subcellular Distribution

Inactive STATs are nucleocytoplasmic shuttling proteins which, due to their size, must traverse the nuclear membrane via specialised structures known as nuclear pore complexes (NPCs). These structures are high-order octagonal channels formed by proteins called

nucleoporins, of which some contain hydrophobic regions rich in phenylalanine and glycine; FG- repeat motifs. (Fahrenkrog et al., 2004). These regions provide contact points for STAT molecules, allowing them to shuttle between the cytoplasm and nucleus in an energy independent manner (Marg et al., 2004). A second, energy-dependent mechanism for the passage of STATs through the NPC also exists in the form of karyopherins. These proteins enable the rapid transport of cargo through the NPC, utilising metabolic energy from the Ran-GTPase, and are called either importins or exportins depending on the direction of transport. For a protein to be recognised as cargo, specific amino acid motifs must be present and exposed. These motifs can either be nuclear localisation signals (NLS) or nuclear export signals (NES) depending on their recognition by either importins or exportins.

Whilst all inactive STAT proteins shuttle through the NPC, the speed and general direction of travel is not universal, leading to different subcellular distribution in resting cells. STAT1 and STAT3 can be observed in both the nucleus and cytoplasm prior to cytokine signalling, although their nuclear presence shows variation across cell-types (Meyer et al., 2002) indicating cytokine-independent regulation of nuclear transport exists. In contrast, STAT2 is found almost exclusively in the cytoplasm of cells due to a strong NES located within the TAD (Frahm et al, 2006). A NES within the coiled-coil domain of STAT1 has also been identified, although it has a much less dramatic effect than that of STAT2 (Begitt et al, 2000). STAT2 also appears to shuttle between the cytoplasm and nucleus much faster than STAT1 (Frahm et al, 2006) leading to the postulation that during type-1 IFN signalling STAT1 contributes to the rapid accumulation of ISGF3 by blocking the strong NES of STAT2.

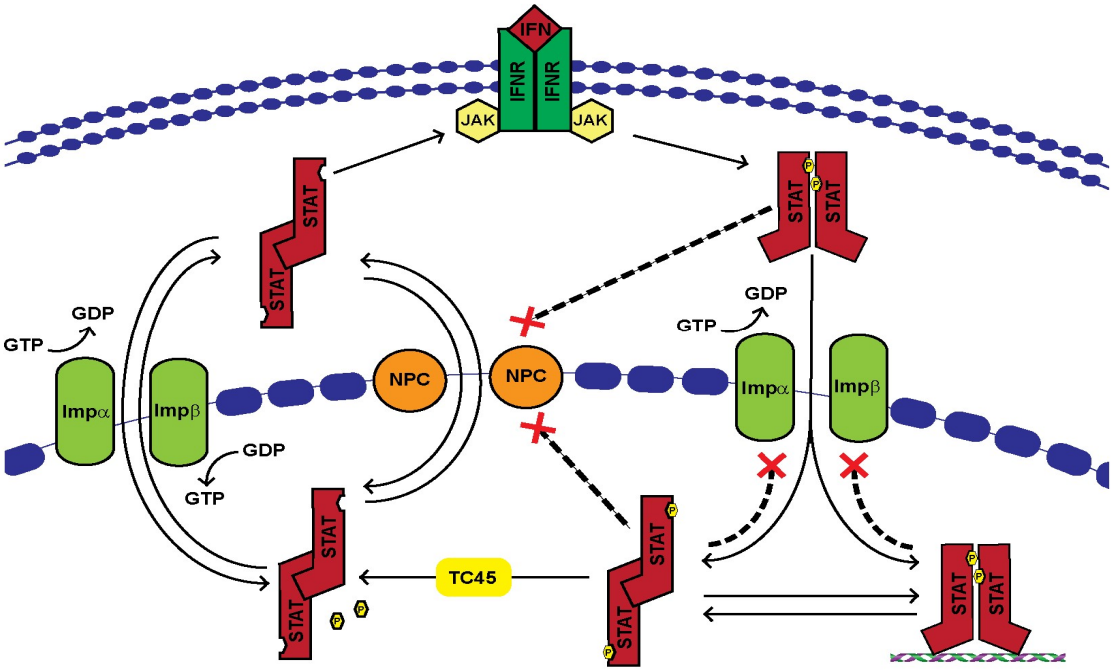

Figure 1.5: *STAT nucleocytoplasmic shuttling. Unphosphorylated STAT proteins can shuttle across the nuclear membrane either through energy-independent interactions with the nuclear pore complex (NPC) or by active transport across the RanGTP/GDP gradient by the importin proteins. Following phosphorylation, STATs can only enter the nucleus via the importin route and cannot be exported from the nucleus until dephosphorylation by the TC45 phosphatases. TC45 cannot inactivate STATs until the phosphate group is exposed.*

The activation of STAT proteins dramatically alters their cellular distribution, leading to an accumulation within the nucleus. This occurs as a result of a change in their interaction with the NPC. Activated STATs require the energy-dependent importin factors to enter the nucleus. During IFN signalling, the formation of a dimer specific NLS by conserved amino acid sequences in the DNA binding domains of STAT1 and STAT2 facilitates such import (Melen et al, 2001). The karyopherin, importin α5, has been identified as the sole facilitator of GAF and ISGF3 nuclear import (Fagerlund et al, 2002). As such the STAT-importin α5 interaction is targeted by many viruses, including Ebola and Hepatitis B, in order to suppress IFN signalling (Xu et al, 2014; Chen et al, 2013). At the same time, activated STATs cannot be exported from the nucleus until they are dephosphorylated (ten Hoeve et al, 2002). Dephosphorylation of STATs requires the exposure of the key tyrosine residue to the

phosphatases, however DNA binding stabilises a dimer conformation that prevents this. Thus the DNA off-rate of STATs correlates to their export during cytokine signalling. Indeed, mutations that disrupt the DNA binding increase the rate of dephosphorylation and reduce nuclear retention (Meyer et al, 2003). This combination of energy-dependent import and retention leads to an observable nuclear accumulation of STATs after as little as 10 minutes of cytokine signalling (Schindler et al, 1992). Upon the termination of cytokine signalling, the gradual inactivation of STAT proteins in the nucleus allows both the carrier-free and energy-dependent mechanism of STAT shuttling to result in their redistribution throughout the cell.

1.3.2. STAT Dimer Conformations

As signal transducers, the movement of STATs from the cytoplasm to the nucleus is critical to their function and thus much research has been focused on understanding how this is regulated. The major change in import/export routes initiated by cytokine signalling is attributed to an altered interaction with the nuclear transport machinery (Vinkemeier, 2004). This change in behaviour stems from a transformation in STAT dimer conformation.

As mentioned previously, STATs exist as dimers both before and during activation. However STATs may oscillate between two dimer conformations, parallel and anti-parallel. Activation of STATs at the receptor prompts the formation of dimers in the parallel conformation through reciprocal SH2-phosphotyrosine interactions. This dimer is the classic STAT transcription factor which can interact with the nuclear import machinery, bind DNA and induce target gene transcription. Parallel STAT dimers have been shown to use the amino-terminal domain as an interaction surface, facilitating dimer polymerisation along DNA (Xu et al, 1996) which is essential for the activation of type II, but not type I, IFN target genes (Begitt et al, 2014). Furthermore, this conformation is associated with nuclear accumulation of STATs as it can bind to importin α5 and target DNA sequences, whilst protecting the STATs against tyrosine dephosphorylation required for their export. Whilst it is believed that the parallel conformation typically requires activation of STATs, it has been suggested that in high cellular concentrations inactive STAT1 and STAT2, along with IRF9, may form U-ISGF3 activating a subset of genes independent of IFN and subsequently linked to resistance to cell death following radiation-induced DNA damage (Cheon et al, 2013).

Prior to activation STATs interact via their amino-terminal domains to form anti-parallel dimers independent of the SH2 domain interaction (Mao et al., 2005). These dimers are nucleocytoplasmic shuttling proteins and their role in STAT function is not fully understood. They do not appear essential for either receptor recruitment or activation of STAT1 as mutations that destabilise this interaction do not inhibit STAT1 activation (Mertens et al, 2006).

There is also substantial evidence that activated STATs can transition from a parallel to a phosphorylated anti-parallel conformation (Wenta et al., 2008). These phosphorylated anti-parallel dimers are essential for the inactivation of STAT1, as phosphatases cannot access the key tyrosine residues whilst they are masked by STAT SH2 domains. Accordingly, mutations which prevent the formation of anti-parallel dimers are associated with defects in STAT1 dephosphorylation (Mertens et al, 2006) with clinical implications manifesting in chronic mucocutaneous candidiasis (Liu et al., 2011). In an interesting contrast, anti-parallel pSTAT1 dimers may polymerise via concurrent SH2 interactions to form paracrystals (in the absence of SUMO-modification) which also prolongs the nuclear presence of pSTAT1 by blocking access to phosphatases (Droescher et al, 2011).

Whilst the precise mechanism for transition between parallel and anti-parallel dimer conformations is not yet fully understood, it is clear that there is a functional purpose for each in IFN signalling. A greater understanding of the different consequences for each conformation before and during IFN signalling would shed further light on how this vital system is regulated.

1.3.3. Regulation of STAT Activity

The response to a cytokine is not binary, therefore the result of IFN signalling is influenced by the context in which it occurs. It is highly unlikely that cells are at any point exposed to just one external stimulus at any one time and points of signal crosstalk exist not only across the various cytokines but even between the different types of IFN. As the carriers of the external stimuli to the nucleus, much of this crosstalk converges on the STAT proteins. STATs can be regulated by their expression or by a range of post-translational modifications.

Whilst phosphorylation of a conserved tyrosine residue is essential for the activation of STATs, several other residues can also be modified in this way. STAT1 possesses a serine residue at position 727 within the TAD that works synergistically with the classical tyrosine to enhance the transcriptional potency. This is observed in murine macrophages as a mechanism utilised by Toll-like receptor (TLR) 2 and TLR4. In these cases, phosphorylation of the serine residue is carried out by members of the mitogen-activated protein kinase (MAPK) and protein kinase C (PKC) families (Rhee et al, 2003). STAT2 is also phosphorylated at serine 287 in the coiled-coil domain, however in this case it acts to negatively regulate the anti-viral and anti-proliferative effects of IFN signalling (Steen et al, 2013; Steen and Gamero, 2013).

Negative regulation of IFN signalling is classically attributed to the SOCS protein family. Expression of SOCS1 is directly upregulated by IFN signalling and so acts as a negative feedback loop. Once expressed, SOCS1 has been shown to interact with the receptor/JAK complex preventing further STAT activation via two methods; preventing STAT access to the JAK/receptor complex (Yasukawa et al, 1999) whilst also targeting the complex for degradation through ubiquitin ligase activity (Vuong et al, 2004). By inhibiting the reactivation of STATs, SOCS1 works with the nuclear TC45 phosphatases to diminish the amount of activated STAT following a cytokine signal (ten Hoeve et al, 2002). Unsurprisingly, loss of SOCS1 protein results in a loss of control over the IFN response; SOCS1 -/- mice show increased levels of pro-inflammatory cytokines and nitric oxide in response to LPS and other TLR ligands (Yoshimura et al, 2007).

Whilst SOCS1 and TC45 are the quintessential STAT1 negative regulators, other proteins also alter the response to IFNs. Two small protein families are particularly associated with IFN; SUMO and ISG15. In both cases, these small proteins are bound to target proteins by a ligase. STAT1 is the only member of the family to be targeted by SUMO, on account of its recognition motif WExV just upstream of the key tyrosine at position 701. SUMO modification of STAT1 results in a semi-phosphorylated STAT1 homodimer, which in turn disrupts the formation in the nucleus of paracrystals thus making STAT1 more susceptible to dephosphorylation (Droescher et al, 2011). This process can be ablated by mutation within the SUMO recognition motif and results in both type-1 and type-2 IFN hypersensitivity (Maarifi et al, 2015; Begitt et al, 2011). Clinically, the inverse case can be seen, where a

mutation produces a *de novo* SUMO recognition site at a corresponding position in STAT3. Although SUMO conjugation of STAT3 in these patients has not yet been shown directly, the subsequent phenotype shows diminished STAT3 activation and an immune deficiency known as hyper IgE-syndrome (He et al, 2012). ISG15 is an interesting and, as yet, incompletely understood protein, which is highly upregulated in response to IFN. It has been shown to bind STAT1, JAK1 and several proteins that are involved in the innate immune system (Zhang and Zhang, 2011). It is a positive regulator of IFN signalling; cell lines with increased ISG15 modification show prolonged STAT1 activation and gene transcription in response to IFN (Malakhova et al, 2003). In light of this, ISG15ylation is thought to stabilise target proteins, possibly by competing with ubiquitin, until it is removed by a deubiquitinating protease called USP18 (Malakhov et al, 2002; Zhang and Zhang, 2011).

All organisms must maintain a balance between possessing a highly sensitive immune system and limiting the self-harming potential of such a system. As an example, sepsis is an uncontrolled immune response to infection that causes systemic organ damage, shock and ultimately death. In England, approximately 120,000 people suffered from sepsis in 2013-2014 (Hospital Episode Statistics, Health and Social Care Information Centre 2015). The regulation of STATs in IFN signalling is of great importance in this context, as it forms part of the first response and thus plays a role in determining the level of subsequent action by the immune system. Thus, it is no surprise that a surfeit of STAT regulating mechanisms have been uncovered. Our understanding of these mechanisms is crucial in providing better treatments for immune disorders and improved the use of IFN as a treatment.

1.4. Areas of Limited Understanding in the Current Literature

STATs have a well characterised and relatively simple model of action, however this does not easily fit with the fact that over 50 different cytokines converge upon the 7 member STATS. Although these cytokines do show substantial overlap in terms of target genes, the phenotypical outcomes are often highly distinct. Furthermore, the response to any given cytokine can vary greatly depending on the cell-type and surrounding environment. Thus, it is not a great surprise that the clinical outcome of IFN treatment lacks the predictability of antibiotics.

Several questions remain regarding the function and regulation of STATs, most of which require further investigation of known mechanisms. ISG15 and SOCS function are growing areas of research in STAT regulation which may show promise as therapeutic targets of immune disorders in the future but as yet are not sufficiently understood. Similarly, the influence of SUMO on STAT1 function is now acknowledged and further research may allow clinical manipulation of this system. However, some are as yet complete mysteries, such as how STAT1 and STAT3 homodimers share the same target DNA sequence (GAS) but show different gene expression profiles; even in response to cytokines that activate both (Hirahara et al., 2015).

No STAT appears to have had as little attention as STAT2 in recent years. This is likely due to the fact that, unlike STAT1 and STAT3 which are involved in many cytokine signalling pathways, STAT2 appears to be solely responsive to type-1 and type-3 IFN. Thus, much of the recent literature on STAT2 focuses on its inhibition by viruses in order to evade the immune system (Parisien et al, 2002; Grant et al, 2016). Indeed the loss of STAT2 in patients and animals prevents the upregulation of hundreds of genes in response to these crucial anti-viral cytokines, predictably resulting in increased susceptibility to infection (Park et al, 2000; Hambleton et al, 2013). However many aspects of STAT2 deficiency, and hence function, are unexplained. For example, the genetic deletion of STAT2 appears to exacerbate experimental sepsis despite the opposite phenotype being observed when the other components of type-1 IFN are removed instead (Alazawi et al, 2013). Similarly, some patients that are deficient in STAT2 present surprisingly mild phenotypes and may still resist viral infections (Hambleton et al, 2013). These data suggest that STAT2 has other roles in cytokine signalling beyond being the canonical signal transducer to type-1/3 IFNs.

One such aspect that requires investigation is the binding behaviour of STAT2 prior to IFN signalling. While it is now accepted that STATs form dimers both before and during cytokine signalling, STAT2 appears uniquely incapable of homo-dimerisation and instead forms heterodimers with STAT1 (Braunstein et al, 2003; Ota et al, 2004; Levy and Darnel, 2002). The hetero-dimerisation of STAT1 and STAT2 prior to activation has not been investigated despite STAT2 being required for the recruitment of STAT1 to the type-1 IFN receptors (Leung et al, 1995; Li et al, 1997). Strikingly, an observation that STAT1 showed impaired nuclear translocation in cells overexpressing STAT2 (Melen et al, 2003) has not yet been

followed up despite this inhibition taking place during type-2 IFN signalling, which STAT2 has no known role in.

1.5. Thesis Aims

The work presented in this thesis was carried out with the intention of elucidating the existence and functional role of STAT1-STAT2 heterodimers before and during IFN signalling. Subsequently the role of STAT2 in the type-2 IFN signalling pathway was analysed. In detail the questions which drove this work were as follows:

- Does STAT1 form heterodimers with STAT2 prior to IFN signalling?
- If so, does the N-domain facilitate this interaction?
- Are STAT1-STAT2 heterodimers required for type I IFN signalling?
- What is the consequence and role of heterodimers during the type II IFN response?

In order to investigate these questions a variety of methodologies, including fluorescence microscopy, biochemical experimentation, flow assisted cell sorting and other biological assays of IFN response were utilised.

2. Materials and Methods

2.1. Materials

2.1.1. Lab-made buffers and solutions

A variety of lab-made buffers and solutions were utilised in this thesis and are listed alphabetically in the table below. Unless otherwise stated, these buffers were prepared in de-ionised water and, where required, were adjusted to the correct pH using a pH-Meter 540 GLP (WTW, Weilheim). All buffers that required sterilising were autoclaved at 120°C.

Reagent	Preparation
Agar Plates with Antibiotic	Autoclaved LB Medium with 0.15% (w/v) Agar (Fisher Scientific), then either 0.001 % (w/v) Ampicillin (Sigma) or 0.003% (w/v) Kanamycin (Sigma) added to solution. Cast into plates.
Blocking Solution	TBS-T with 4% (w/v) Marvel dried milk.
Casting Gel buffer (4x concentrated)	1.5 M Tris (Fisher Scientific) and 0.4% (w/v) SDS (Sigma). pH=8.8. Diluted in deionized H_2O upon use.
Lysogeny Broth (LB) Medium	1% (w/v) NaCl (Fisher Scientific), 1% (w/v) Yeast Extract (Oxoid) and 0.5% (w/v) Bacteriological Peptone (Oxoid). Autoclaved prior to use, pH=7.0.
Lysis Buffer	50 mM Tris-HCl (Tris base at pH=8.0 with HCl), 100 mM EDTA (Calbiochem), 100 mM NaCl (Fisher Scientific) and 1% (w/v) SDS (Sigma).
PBS	Dulbecco's PBS tablets (Oxoid) at 1 tablet per 100 mL H_2O.

DNA-Loading Buffer (10x concentrated)	10x concentrated TAE buffer with 30% (v/v) Glycerol (Courtin and Water) and 0.25% (w/v) Bromphenylblue (EuroBio). Diluted in sample mix upon use.
SDS Protein-Loading Buffer	125 mM Tris-HCl, 25% (v/v) Glycerol (Courtin and Water), 4% (w/v) SDS (Sigma), 0.7 M DTT (MP Biomedicals). pH adjusted to 6.8 and small amount of Bromphenylblue (EuroBio) added.
SDS Running Buffer (10x concentrated)	2M Glycine (Fisher Scientific), 250mM Tris (Fisher Scientific) and 1% (w/v) SDS (Sigma). Diluted in deionized H_2O upon use.
SDS Transfer Buffer (10x concentrated)	0.48 M Tris (Fisher Scientific), 13 mM SDS (Sigma) and 0.39 M Glycine (Fisher Scientific). Diluted in a 7:2 Deionized H_2O:Methanol (Fisher Scientific) solution upon use.
Stacking Gel Buffer (4x concentrated)	0.5 M Tris (Fisher Scientific) and 0.4% (w/v) SDS (Sigma). Diluted in deionized H_2O upon use.
Stripping Buffer	25mM Glycine (Fisher Scientific) and 2% (w/v) SDS (Sigma). pH adjusted to 2.0.
TAE Buffer (10x concentrated)	0.4 M Tris (Fisher Scientific), 1.14% (v/v) acetic acid and 0.01 M EDTA (Calbiochem). Diluted in deionized H_2O upon use.
TBS (10x concentrated)	1.4 M NaCl (Fisher Scientific) and 0.1 M Tris (Fisher Scientific). pH adjusted to 7.3. Diluted in deionized H_2O upon use.
TBS-T	TBS with 0.0005% (v/v) Tween-20 (Sigma).
TE Buffer	10 mM Tris (Fisher Scientific) and 1 mM EDTA (Calbiochem). Adjusted to pH=8.0

WCE Buffer (supplemented)	50 mM Tris (Fisher Scientific), 2 mM EGTA (Roth), 0.2 mM EDTA (Calbiochem), 1 mM Na_3VO_3, 50 mM NaF (Roth), 280 mM NaCl (Fisher Scientific) and 10% (v/v) Glycerol (Courtin and Water). Prior to use supplemented with 1 mM DTT (MP Biomedicals), 0.1 mM PMSF(Sigma), 0.05% (w/v) NP40 (Roche) and Complete protease inhibitor cocktail (Roche).
Low-salt WCE Buffer (supplemented)	10 mM KCl (Fisher Scientific), 1 mM EDTA (Calbiochem), 20mM HEPES (Roth), 0.1 mM Na_3VO_3 and 10% (v/v) Glycerol (Courtin and Water). Prior to use supplemented with 1 mM DTT (MP Biomedicals), 0.1 mM PMSF(Sigma), 0.02% (w/v) IGEPAL (Sigma) and Complete protease inhibitor cocktail (Roche).
IP Buffer	10 mM KCl (Fisher Scientific), 1 mM EDTA (Calbiochem), 20 mM HEPES (Roth), 150 mM NaCL (ThermoFisher), 0.1 mM Na_3VO_3 and 10% (v/v) Glycerol (Courtin and Water). Prior to use supplemented with 1 mM DTT (MP Biomedicals), 0.1 mM PMSF(Sigma), 0.02% (w/v) IGEPAL (Sigma) and Complete protease inhibitor cocktail (Roche).

2.1.2. Cytokines and other treatments.

IFN-γ, both human (#407306) and mouse (#407320) were purchased from Merck Millipore, human IFN-β (#11415-1) was obtained from PBL assay science. Standard IFN treatment was for one hour with 50 U/ml IFN-γ or 500 U/ml IFN-β in growth medium, unless stated otherwise. Other treatments used in this thesis include LPS (L7895) from Sigma and ratjadone (#553590) purchased from Merck Millipore.

2.1.3. Cell Lines and Cell Culture reagents

A variety of cell lines were utilised in this thesis and are presented in the following **Table 2.2**

Cell Line	Species	Description	Supplier
HeLa S3	Human	Cervix Carcinoma	Deutsche Sammlung von Mikroorganismen und Zellkulturen, GmbH
U6A	Human	Fibrosarcoma, STAT2 deficient.	Kind gift from Dr G. Stark
U6A-STAT2	Human	Fibrosarcoma, U6A cells stably reconstituted with YFP-tagged STAT2 construct.	Produced by Vinkemeier lab during the course of this thesis as described in Ho et al, 2016
U6A-STAT2 L82A	Human	Fibrosarcoma, U6A cells stably reconstituted with YFP-tagged STAT2 L82A construct	Produced by Vinkemeier lab during the course of this thesis as described in Ho et al, 2016
U3A	Human	Fibrosarcoma, STAT1 deficient	Kind gift from Dr G. Stark
2fTGH	Human	Fibrosarcoma, parental cell line of U6A and U3A	Kind gift from Dr G Stark
Wild-type macrophage	Mouse	Immortalised bone-marrow derived macrophages from 129SvJ mice	Kind gift from Drs W Alazawi and A Gamero
STAT2 -/- bone-marrow derived macrophage	Mouse	Immortalised bone-marrow derived macrophages from STAT2 -/- mice (129SvJ background)	Kind gift from Drs W Alazawi and A Gamero

The cell culture media used in this thesis, Dulbecco's modified essential medium (DMEM), along with other cell culture reagents such as foetal bovine serum (FBS), phosphate

buffered solution (PBS), Trypsin and Penicillin/Streptomycin solution were purchased from Sigma.

2.1.4. Plasmids and Constructs

The following **Table 2.3**, lists the plasmids and expression constructs that were used in this thesis. The specific details of their production are provided in the referenced literature whilst the general methods used to generate them are found in section **2.2**.

Name	Description	Source/Reference
pEYFP-N1	Mammalian expression vector that allows N-terminus fusion to YFP	Clontech, Palo Alto, CA
pEYFP-N1 STAT2 **(1)**	Human STAT2 in pEYFP-N1	Kind gift from Dr J Piehler
pEYFP-N1 STAT2 ΔNES	Derived from **(1)** with introduction of LL737/741AA mutation	Ho et al, 2016
pEYFP-N1 STAT2 ΔC	Derived from **(1)** with the deletion of aa 703-851	Ho et al, 2016
pEYFP-N1 STAT2 L81A	Derived from **(1)** with the mutation L81A	Ho et al, 2016
pEYFP-N1 STAT2 LL81/82AA	Derived from **(1)** with the mutation LL81/82AA	Ho et al, 2016
pEYFP-N1 STAT2 L82A	Derived from **(1)** with the mutation L82A	Ho et al, 2016
pEYFP-N1 STAT2 Untagged	Derived from **(1)** with the inclusion of a stop codon between STAT2 and YFP sequence	Ho et al, 2016
pEYFP-N1 STAT2 Chimera **(2)**	Chimeric molecule comprised aa 1-571 of STAT2, aa 573-710 of STAT1 and finally aa 701-851 of STAT2, produced using SOE PCR.	Ho et al, 2016/Heim et al, 1995

pEYFP-N1 STAT2 Chimera R602L	Derived from **(2)** with the mutation R602L contained within the STAT1 aa sequence.	Ho et al, 2016
pECFP-N1 STAT1 **(3)**	Human STAT1 in pECFP-N1	Droescher et al, 2011
pECFP-N1 STAT1 F77A	Derived from **(3)** with the inclusion of the F77A mutation.	Droescher et al, 2011
pEGFP-N1 STAT1 **(4)**	Human STAT1 in pEGFP-N1	Begitt et al, 2000
pEGFP-N1 STAT1 F77A	Derived from **(4)** with the inclusion of the F77A mutation.	Meyer et al, 2004
pEGFP-N1 STAT1 LL308/312AA	Derived from **(4)** with the inclusion of the LL308/312AA mutation.	Begitt et al, 2000
pCMV-FLAG-N	Mammalian expression vector that allows the N-terminus fusion of FLAG sequence	Clontech, Palo Alto, CA
pCMV-FLAG-N STAT1 **(5)**	Human STAT1 with FLAG tag sequence at C-Terminal end	Meyer et al, 2002
pCMV-FLAG-N STAT1 F77A	Derived from **(5)** with the inclusion of the F77A mutation.	Ho et al, 2016
pCMV-FLAG-N STAT1 Y701F	Derived from **(5)** with the inclusion of the Y701F mutation.	Ho et al, 2016
pCMV-FLAG-N STAT1 F77A/Y701F	Derived from **(5)** with the inclusion of the F77A and Y701F mutation.	Ho et al, 2016

The production and maintenance of the plasmid stocks was carried out using the DH5α strain of *E. coli* grown on LB agar plates containing either ampicillin or kanamycin, both of which were purchased from Sigma. All restriction digest enzymes were supplied by NEB. The methods used in the generation of these plasmids is covered in section **2.2.1**.

2.1.5. Antibodies

Several primary antibodies were used in this thesis and are presented in the following **Table 2.3.**

Antibody	Species	Supplier	Application
α-STAT1 p84/p91 (C-24) sc-345	Rabbit, polyclonal	Santa Cruz Biotechnology	Immunoblotting, Immunofluorescence
α-phosphoSTAT1 Y701 (#9171)	Rabbit, polyclonal	Cell Signaling Technology	Immunoblotting, Immunofluorescence
α-STAT2 (C-20) sc-476	Rabbit, polyclonal	Santa Cruz Biotechnology	Immunoblotting
α-phosphoSTAT2 Y690 (#07-224)	Rabbit, polyclonal	Merck-Millipore	Immunoblotting
α-STAT2 (L-20) sc-950	Rabbit, polyclonal	Santa Cruz Biotechnology	Immunoblotting
α-STAT1 (#610116)	Mouse, monoclonal	BD Transduction Laboratories	Immunoblotting
α-β-Actin (AC-15)	Mouse, monoclonal	Sigma	Immunoblotting
α-FLAG (M2)	Mouse, monoclonal	Sigma	Immunoblotting
α-phospho (S93) HP1γ (ab45720)	Rabbit, polyclonal	Abcam	Immunofluorescence
Alexa Fluor-488 anti-mouse IA/I-E (107615)	Rat, monoclonal	Biolegend	Flow Cytometry
Alexa Fluor-488 rat IgG2b, κ isotype control (400625)	Rat, monoclonal	Biolegend	Flow Cytometry
Alexa Fluor-488 anti-mouse F4/80 (123119)	Rat, monoclonal	Biolegend	Flow Cytometry
PerCP anti-mouse IA/I-E (107623)	Rat, monoclonal	Biolegend	Flow Cytometry

PerCP Rat IgG2b, κ Isotype Control (400629)	Rat, monoclonal	Biolegend	Flow Cytometry
APC anti-human HLA-A,B,C (311409)	Mouse, monoclonal	Biolegend	Flow Cytometry
APC-conjugated mouse IgG2a,k isotype control (400219)	Mouse, monoclonal	Biolegend	Flow Cytometry

2.1.5.1. Secondary antibodies and fluorescent probes.

The secondary antibodies utilised for immunoblotting, IRDye 800CW donkey anti-rabbit (925-32213) and IRDye 800CW donkey anti-mouse (925-32212) were purchased from Licor. Where spectral distinction between two primary antibodies was required, AlexaFluor 680 goat anti-Rabbit (A27042) or AlexaFluor 680 Donkey anti-mouse (A28183) from ThermoFisher were used in conjunction with an IR800 secondary antibody. Immunofluorescence studies utilised the decoration of primary antibodies with either Cy3 AffiniPure donkey anti-mouse (715-165-150, Jackson ImmunoResearch Laboratories) or Cy3 goat anti-rabbit (A10520, ThermoFisher) secondary antibodies.

2.1.6. Software

Visualization and quantitative immunoblot analysis was performed using Image Studio Lite (Li-Cor, version 3.1). Axiovision 4.7 (Zeiss) was used in the capture and export of fluorescent microscopy images using the Axiocam CCD camera and Zeiss AxioPlan 2 wide-field microscope. The recording of fluorescent images from the DeltaVision Elite deconvolution microscope in conjunction with a CoolSNAP HQ2 CCD camera was performed using the Resolve 3D software (Softworx). Line scan analyses were done using Image J software. Microsoft Excel (Microsoft) was used for the handling of raw data from immunoblot quantification, line scan analyses and parasitic replication assays, whilst statistical analyses and the generation of graphs for figures were performed using GraphPad Prism 5.03 (GraphPad). All data and graphs from flow cytometry assays were handled using Kaluza Analysis software (Beckman). The compilation and handling of figures were completed on Adobe Illustrator CS6.

2.2. Methods

The following sections describe the methods used to generate the materials and data presented in this thesis. For the consistency of all buffers, please refer to Table 2.1. The source of all pre-supplied buffers and solutions will be indicated in the text.

2.2.1. Molecular Cloning and maintenance of plasmid constructs

The generation and maintenance of new constructs was performed using the following kits. Site directed mutagenesis was performed using the QuikChange II Site-directed mutagenesis kit from Stratagene. The purification of restriction enzyme digestion products was performed using the NucleoSpin kit (Machery-Nagel). The production of large quantities of high quality plasmid DNA was performed using PureLink Maxiprep (Sigma) columns. These kits were used in line with the manufacturer's instructions in conjugation or as part of the procedures detailed in this following section.

2.2.1.1. Polymerase Chain Reaction (PCR)

The generation of DNA fragments containing new mutations were generated using the Pfu Ultra DNA polymerase from Agilent. Each reaction contained 50 ng of template DNA, 125 ng each of forward and reverse mutagenesis primers, 1.25 mM of each dNTP and 1.25 U Polymerase in a total volume of 50 µL 1 x reaction buffer (Agilent). Amplification was performed using a Mastercycler gradient (Eppendorf). The program used to amplify target DNA utilised a 2 minute denaturation stage at 95°C, followed by 14 cycles of the following program: a 30 second denaturation at 95°C, followed by a 30 second annealing stage and an elongation stage at 72°C. The temperature at the annealing stage was dependent on the calculated melting temperature (T_m) of the primer pair used. This temperature was calculated using the equation $T_m = 81.5°C + 0.41(\%GC) – (675/\text{number of bases} + \%$ mismatch) as provided in the manufacturer's protocol. The duration of elongation stage was calculated as 0.12 seconds per base pair in template DNA. Upon completion of the 14 cycles, a final 10 minute elongation stage at 72°C was performed. In reactions designed to introduce point mutations, destruction of remaining template DNA was performed via incubation with 1 µL of DPN1 restriction enzyme at 37°C. The resulting DNA was then either amplified in bacteria or subjected to further molecular cloning techniques such as restriction digestion.

2.2.1.2. Splicing by Overlap Extension (SOE) PCR

The generation of a chimeric STAT2 was generated using a near identical technique to that described in (Heim et al, 1995). In essence, three separate PCR amplifications were performed using primer pairs which generated DNA fragments encoding aa 1-571 of STAT2 (A), aa 573-710 of STAT1 (B), and aa 701-851 of STAT2 (C). Each fragment contained an overlap sequence with the other which it was to be fused to. Fragment A contained an

overlap at the 3' end which matched the 5' end of B; fragment C possessed an overlap sequence at the 5' end which was identical to the 3' sequence contained in B; whilst fragment B had an overlap with A and C at the 5' and 3' ends respectively. The fragments were isolated using agarose gel electrophoresis and purification. Two rounds of SOE PCR were performed in order to fuse fragment A and B as well as fragment B to C. These two larger PCR fragments were purified and subjected to a final SOE PCR, which encoded the chimeric STAT2. This fragment possessed restriction sites at the 5' and 3' ends which were subsequently used to clone the DNA into the pEYFP-N1 expression vector.

2.2.1.3. Restriction digestion of DNA

Restriction digests were performed using enzymes acquired from NEB in reaction buffer supplied, according to the manufacturer's instructions. Digestion reactions of 50 µL containing either 0.5 µg vector DNA or 1 µg of insert DNA were performed at 37°C for 2 hours. During vector digests, 1 µL of calf intestinal phosphatase (CIP) was introduced for the final 30 minutes in order to prevent re-ligation.

2.2.1.4. DNA agarose gel electrophoresis

The isolation of PCR and restriction digestion products was performed using a gel consisting of 1.5% low melting point agarose (Melford) in 1 x TAE buffer supplemented with 0.5 µg/mL ethidium bromide (ThermoFisher). DNA samples were loaded in 1 x DNA loading buffer and run alongside 1Kb DNA ladder sample (Invitrogen). Electrophoresis was run at a maximum of 85V for 60 to 90 minutes using a B1, B1A separation system from Owl and an Amersham EPS 301 power supply. Bands required for isolation were excised under low UV and purified using the Nucleospin Kit from Machery-Nagel according to manufacturer instructions.

2.2.1.5. Ligation of DNA

The ligation of DNA vectors and inserts prepared over the course of this work were performed using 20 µL reactions containing 1 µL of T4 DNA Ligase (NEB), 1.5 µL of vector DNA and 6 µL insert DNA in 1 x T4 DNA Ligase buffer as supplied. Reactions were run for 30 minutes at room temperature. Subsequent transformation of DH5α bacteria used 5 µL of ligation product.

2.2.1.6. Transformation of Bacteria

Competent DH5α cultures were thawed from -80°C storage on ice and received 0.02 M β-mercaptoethanol (Fluka). After 15 minute incubation on ice, 100 ng of plasmid DNA or 5 µL of ligation product for amplification was added to culture, followed by a further 30 minute incubation on ice. DH5α transformation performed via 45 second heat shock at 42°C followed by immediate 5 minute incubation on ice. Cultures were fed 400 µL LB medium and incubated at 37°C (shaking vigorously at 200 rpm) for one hour for sufficient expression of plasmid to confer antibiotic resistance. 50-100 µL of culture seeded on to LB Agar plates

(see Prepared Reagents) containing appropriate selective antibiotic. Cultures were incubated overnight at 37°C.

Transformed DH5α colonies on agar plates selected for suspension culture. One colony grown in 5 mL LB medium (with selective antibiotic) at 37°C for 6-8 hours before being fed 95 mL fresh LB medium (again containing selection antibiotic) and grown overnight at 37°C (shaking vigorously). Plasmid isolated from bacterial suspension using PureLink MaxiPrep kit (unless stated otherwise, all reagents from Sigma) according to instructions. The purified DNA concentration was measured by spectrophotometric analysis using the NanoDrop 2000 (Thermo Scientific) and purity measured using 260/280 ratio (1.8-2.2 considered sufficiently 'pure'). Plasmid DNA stored at -20°C until use.

2.2.2. Cell culture techniques

The following section describes the general techniques used to maintain cell lines and to treat with cytokines and other agents. Other *in vitro* assays, and the specific preparation of cells required for them will be described in later sections.

2.2.2.1. Initiation of mammalian cell lines

Cell stocks, stored in 1 mL Foetal Bovine Serum (FBS, Sigma) with 10% Dimethylsulphoxide (DMSO, Sigma), were initiated from liquid nitrogen stores. Cells were thawed by placing vials in lukewarm water and immediately added to 9 mL Dulbecco's modified Eagle's medium (DMEM, Invitrogen) before centrifugation and aspiration of supernatant to remove DMSO. Cell pellets were resuspended in 13 mL DMEM and seeded onto a 10 cm diameter culture dish (TPP).

2.2.2.2. Cultivation of mammalian cells

All mammalian cell lines, listed in **Table 2.2**, were grown in DMEM, containing 10% Foetal Calf Serum (Sigma) and 0.5% Penicillin/Streptomycin (Sigma) at 37°C in humidified 5% (v/v) CO2 atmosphere. Cells were cultured in 10 cm diameter culture dishes (TPP) at a volume of 13 mL per dish. Cells confluency was inspected by light microscopy every 48 hours. Cultures over 70% confluent were passaged in order to avoid changes in cell behavior through environmental pressure caused by high or low cell density. Cells were washed once with Phosphate Buffered Saline (PBS, Sigma) to remove any traces of DMEM prior to incubation at 37°C in Trypsin (Sigma) for approximately 1 min. Cells were completely detached by agitation and the activity of trypsin terminated by addition of fresh DMEM (in order to achieve a dilution of 1:[confluency/10]). 1 mL of the resulting cell solution was seeded onto a new tissue culture plate with 12 mL fresh DMEM and returned to 37°C. In the instances of a low observed confluency (<70%), cells were washed once with 10 mL PBS and fed 13 mL fresh DMEM, inspected ~24 hours later until over 70% confluent prior to passage.

2.2.2.3. Preparation of frozen cell stocks

Cell cultures were grown to a confluence of around 80%. Cells were subsequently washed with 10 mL PBS and incubated with Trypsin to facilitate detachment. Detached cells were subjected to 300 x g for 10 minutes (room temperature) using centrifugation to form a pellet. Cells were then resuspended 3 mL of a 'freezing mixture' consisting of 10% (v/v) DMSO in FBS, before being rapidly aliquoted into 1 mL cryo-vials. The cells were then stored at -80°C in an isopropanol filled cryo-freezing container overnight. The following day, frozen cell samples were transferred into liquid nitrogen storage.

2.2.2.4. Transfection of cells

Cells were prepared for transfection during passage. Following detachment by trypsin and initial dilution with complete DMEM, 15 µL sample of cell solution was loaded into a haemocytometer cell counting chamber for estimation of cell concentration. Cells were diluted to 1 x 10^5 cells/mL and seeded on to 12-well tissue culture plates (1 mL per well). Cells for fluorescent microscopy analysis were seeded onto 12-well plates with coverslips. Cells were incubated at 37°C overnight. Cell confluency inspected prior to transfection (within 50-70% was considered optimal, in accordance with supplier recommendations). In accordance with Lipofectamine LTX/Plus supplier protocol (ThermoFisher), the Plus reagent (3 µL per well) was incubated at room temperature for 15 minutes, with serum and antibiotic-free DMEM (50 µL per well) and DNA (0.5 µg per well) to allow reagent-DNA complex formation. In an equal volume of serum-free DMEM, Lipofectamine LTX (3 µL per well) was diluted to form a second mixture. The two mixtures were then mixed and incubated together for a further 15 minutes at room temperature. Cell culture medium was then replaced with fresh complete DMEM (0.9 mL per well) and transfection mixture (100 µL per well). Cells incubated at 37°C and transfection efficiency inspected after 24 and 48 hours. Transfection efficiency could be estimated using fluorescent microscopy of live cell cultures prior to performing stimulation assays. Optimum transfection efficiency (on average ~40% of total cells) was found to take place following approximately 48 hours incubation in transfection complex containing medium. The generation of reconstituted U6A cells with stable transfections is detailed in Ho et al, 2016 and was achieved by growth in selection medium; whole DMEM containing 400 µg/mL G418 (A1720) following transfection with pEYFP-N1 STAT2 or pEYFP-N1 STAT2 L82A.

2.2.2.5. Treatment of cells

The standard interferon treatment of cells consisted of either IFN-γ (at 50 U/mL) or IFN-β (at 500 U/mL) in DMEM for one hour at 37°C. Other treatments used in this work include Ratjadone (Calbiochem), Puromycin (Invitrogen) and LPS (Sigma). Unstimulated controls were included in every experiment and were simultaneously fed fresh DMEM without IFN or treatment reagent. Concentrations and exposure times for specific assays are detailed with their respective results.

2.2.2.6. Isolation of peritoneal cells from mice

STAT2 -/- or wildtype mice were sacrificed by UK Home Office approved schedule one procedure. Subsequently, the peritoneal cells were isolated by lavage procedures as described by (Ray and Dittel, 2010). Briefly, the peritoneal membrane was exposed and a 27g needle was used to inject 5 mL of ice-cold PBS containing 3% (v/v) FBS. The peritoneum was gently massaged to facilitate the detachment of cells from internal organs prior to the extraction of the cell suspension using a 25g needle. Cells were then pelleted by centrifugation at 400 x g for 5 minutes (4°C) and resuspended in either PBS or complete DMEM (as previously defined in **2.2.2.2**).

2.2.2.7. Maintenance of *Toxoplasma gondii*

Toxoplasma gondii were provided by Dr Gereon Schares. The growth and purification of tachyzoites was performed as described by (Elsheikha et al, 2006). In short, the parasite was maintained within a host mammalian cell line, specifically Madin-Darby Canine Kidney (MDCK) cells, in DMEM supplemented with 5% FBS, 2 mM glutamine, and 1% (v/v) antibiotic-antimycotic solution (Gibco). Purification of *T. gondii* from their feeder cell cultures was achieved by passage through PD-10 desalting columns followed by centrifugation at 1000 × g. The parasite pellet was subsequently resuspended in fresh culture medium and counted with an improved Neubauer haemocytometer.

2.2.3. Preparation and fluorescent analysis of fixed cells

For microscopic analysis, cells were grown on sterile glass coverslips. Following transfection and treatment, cells were washed once with PBS (1 mL per well). Fixation of cells was subsequently carried out via 15 minute incubation (room temperature) in ice-cold methanol (0.5 mL per well, Fisher-Scientific). Methanol was removed via three washes with PBS (0.5 mL per well) prior to one wash in distilled H_2O. Cells used in GFP single and YFP/CFP co-stransfection experiment were subsequently mounted onto slides using FluorPreserve reagent (Merck Millipore) and stored in away from light (4°C).

For immunofluorescent assays, cells were grown, treated and fixed as above. Cells were then blocked for 1 hour (4 °C) in 20 % (v/v) FBS in PBS. Endogenous proteins were then labelled one of the following primary antibodies: 0.4 µg/ml anti-STAT2 (sc-476), 0.2 µg/ml anti-STAT1 (sc-345), 4 µl/ml anti-STAT1 (phospho-Tyr701) (#7649) or 5 µg/ml anti-HP1γ (phospho-Ser93) (ab45720). Incubation with primary antibodies was performed in 20 % (v/v) FBS in PBS overnight at 4°C. Unbound primary antibody was washed from cells three times using PBS. This was followed by Cy3-decoration with the appropriate species-specific secondary antibody at a concentration of 0.75 µg/mL in 20 % (v/v) FBS/PBS solution for 1 hour (room temperature). Excess secondary antibody was removed by a further two washes

with PBS before nuclei were counterstained using 5 µg/ml Hoechst 33285 (Sigma) for 5 minutes and coverslips mounted onto slides as described previously.

The slides were examined by conventional wide-field indirect immunofluorescence using a Zeiss Axioplan 2 microscope and Axiocam CCD camera with the following filter settings: DAPI/Hoechst, excitation (ex) 359 nm/emission (em) 461 nm; Cy3 ex 595 nm/em 620 nm; and YFP, ex 520 nm/em 532 nm. The acquisition and export of images from this microscope was achieved utilising the AxioVision 4.7 software.

Alternatively, deconvolution microscopy was performed using the DeltaVision Elite microscope (GE Lifesciences) in conjunction with a CoolSNAP HQ2 CCD camera (Photometrics). In this case the following filter sets were used to detect: CFP, ex 438 nm/em 470 nm; YFP, ex 513 nm/em 559 nm; Cy3, ex 575 nm/em 632 nm; and DAPI/Hoechst, ex 390 nm/em 435 nm. Image acquisition and automatic deconvolution of images were achieved using the Resolve 3D software from softWoRx.

2.2.4. Whole Cell Extraction for Immunoblotting

Following the completion of cell treatments, culture medium removed and cells were washed once with ice-cold PBS. Whole Cell Extraction (WCE) buffer supplemented with a cocktail of phosphatase and protease inhibitors was then applied to cultures. 120 µL of supplemented WCE buffer was added to each well (of a 12 well plate). Cells were subsequently detached from well surface via scraping and agitation via gentle pipetting up and down. Cell suspensions were transferred to pre-cooled 1.5 mL microtubes and incubated on ice for 30 minutes to enable cell lysis to occur. Insoluble protein was pelleted by centrifugation at 16,000 x g for 15 minutes (4°C). 90 µL of supernatant was extracted and either utilised for Bradford assay or denatured via 5 minute 95°C incubation with 1 x SDS protein sample buffer and stored at -20°C prior to SDS-Polyacrylamide gel electrophoresis.

2.2.5. Low-Salt Whole Cell Extraction for Immunoprecipitation

Cells for immunoprecipitation were lysed in a low salt buffer in order to preserve protein structure and protein-protein interactions. Cultures were grown in a 10 cm dish and treated as described in **2.2.2.5** prior to a single wash with ice-cold PBS. Supplemented low salt WCE buffer was added to dishes prior to scraping cells from dish and transferring to pre-cooled 1.5 mL microtubes. Cell suspensions were incubated on ice for 5 minutes before manual lysis was performed using a Teflon dounce homogenizer. The lysates were incubated for a further 10 minutes on ice. Insoluble protein was pelleted via 5 minute centrifugation at 16,000 x g (4°C). The majority (90%) of the sample was snap frozen on dry ice prior to immunoprecipitation experiments. The remaining 10% was utilised for either Bradford assay

to assess protein concentration or boiled for 5 minutes at 95°C in 2 x SDS loading buffer for immunoblot analysis and input control.

2.2.6. Bradford quantification of protein concentration

In a 96-well plate, 5 µL whole cell extract samples prepared in duplicate, in 45 µL sterile distilled H_2O. Standard protein solutions prepared in duplicate using 50 µL sterile distilled H_2O containing known concentrations of bovine serum albumin. Samples and standard solutions received 50 µL Bradford reagent (Bio-Rad), diluted 1:3 in sterile de-ionised H_2O and thorough mixing. Protein concentration analysed via spectrophotometry on SpectraMax 340pc plate reader (Molecular Devices). Results obtained from known standards used to form a standard curve, concentrations of samples were calculated using the formula for line of best fit of the standard curve.

2.2.7. SDS-Polyacrylamide Gel Electrophoresis (SDS-PAGE)

Cell extracts were separated by electrophoresis through SDS-polyacrylamide gels. Casting gels with 10% acrylamide concentration prepared from 30% acrylamide/bisacrylamide (Sigma) diluted with de-ionised H2O and casting gel buffer (see Prepared Reagents). Immediately prior to casting, 20 µL TEMED (N,N,N',N'-Tetramethylethylediamine, Sigma) and 0.01% (w/v) ammonium persulphate (APS, Fluka/Sigma) was added to initiate polymerisation of the gel. After polymerisation of casting gel was complete, stacking gel was prepared, layered on top. Stacking gel consisted of 30% acrylamide/ bisacrylamide diluted to a final concentration of 3.3% with de-ionised H2O and stacking gel buffer (see Prepared Reagents). Polymerisation was initiated prior to casting by addition of 20 µL TEMED and 0.02% (w/v) APS. 50 µg of protein samples (with SDS protein sample buffer) was loaded into gel (calculated using results from Bradford Assay). 3 µL pre-stained molecular weight marker, SeeBlueTM Plus2 (Invitrogen) was used to indicate molecular weight. Electrophoresis was run in Protean® II electrophoresis chamber (Bio-Rad) with SDS running buffer (see Prepared Reagents) and using power supply, EPS E835 (Consort). Electrophoresis was run at 120V to pull samples through stacking gel, and then run at 180V for 45-55 minutes until loading dye began to exit casting gel. Separated protein samples transferred from gel onto nitrocellulose membrane (Protran, Whatman) using Trans-Blot SD Semi-Dry Transfer Cell-System (Bio-Rad). Gel laid on top of nitrocellulose membrane (GE Healthcare) and 'sandwiched' between filter paper soaked in 1 x SDS Transfer Buffer prior to transfer under 18V for 50 minutes using EPS E802 power supply (Consort). Following transfer, membranes incubated for 1 hour (room temperature) in blocking solution.

2.2.8. Protein detection and immunoblot analysis

The detection of proteins on immunoblot membranes was performed following the blocking stage described in **2.2.7.** Primary antibody solutions were prepared at a standard dilution of 1:1000 in 8 mL Tris-Buffered Saline with Tween (TBS-T). Membranes incubated in primary antibody solutions for either 1 hour (room temperature) or overnight (4°C). Unbound primary antibody was removed by washing the membrane three times in TBS-T for 8 minutes. Immunoblots were then incubated with appropriate species-specific IRDye 800CW (LiCor) or AlexaFluor 680 (ThermoFisher) conjugated secondary antibodies, diluted 1:10000 in TBS-T, for 30 minutes (room temperature). Unbound secondary antibody removed following three washes with TBS and one with distilled H2O. Immunoblots were subsequently scanned using Odyssey Infrared Imaging System (LI-COR Biosciences). Prior to re-blotting of membranes with different primary antibodies, membrane-bound antibody complexes were removed via 2 x 20 minute incubations in stripping buffer (65°C). Membranes rinsed 3 x with TBS and incubated at room temperature in blocking solution, followed by 3 more TBS rinses before application of new primary antibody.

2.2.9. Immunoprecipitation

For STAT1 immunoprecipitation experiments, HEK 293T cells were transfected with expression vectors for untagged STAT2 and FLAG-tagged STAT1 variants. Transfected confluent cell were cultured on a 10 cm dish and were left either untreated or treated for 1 hour with 500 U/ml IFN-β. Extraction of samples for immunoprecipitation was performed as described in **2.2.5**. The fraction of the WCE extracts that was not snap frozen for immunoprecipitation was used in quantitative immunoblot experiments in order to measure the expression of the different FLAG-tagged constructs. This data was used to normalise the FLAG-tagged protein content of the immunoprecipitation reactions. Anti-FLAG M2 magnetic beads (Sigma) were equilibrated to the IP buffer for 1 hour (4°C) before the immunoprecipitation reaction was performed. The snap frozen fractions were thawed and FLAG concentration appropriately normalised with WCE extracts of untreated HEK-293T cells. Each 1 mL immunoprecipitation reaction contained 40 µL of the equilibrated anti-FLAG beads and 500 µg of protein sample, incubated together on a slow rotation for 4 hours (4°C). Magnetic beads and bound protein were isolated from the supernatant and washed twice with fresh IP buffer. Bound proteins were released from beads via re-suspension in 2 x SDS loading buffer and subsequent boiling at 95°C. Beads were pelleted by centrifugation at 16,000 x g for 2 minutes. The protein containing supernatant was then run alongside the input control in SDS-PAGE and immunoblotting assays.

2.2.10. Nitric oxide (NO) assay

Immortalized mouse macrophages were seeded into 10 cm tissues culture plates at a density of 1 x 10^6 cells/well. Cultures were then left to grow in full DMEM growth medium or were primed in growth medium containing 0.5 U/ml IFN-γ for 48 hours. Cells were subsequently washed with PBS, detached and seeded onto 96-well plates at a density of 1 x 10^4 cells/well. Cells were incubated in triplicate for further 36 hours in growth medium without or with IFN-γ and/or LPS as indicated. NO production was subsequently assessed by nitrite determination using Griess assay (Promega) according to manufacturer's instructions. Briefly, 50 µL of cell culture medium was transferred to a new 96-well plate. In addition, a set of standard samples was prepared using the provided 100µM nitrite ranging from 100 µM to 1.56 µM. Sequential addition of sulfanilamide and N-1-napthylethylenediamine dihydrochloride (NED, both Promega), separated by 10 minute incubation at room temperature, and resulted in a straw-yellow colour which shifted to become a pink with an increased presence of NO. The samples were measured by spectrophotometry using a SpectraMax 340pc plate reader (Molecular Devices) using a filter set to 545 nm. Nitric oxide concentration was calculated using the standard curve produced by the nitrite samples.

2.2.11. IFN-γ anti-parasitic activity assay

Macrophages and U6A cells were plated on poly-L-lysine (Sigma) coated 24-well culture plates at a density of 4 x 10^4 cells per well. Cells were then grown in 1 mL full DMEM growth medium for 15 hours. Prior to exposure to parasite, cells were left untreated or treated for 48 h with IFN-γ at various concentrations in triplicate wells. Tachyzoites, cultured and purified as described in **2.2.2.7**, were then added to cell cultures at a multiplicity of infection (MOI) of 3. Cells were incubated for 5 hours at 37°C in IFN-free growth medium, in order to permit parasite entry, following which any unattached parasites were washed away with PBS. The infected cell cultures were fed 1 mL fresh DMEM growth medium that contained the same IFN-γ concentration as before. 100 µL samples of infected cell culture supernatant were taken at the indicated time points and extracellular parasite load was calculated using a Neubauer haemocytometer. Supernatant sampling of infected cultures was immediately followed by the replacement with the appropriate growth medium such that IFN-γ concentrations were maintained. Data from at least two biological replicates were evaluated per well, and averages were calculated.

2.2.12. Fluorescence assisted cell-sorting (FACS)

Following the indicated treatment or isolation of cells, Fc receptor blocking was performed for 5 minutes in ice-cold PBS containing 0.2% heat-inactivated mouse serum (MS, Sigma).

Cells were subsequently spun at 300 x g for 5 minutes (4°C) and resuspended in the 0.2% MS/PBS solution. 100 µL antibody reactions containing ~2.5 x 10^5 cells were prepared in this buffer and incubated at room temperature for 20 minutes. The following antibody concentrations were used to detect MHC class II expression on immortalised mouse macrophages; 4 µg/mL Alexa Fluor-488 rat anti-mouse IA/I-E or 4 µg/mL Alexa Fluor-488 rat IgG2b,k isotype control. Detection of MHC class II expression on primary mouse macrophages isolated using peritoneal lavage was performed using either 4 µg/mL PerCP rat anti-mouse IA/I-E or PerCP rat IgG2b,k isotype control in conjunction with 4 µg/mL Alexa Fluor-488 rat anti-mouse F4/80. The detection of human MHC Class I on U6A cells were similarly performed using 3.2 µg/ml APC-conjugated anti-human HLA-A,B,C or APC-conjugated mouse IgG2a,k isotype control. The detection of early apoptosis and necrosis was performed using the FITC Annexin V Apoptosis Detection Kit (#640914) as described by the manufacturer Biolegend, with the exchange of Biolegend's cell staining buffer for 0.2% MS/PBS. Immediately before FACS using FC500 (Beckman-Coulter) or LSRII flow cytometers (Beckman-Coulter), cell suspensions were passed once through a 20G needle on a 1 ml syringe. FACS data were processed using Kaluza analysis software (Beckman Coulter, version 1.3), in all analyses cells were gated for viability using forward and side scatter patterns with the same gate used consistently for each cell type.

2.2.13. Statistical analyses

The statistical significance of data in this work was calculated by Student's t-test (* denotes $p < 0.05$; ** $p < 0.01$; and *** $p < 0.001$; n. s. denotes $p > 0.05$) using GraphPad Prism 5.03 (GraphPad).

3. Results

STAT2 binds to and alters STAT1 subcellular distribution before and during IFN signalling.

3.1. Introduction

STATs are latent transcription factors that shuttle between the nucleus and cytoplasm. This is a key property of this family of proteins as they must be accessible to receptors at the cell surface and also reach target genes within the nucleus. Cytokines trigger the activation of STATs that subsequently results in their nuclear accumulation, allowing them to initiate gene transcription. Following the termination of the signal the STAT proteins are inactivated and redistribute throughout the cell in preparation for further signalling. Whilst many of the mechanisms that govern this nucleocytoplasmic shuttling behaviour have been studied, several aspects require further investigation. For example, the distribution of STAT proteins varies not only between the individual members but also in a cell-type specific manner. Both the cause and consequences of this are not yet fully understood.

STAT1 and STAT2 are intrinsically linked to interferon signalling. Interferon binding to their receptors results in recruitment of STATs to the receptor and its associated JAK. This results in phosphorylation of a key tyrosine residue at the amino-terminal end of the transactivation domain. Following this modification, STATs are activated and carry the signal from the cell surface to the nucleus, where they facilitate the transcription of genes by binding to specific sequences within their promoter regions. In response to both type I and type III interferon, STAT1 and STAT2 form heterodimers that incorporate a third protein, IRF9, to form the ISGF3 complex. This complex accumulates within the nucleus of cells and drives transcription. In contrast, type-2 IFN activates STAT1 alone. In this case, it is a STAT1 homodimer that drives the transcriptional response whilst STAT2 is considered to be inert.

It is now widely accepted that most STATs exist as dimers prior to cytokine signalling. This inherent dimerisation is dependent on interactions between the amino-terminal domains and is termed the anti-parallel conformation. STAT2 is the exception to this model as there is no physiologically relevant evidence that it can form homodimers, even after activation. This chapter explores the potential for STAT2 to bind to its most notable partner, namely STAT1, before IFN stimulation and during type-2 IFN signalling when STAT1 is activated but STAT2 is not. The biological consequences of STAT1-STAT2 hetero-dimerisation for type-2 IFN signalling *in vitro* is investigated and discussed in **Chapter 4**. Some characterisation of STAT1-dependent immune responses in a genetically modified mouse strain that lacks STAT2 is described in **Chapter 5**.

3.2. Effect of STAT2 on the subcellular distribution of STAT1 before IFN signalling

STAT1 and STAT2 have both been shown to constantly shuttle between the nucleus and cytoplasm of cells. Despite this, the amount of STAT within each compartment can vary depending on the STAT and the cell type. STAT2 is observed almost exclusively in the cytoplasm due to a strong NES in the carboxyl-terminal domain, whilst STAT1 can be observed in both the cytoplasm and nucleus in many cell types. In light of this differential distribution, it was hypothesised that if STAT1 and STAT2 interact prior to IFN they could influence the subcellular distribution of one another.

3.2.1. STAT1 shows an altered distribution in cells lacking STAT2

A vital tool in early IFN research was the development of mutant cell lines lacking separate components of the Jak-STAT pathway. These mutants were derived from a human fibrosarcoma cell line, 2fTGH, which contains the *E. Coli* gene *gpt* upstream of an IFN-inducible gene (McKendry et al, 1991). Chemical mutagenesis followed by selection with type-1 IFN and 6-thioguanine allowed the establishment of mutant cell lines that were unresponsive to IFN. One of the cell lines generated, U6A, has lost IFN responsiveness specifically because it does not express STAT2. To elucidate whether STAT2 has an influence on the subcellular distribution of STAT1, a comparison of the two cell lines was performed.

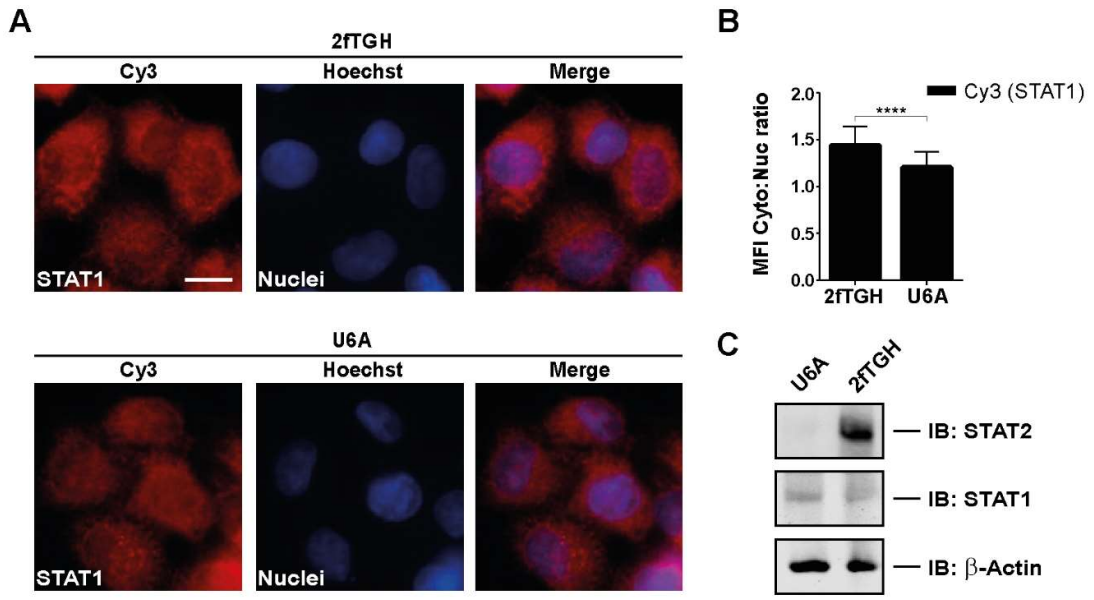

Fig 3.1 *Altered subcellular distribution of STAT1 in cells lacking STAT2* **A -** Fluorescent microscopy showing the subcellular distribution of STAT1 detected by Cy3-decorated anti-STAT1 antibody, nuclear counterstained with Hoechst. Scale bar = 10 µm **B** – The cytoplasmic: nuclear ratio of mean fluorescent intensity of Cy3-decorated STAT1 in cells was measured by line scan analysis. Data represents at least 25 cells from 2 independent experiments. **C** – Whole cell extracts from U6A and 2fTGH lines were analysed by western blot using anti-STAT1, and anti-STAT2 antibodies. Protein loading was confirmed by re-probing with anti-β-Actin antibody.

Subcellular distribution of proteins can be determined by immunofluorescence; a technique that involves the detection of a target protein in fixed cells using antibodies. 2fTGH and U6A cells were fixed and permeabilised in ice-cold methanol. STAT1 was then detected via incubation with anti-STAT1 antibody and subsequent decoration with a secondary antibody conjugated to the fluorophore Cy3. Wide-field fluorescent microscopy was used to visualise the distribution of STAT1 in 2fTGH and U6A cells (**Figure 3.1A**). Fluorescence intensity can be measured and subsequently approximated to protein concentration.

The intensity of Cy3-fluorescence was used to compare the STAT1 concentration within the cytoplasm and nucleus of a given cell. The nucleus was identified by counterstaining with Hoechst, which intercalates with DNA and emits a different wavelength to Cy3 (**Figure 3.1A**). The mean Cy3 intensity within a cell cytoplasm was divided by the respective intensity in the nucleus to calculate a ratio of fluorescence. This was used as a proxy for the distribution of STAT1 within each cell line, with values above 1 indicating an increased cytoplasmic STAT1 concentration compared to the nucleus. When analysed in this way, STAT1 distribution was

more cytoplasmic in the 2fTGH (approx: 1.4) cells compared to the STAT2 deficient U6A (approx: 1.2, **Figure 3.1B**). Despite showing a less cytoplasmic distribution in the U6A cells, STAT1 nonetheless had a cytoplasmic:nuclear ratio above 1, indicating a higher amount of STAT1 in the cytoplasm compared to the nucleus. Finally, western blot analysis was used to confirm the lack of STAT2 in the U6A cell line (**Figure 3.1C**) as described by McKendry and colleagues (1991).

3.2.2. STAT1 co-localises with STAT2 within the cytoplasm of resting cells

Following the observation that cells lacking STAT2 expression show an altered subcellular distribution of STAT1, this phenomenon was characterised by overexpression in Hela-S3 cells of STAT1 and STAT2, conjugated to cyan (CFP) and yellow (YFP) fluorescent proteins respectively. HeLa-S3 cells were transfected with either STAT1-CFP or STAT2-YFP alone or in combination.

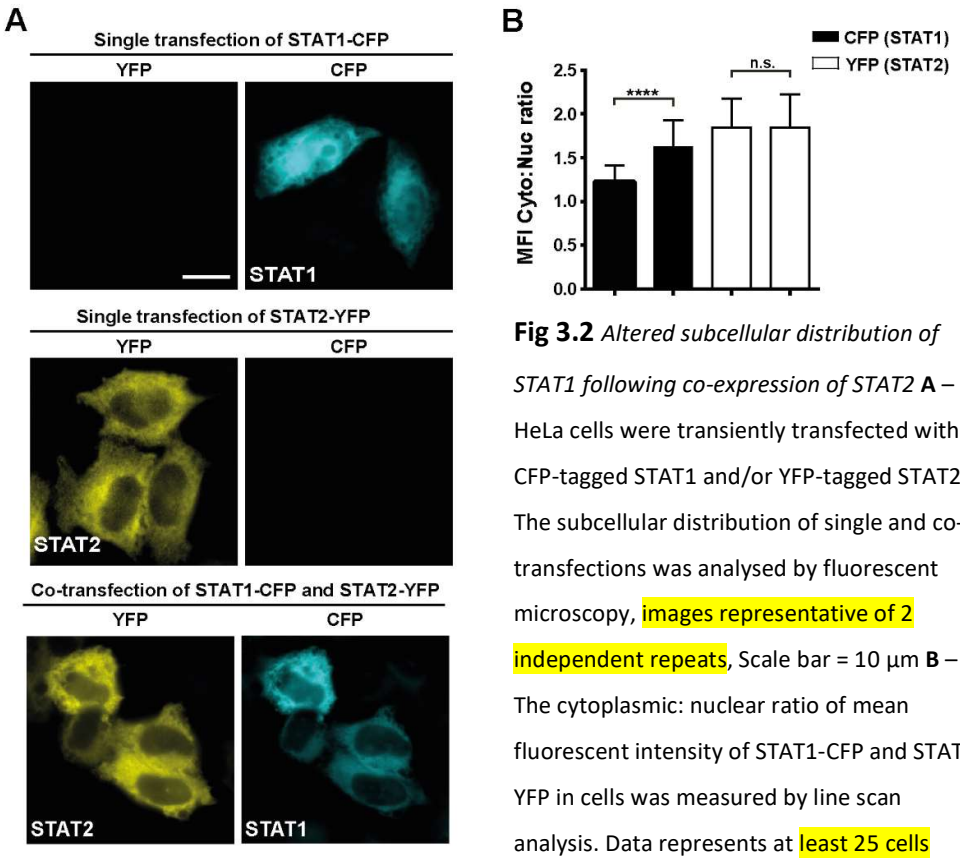

Fig 3.2 *Altered subcellular distribution of STAT1 following co-expression of STAT2* **A** – HeLa cells were transiently transfected with CFP-tagged STAT1 and/or YFP-tagged STAT2. The subcellular distribution of single and co-transfections was analysed by fluorescent microscopy, images representative of 2 independent repeats, Scale bar = 10 µm **B** – The cytoplasmic: nuclear ratio of mean fluorescent intensity of STAT1-CFP and STAT2-YFP in cells was measured by line scan analysis. Data represents at least 25 cells across 2 independent experiments. **** = $p<0.001$, n.s = $p>0.05$.

Fluorescence microscopy of fixed cells revealed that STAT1 was present throughout the cell, in both the nucleus and cytoplasm (**Figure 3.2A, upper panels**). In contrast, STAT2 was primarily located within the cytoplasm of cells (**Figure 3.2A, middle panels)**. STAT2 is predominantly present in the cytoplasm of cells due to a strong NES contained within the C terminal domain (Reich and Banninger, 2004). In addition, single transfection experiments confirmed that YFP and CFP-tagged proteins were spectrally distinct. In cells expressing both STAT1-CFP and STAT2-YFP, co-localisation of the proteins within the cytoplasm of the cell was observed (**Figure 3.2A, lower panels).**

As in **Figure 3.1**, line scan analysis of micrographs was performed to quantify the changes in STAT1 and STAT2 distribution. STAT2 was found to have the highest cytoplasmic:nuclear ratio and this distribution was unaffected by the co-expression with STAT1 (**Figure 3.2B**). In contrast, whilst STAT1-CFP already showed a slightly higher concentration within the cytoplasm compared to the nucleus (approx. 1.2, **Figure 3.2B**), co-expression with STAT2-YFP significantly shifted the ratio further above 1.2 to approximately 1.6, thus confirming that STAT2 was capable of altering the subcellular distribution of STAT1.

3.2.3. Subcellular redistribution of STAT1 by STAT2 requires CRM1-dependent export signal in the C terminal domain

The co-localisation of STAT1 and STAT2 occurs within the cytoplasm of cells (**Figure 3.2A**). Although it is constantly shuttling between the cytoplasm and nucleus, STAT2 is actively transported from the nucleus to the cytoplasm in resting cells in a CRM1-dependent manner which results in the vast majority of STAT2 existing within the cytosol of cells. CRM1 can be inhibited by small molecule ratjadone or leptomycin B (Meissner et al, 2004) and causes the distribution of STAT2 to change from a cytoplasmic to pancellular state (Frahm et al, 2006). HeLa cells expressing STAT2-YFP were treated with ratjadone for up to 6 hours before fixation and visualisation of STAT2 distribution. STAT2-YFP presence within the nucleus increased after at least 4 hours (**Figure 3.3A**), in line with behaviour previously described in the literature (Frahm et al, 2006).

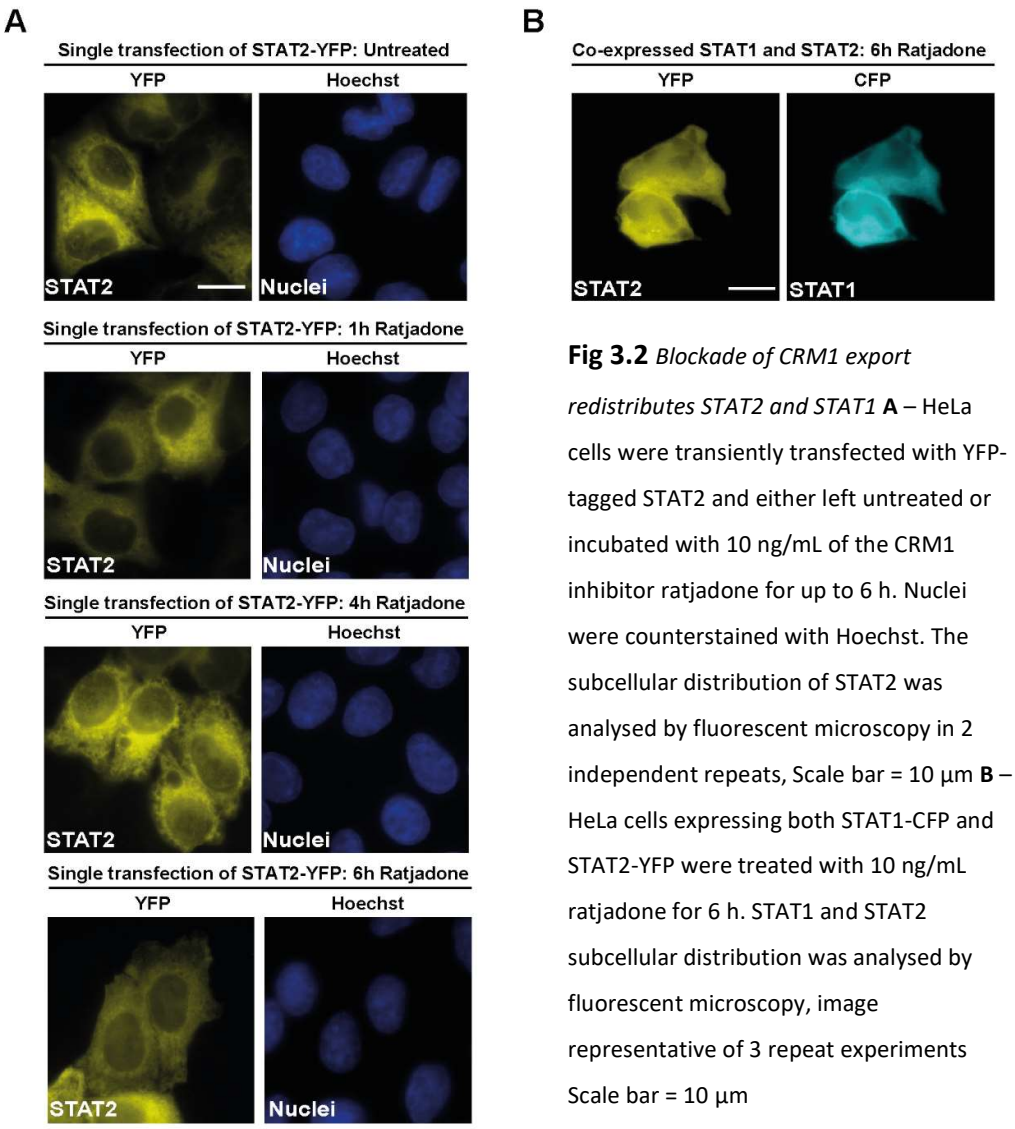

Fig 3.2 *Blockade of CRM1 export redistributes STAT2 and STAT1* **A** – HeLa cells were transiently transfected with YFP-tagged STAT2 and either left untreated or incubated with 10 ng/mL of the CRM1 inhibitor ratjadone for up to 6 h. Nuclei were counterstained with Hoechst. The subcellular distribution of STAT2 was analysed by fluorescent microscopy in 2 independent repeats, Scale bar = 10 µm **B** – HeLa cells expressing both STAT1-CFP and STAT2-YFP were treated with 10 ng/mL ratjadone for 6 h. STAT1 and STAT2 subcellular distribution was analysed by fluorescent microscopy, image representative of 3 repeat experiments Scale bar = 10 µm

The effect of CRM1-dependent export inhibition on the STAT1 and STAT2 co-localisation was investigated. HeLa cells expressing both STAT1-CFP and STAT2-YFP were treated for 6 hours with ratjadone. As seen in the single transfections STAT2-YFP was detected throughout the cell rather than restricted to the cytoplasm (**Figure 3.3B**, left). Concurrently, STAT1-CFP was also localised in both the nucleus and cytoplasm of cells following CRM1-export block - (**Figure 3.3B**, right). Thus the redistribution of STAT1 to the cytoplasm in the presence of STAT2 observed in **Figure 3.2A** required nuclear export.

STAT2 is recognised by the CRM1 export machinery due to a NES located within the C terminal domain (Banninger and Reich, 2004). The mutation to alanine of two lysine residues at position 737 and 741 within the C terminal domain of STAT2 has been shown to

inactivate the NES and result in an even distribution of STAT2 throughout the cell (Frahm et al, 2006). A YFP-tagged STAT2 containing the two point mutations of these residues was produced to create the STAT2-ΔNES. In addition, a truncated STAT2 (aa 1-702) that lacked the C terminal domain entirely was also constructed and termed STAT2-ΔC (**Figure 3.4A**). The distribution of these STAT2 variants in HeLa cells was observed by fluorescence microscopy. In comparison the WT, the STAT2-ΔNES showed a similar cytoplasmic distribution (**Figure 3.4B**, middle panels) which was in contrast to the results described in the literature. The truncated STAT2 (STAT2-ΔC), however, was clearly present in both the cytoplasm and nucleus of transfected cells (**Figure 3.4B**, lower panels).

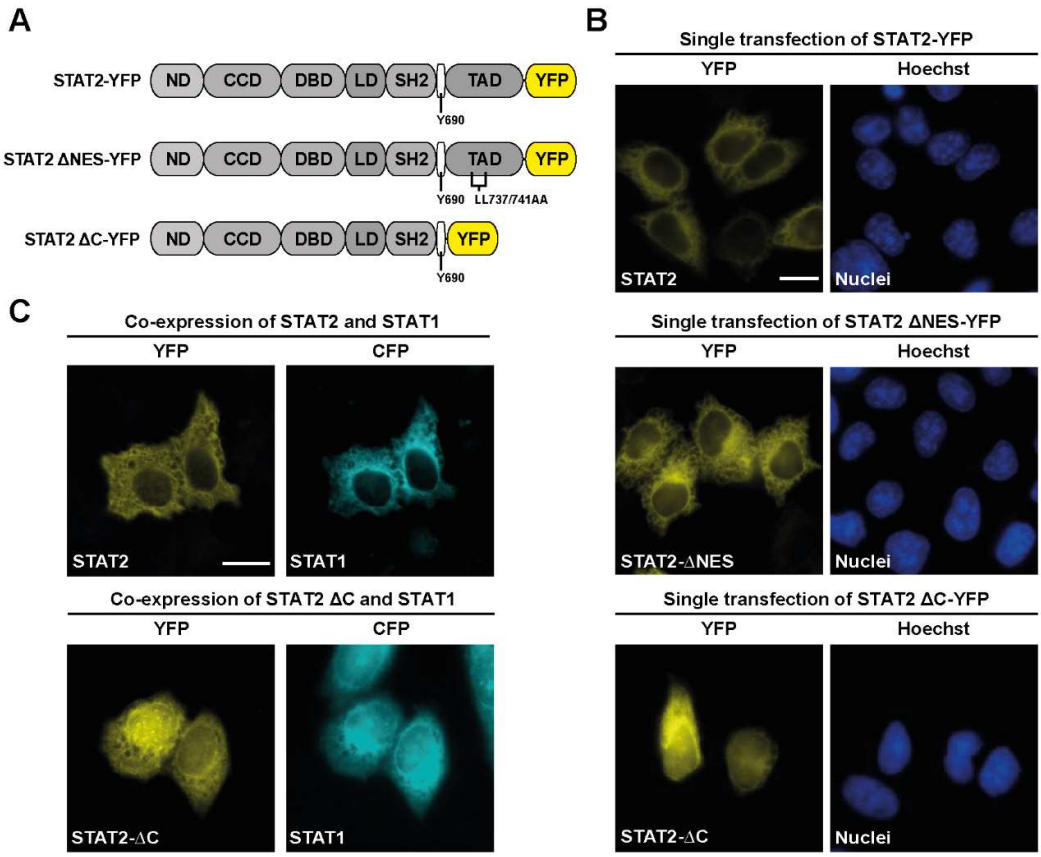

Fig 3.4 *Cytoplasmic co-localisation of STAT2 and STAT1 is dependent on the C-terminal domain of STAT2* **A –** Schematics of STAT2-YFP fusion variants used **B** – Fluorescent microscopy showing the resting subcellular distribution of STAT2-YFP constructs expressed in HeLa cells. Nuclei counterstained with Hoechst. Scale bar = 10 µm **C** – CFP-tagged STAT1 was co-expressed in HeLa cells with either YFP-tagged STAT2 or truncated (aa 1-702) STAT2 ΔC. Subcellular distribution of constructs were determined by fluorescence microscopy. Scale bar = 10 µm. All images are representative of a least 2 experimental repeats.

YFP-tagged STAT2 and truncated STAT2 ΔC were co-expressed with STAT1-CFP in HeLa cells and the subcellular distribution of both proteins was observed by fluorescence microscopy. As seen in **Figure 3.2A**, wild type STAT1 and STAT2 co-localised within the cytoplasm of cells (**Figure 3.4C**, upper panels). However, in cells expressing the truncated STAT2 ΔC, STAT1 and STAT2 were present in both the cytoplasm and nuclei (**Figure 3.4C**, lower panels). To this end, the redistribution of STAT1 to the cytoplasm in the presence of STAT2 was dependent on both CRM1 and the C-terminal domain of STAT2.

3.2.4. STAT1 co-localisation with STAT2 is dependent on key residues in their respective N domains

STAT proteins can dimerise independent of cytokine signalling through mutual interactions of their N domains (Mao et al, 2005) although observations of this phenomenon have thus far been restricted to homodimers. Several point mutations within STAT1 have been identified that disrupt activation-independent homodimer formation, including Phe77Ala and Leu78Ala within the N domain and a Phe172Trp mutation in the coiled-coil domain (Chen et al, 2003). In particular, the Phe77 residue is believed to reside within an interaction interface of the N-domains and contributes to the polymerisation of STAT1 both upon DNA promoter regions and within the nucleoplasm (Begitt et al, 2014; Droscher et al, 2011).

To investigate whether the co-localisation of STAT1 and STAT2 observed in cells could be affected by loss of STAT1 N-domain interface, CFP-tagged STAT1 Phe77Ala (F77A) was co-expressed with STAT2 (**Figure 3.5B**). In contrast to wild type STAT1 which was redistributed to the cytoplasm (**Figure 3.2A**), STAT1 F77A was present in both the nucleus and cytoplasm of cells regardless of the presence of STAT2 (**Figure 3.5B**). As with co-expression with wild type STAT1, the STAT2 distribution was unaffected by the presence of STAT1 F77A. The cytoplasm: nuclear ratio of both CFP and YFP was determined by line scan analysis and used to quantify the subcellular distribution of the proteins. CFP-tagged STAT1 F77A showed a slightly cytoplasmic distribution similar to wild type STAT1 (compare **Figures 3.2B** and **3.5C**) that did not alter significantly after co-expression of STAT2 (**Figure 3.5C**).

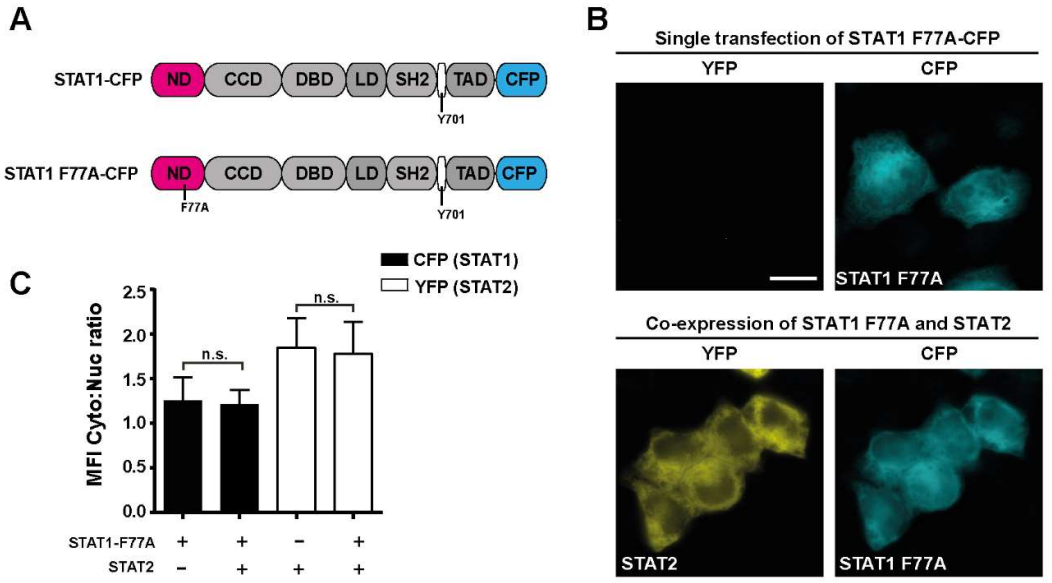

Fig 3.5 *STAT1 F77A subcellular distribution is not altered upon co-expression with STAT2* **A –** Schematics of STAT1-CFP fusion variants used **B** – Fluorescent microscopy showing the resting subcellular distribution of STAT1 F77A-CFP expressed alone or co-expressed with STAT2-YFP in HeLa cells. Scale bar = 10 µm **C** – The cytoplasmic: nuclear ratio of mean fluorescent intensity of STAT1 F77A-CFP and STAT2-YFP in cells was measured by line scan analysis. Data represents at least 25 cells analysed from 3 separate experiments, n.s = p>0.05.

The failure of STAT2 to redistribute STAT1 F77A, indicated that the interaction facilitating STAT1-STAT2 co-localisation required a functional N domain interface. Although STAT2 has yet to be observed as a dimer prior to activation at the receptor, comparison of the amino acid sequences of STAT1 and STAT2 revealed a conserved motif adjacent to the F77A of STAT1 (**Figure 3.6**).

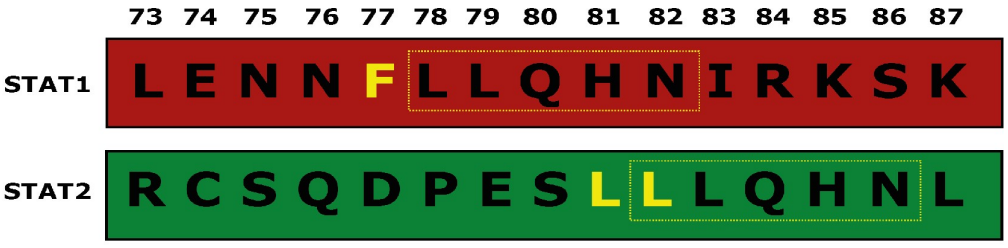

Fig 3.6 *Conserved amino acid motif detected within the N domain of STAT1 and STAT2.* Comparison of amino acid residues 73 to 87 revealed a 5 amino acid motif (boxed) conserved in the N domain of both STAT1 and STAT1. Highlighted in yellow are the amino acids mutated in this thesis.

Two leucine residues at positions 81 and 82 in STAT2 were identified as residing within the reciprocal positions to Phe77 and Leu78 which are known to be essential for N domain interactions of STAT1. A point mutation of Leu81Ala (L81A) was introduced into YFP-tagged STAT2 (**Figure 3.7A**), and was subsequently co-expressed with STAT1. This STAT2 mutant redistributed STAT1 to the cytoplasm of HeLa cells, suggesting that the interaction between STAT1 and STAT2 L81A remained stable (**Figure 3.7B**). The subsequent mutation of Leu82 to alanine in STAT2 resulted in a double mutant LL81/82AA. Expression of this STAT2 variant did not result in a primarily cytoplasmic localisation of STAT1 (**Figure 3.7B**), mimicking the result observed with the STAT1 F77A mutant in **Figure 3.5**. Finally, given the lack of impact of the L81A mutation alone, an YFP-tagged STAT2 construct with a single Leu82Ala mutation was co-expressed with STAT1-CFP. This single point mutation appeared sufficient to disrupt the cytoplasmic shift of STAT1 in the presence of STAT2 (**Figure 3.7B**).

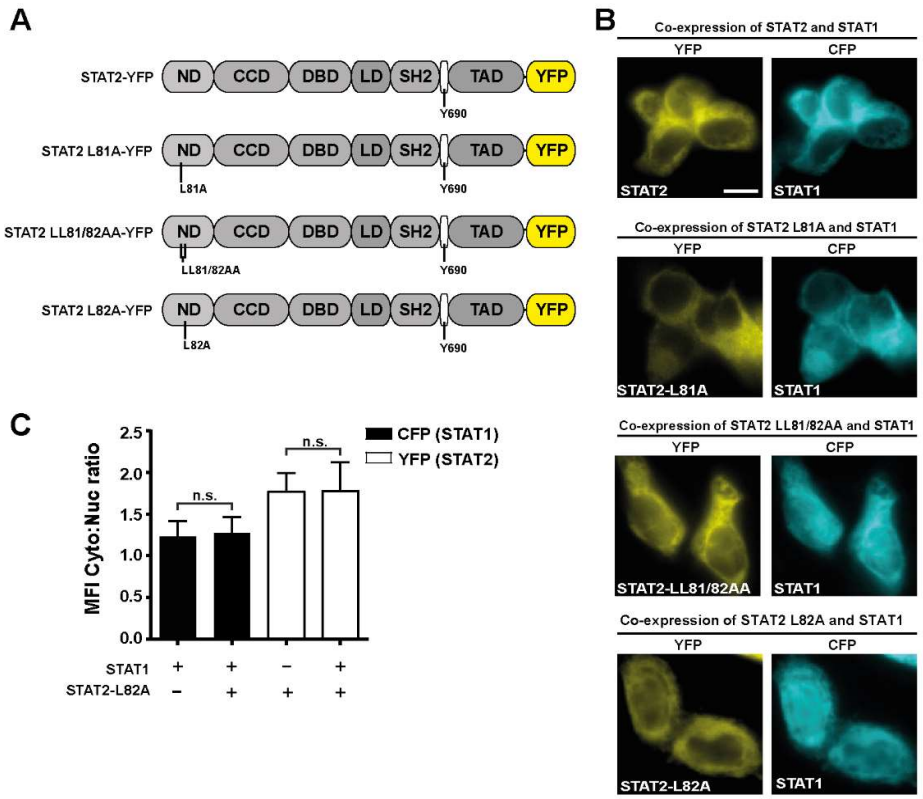

Fig 3.7 Mutations within the N domain of STAT2 abolish redistribution of STAT1 to the cytoplasm **A** – Schematics showing STAT2-YFP mutations used **B** – Fluorescent microscopy showing the resting subcellular distribution of STAT1-CFP co-expressed with various STAT2 mutants in HeLa cells. Scale bar = 10 µm **C** – The cytoplasmic: nuclear ratio of mean fluorescent intensity of STAT1-CFP and STAT2 L82A-YFP in cells was measured by line scan analysis. Data represents at least 25 cells from 2 independent experiments, n.s = p>0.05.

In order to compare the effect of this mutation with that seen in STAT1 F77A expressing cells, line-scan analysis of micrographs was performed. STAT1-CFP distribution in cells was unchanged by the co-expression of STAT2 L82A (**Figure 3.7C**). Similarly, STAT2 L82A showed a highly cytoplasmic distribution comparable with wild type STAT2 (**compare Figures 3.2C and 3.7C**) which did not change upon co-expression with STAT1. These results highlight that the interaction between STAT1 and STAT2 is dependent on a conserved amino acid motif which can be disrupted by single point mutations on either STAT.

3.2.5. STAT1 distribution in cells lacking STAT2 is governed by CRM1 dependent export

STAT1 shows different resting subcellular distribution across various cell types (Meyer et al, 2002), the cause of which is not fully understood. A weak NES within the coiled-coil domain is currently believed to contribute to the subcellular distribution of STAT1 (Begitt et al, 2000). The demonstrated ability of STAT2 to co-localise with STAT1 in the cytoplasm, was a potential contributor to STAT1 distribution that had not been previously considered. In addition STAT1, even in the absence of overexpressed STAT2, had thus far shown a bias towards a cytoplasmic distribution. To clarify this issue the behaviour of STAT1 in the absence of STAT2 was further characterised.

The reported weak NES within the STAT1 CCD is dependent on key lysine residues at positions 308 and 312 (Begitt et al, 2000). As previously shown the F77A mutation in STAT1 abolishes the influence of STAT2 on STAT1 subcellular distribution. These two constructs were compared to wild type STAT1 (**Figure 3.8A**). The nucleocytoplasmic distribution of GFP-tagged wild type STAT1, STAT1 F77A and STAT1 LL308/312AA constructs in the STAT2 deficient U6A cell line was visualised by fluorescence microscopy (**Figure 3.8B**). Whilst all proteins were found throughout the cell, wild type STAT1 and STAT1 F77A both showed a slightly cytoplasmic distribution in untreated U6A cells similar to that observed in HeLa cells earlier (**Figure 3.8B,** upper and middle panels). The mutations within the coiled coil domain appeared to result in a more even distribution of STAT1 throughout the U6A cells (**Figure 3.8B**, lower panels).

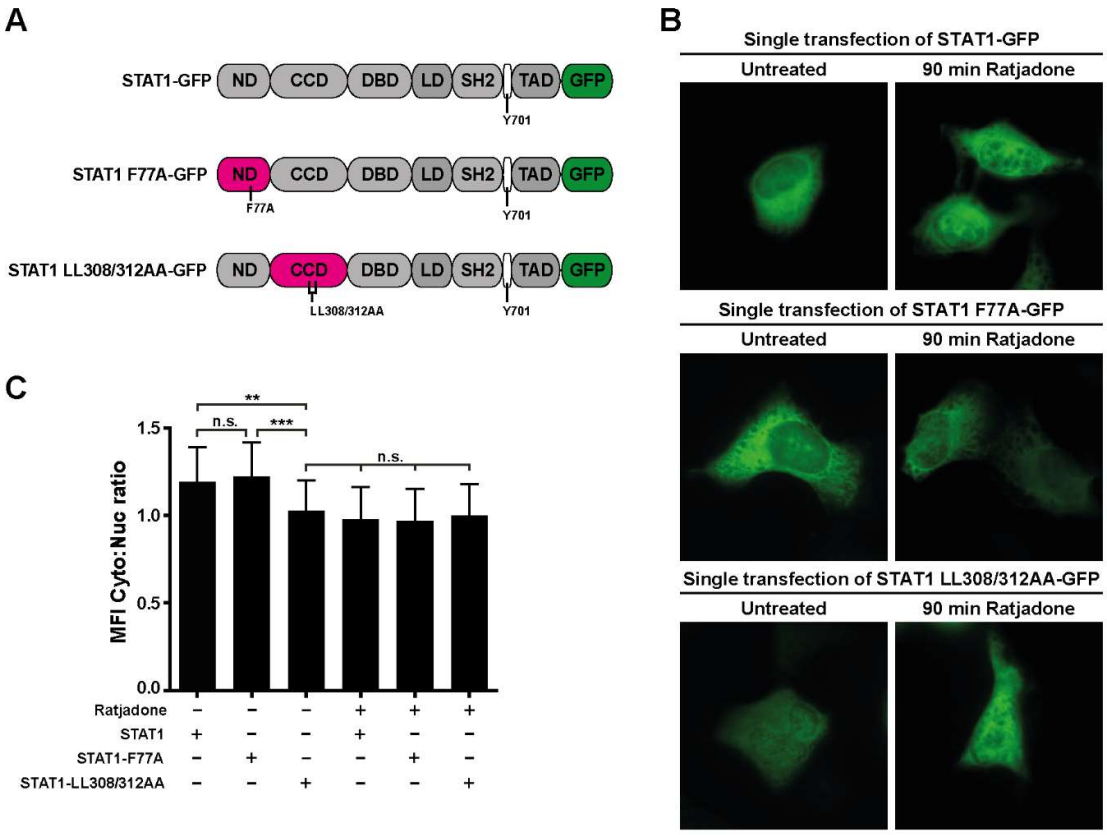

Fig 3.8 *A CRM1 dependent export signal determines STAT1 subcellular distribution in the absence of STAT2* **A** – Schematics showing STAT1-GFP variants **B** – U6A cells expressing STAT1 variants were left untreated (left) or treated for 90 min with 10 ng/mL ratjadone. The resulting subcellular distribution of STAT1-GFP was observed using fluorescence microscopy. Scale bar = 10 µm **C** – The cytoplasmic: nuclear ratio of mean fluorescent intensity of STAT1-GFP variants in U6A cells either untreated or treated for 90 min with 10 ng/mL ratjadone was measured by line scan analysis. Data represents at least 25 cells from 2 independent experiments, ** = $p<0.005$, *** = $p<0.001$, n.s = $p>0.05$.

CRM1-mediated nuclear export was inhibited in U6A cells via treatment with 10 ng/mL of ratjadone for 90 minutes. Under these conditions the subcellular distribution of STAT1 and STAT1-F77A became similar to the STAT1 LL308/312AA NES mutant (**Figure 3B**). Line scan analysis of fluorescent micrographs was performed to confirm this change in behaviour (**Figure 3C**). As observed wild type STAT1 and STAT1 F77A were significantly more cytoplasmic than the NES mutant in the absence of ratjadone. Abolition of CRM1 nuclear export resulted in all STAT1 variants assuming an even distribution between cytoplasm and nucleus (**Figure 3C**). These results confirmed that the previously identified NES within the coiled-coil domain contributes to STAT1 subcellular distribution independent of STAT2.

3.3. Effect of STAT2 on STAT1 subcellular distribution during IFN-γ signalling

Having established that STAT1 and STAT2 co-localise in cells prior to IFN signalling, the effect of this interaction upon IFN-γ treatment was investigated. The currently accepted model assumes that STAT2 is inert during type-2 IFN signalling as it is neither recruited to the receptor nor activated in response to this cytokine. However, the interaction observed between STAT1 and STAT2 in cells appeared to rely on N-domain interactions, which are known for STAT1 and STAT3 homodimers to be stable even after STAT activation (Hirahara et al, 2015). Due to the fact the STAT2 primarily resides in the cytoplasm when inactive, it was postulated that it may have an inhibitory effect on STAT1 nuclear accumulation by facilitating its export.

3.3.1. IFN-γ induced nuclear translocation of STAT1 is enhanced in cells lacking STAT2

As described earlier, the STAT2 deficient U6A and its parental cell line 2FTGH can be used to compare cellular behaviour in the absence of STAT2. The nuclear accumulation of STAT1 in response to IFN-γ was compared between STAT2 deficient U6A cells and the parental 2fTGH cell line. Cells were treated for 1 hour with IFN-γ at a concentration of 1 U/mL before fixation. Activated STAT1 was detected by a Cy3-decorated antibody against pY701-STAT1 and nuclei were counterstained with Hoechst. In both cell lines, activated STAT1 accumulated within the nucleus in response to IFN-γ (**Figure 3.9A**) although in 2fTGH cells a residual presence was also detected in the cytoplasm. To quantify any difference between the cell lines, line scan analysis was used to acquire and compare mean Cy3 fluorescence intensities from within the cytoplasm and nuclei of cells as done before (see **Figure 3.1B**). The cytoplasmic: nuclear ratios of pY701-STAT1 were calculated for each cell line. In contrast to the resting distribution of inactive STAT1, the pY701-STAT1 was predominantly nuclear i.e. the ratio was below 1 in both cell lines. Within U6A cells, however, the proportion of phosphorylated STAT1 that was within the nucleus was significantly higher (**Figure 3.9B**). This result suggested that nuclear accumulation of STAT1 in response to IFN-γ is enhanced in the absence of STAT2.

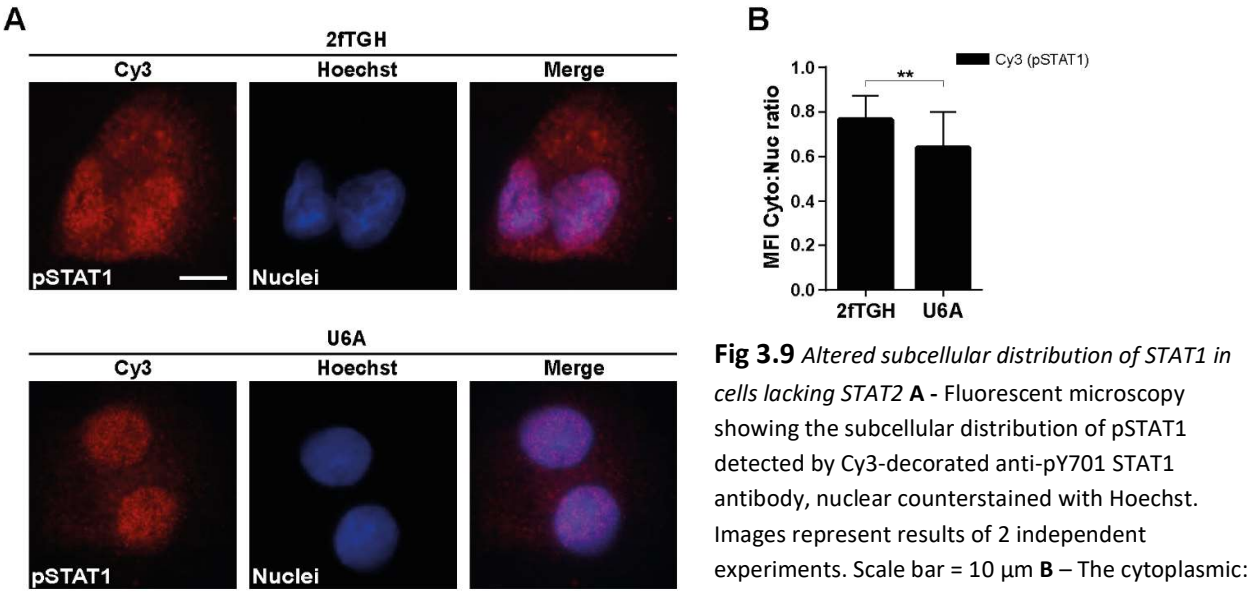

Fig 3.9 *Altered subcellular distribution of STAT1 in cells lacking STAT2* **A -** Fluorescent microscopy showing the subcellular distribution of pSTAT1 detected by Cy3-decorated anti-pY701 STAT1 antibody, nuclear counterstained with Hoechst. Images represent results of 2 independent experiments. Scale bar = 10 µm **B** – The cytoplasmic: nuclear ratio of mean fluorescent intensity of Cy3-decorated STAT1 in cells was measured by line scan analysis. Data represents at least 25 cells.

3.3.2. STAT2 inhibits STAT1 nuclear accumulation but not activation in response to IFN-γ

To follow up the enhanced nuclear accumulation in STAT2 deficient cells the compliment experiment was performed in cells overexpressing STAT2. HeLa cells were transiently transfected with either YFP alone or YFP-tagged STAT2 and treated for 60 minutes with 50 U/mL IFN-γ. Cells were subsequently fixed and permeabilised, before activated STAT1 was detected via Cy3-decorated anti-pY701 STAT1 antibody. In mock transfected cells, YFP was detected in both the cytoplasm and nucleus whilst treatment with IFN-γ resulted in nuclear accumulation of pY701-STAT1 within the cell nucleus (**Figure 3.10A**, upper panels). The expression of STAT2 precluded nuclear accumulation of phosphorylated STAT1, which remained predominantly within the cytoplasm along with STAT2 itself (**Figure 3.10A**). The cytoplasmic: nuclear ratio was analysed by line scanning and this confirmed the vast difference between pY701-STAT1 distribution in mock transfected cells (less than 1) and cells expressing STAT2-YFP (approx. 1.7, **Figure 3.10B**).

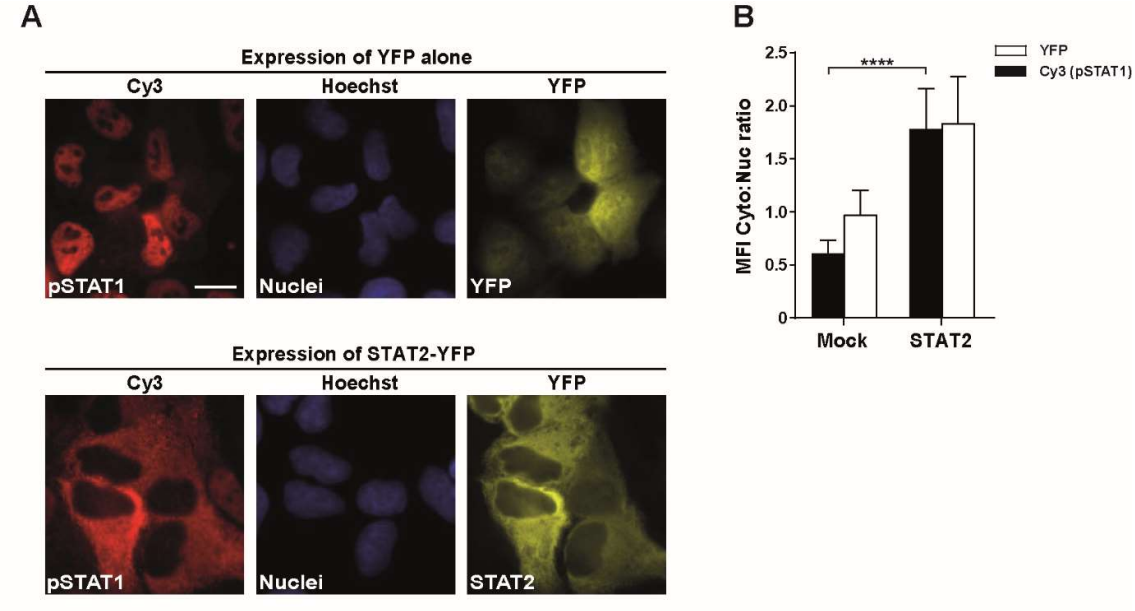

Fig 3.10 *Phosphorylated STAT1 co-localises in the cytoplasm with STAT2* **A -** Fluorescent microscopy showing the subcellular distribution of pSTAT1 detected by Cy3-decorated anti-pY701 STAT1 antibody, nuclear counterstained with Hoechst. Scale bar = 10 µm **B** – The cytoplasmic: nuclear ratio of mean fluorescent intensity of Cy3-decorated STAT1 in cells was measured by line scan analysis. Data represents at least 25 cells.

The nuclear accumulation of STAT1 upon IFN-γ signalling is dependent on recruitment and activation at the receptor-JAK complex. As the expression of STAT2-YFP in cells inhibited nuclear accumulation of pY701-STAT, the effect of STAT2 expression on STAT1 activation was assessed. HeLa cells were transiently transfected with either YFP or YFP-tagged STAT2. Cells were left untreated or treated for 1 hour with either IFN-β (500 U/mL) or IFN-γ (50 U/mL). Western blot analysis of STAT1 and STAT2 expression and activation was performed (**Figure 3.11**). The expression of endogenous STAT1 was unaffected by the expression of STAT2 (**Figure 3.11A**, compare lanes 1, 3, 5 to 2, 4, 6). Phosphorylated STAT1 was detected in cells treated with either IFN-β or IFN-γ (**Figure 3.11A,** lanes 3, 4, 5 and 6). In contrast, neither the endogenous STAT2 nor STAT2-YFP was activated in response to IFN-γ (**Figure 3.11A**, lanes 3 and 4). This result was in line with the current literature, however both STAT-YFP and endogenous STAT2 were phosphorylated in cells treated with IFN-β, a type-1 IFN (**Figure 3.11A**, lanes 5 and 6).

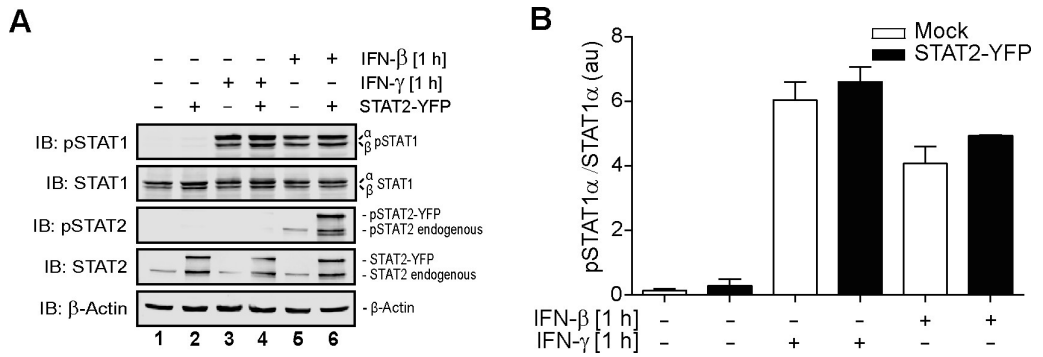

Fig 3.11 *STAT1 activation is unaffected by the expression of STAT2* **A** – Western blot (IB) analysis of STAT1 phosphorylation in HeLa cells mock or transiently transfected with STAT2-YFP. Cells were left untreated or treated for 1 hour with either IFN-γ or IFN-β. IBs were probed with antibodies against pY701-STAT1, STAT1, pY690-STAT2, STAT2 and β-Actin. **B** – The band intensity of phosphorylated and total STAT1α was quantified and used to calculate STAT1 activation. Bars represent mean ± S.D. from 3 independent experiments.

The activation of STAT1α in the presence of STAT2-YFP was compared by analysis of western blot band intensity. The signals detected for phosphorylated STAT1α were normalised to the total expression of STAT1α (**Figure 3.11B**). This analysis revealed that STAT1 activation in response to IFN was found to be unaffected by the expression of STAT2-YFP. Consequently the inhibition of receptor recruitment or phosphorylation of STAT1 was ruled out as a cause of impaired STAT1 nuclear accumulation in the presence of STAT2.

3.3.3. Inhibition of activated STAT1 nuclear translocation is independent of nuclear export but dependent on N domain interactions

Given that nuclear export and N domain interactions between STAT1 and STAT2 were essential for the redistribution of STAT1 prior to IFN signalling, the contribution of these two factors was investigated. Hela cells were transiently transfected with the export mutant STAT2-ΔC and the N domain mutant STAT2 L82A. The subcellular distribution of phosphorylated STAT1 was analysed by fluorescent microscopy detecting Cy3 bound to anti-pY701-STAT1 antibody. In cells expressing STAT2-ΔC, phosphorylated STAT1 remained predominantly within the cytoplasm (**Figure 3.12A,** left) similar to cells expressing wild type STAT2. In contrast, the expression of STAT2 L82A, did not prevent phosphorylated STAT1

from accumulating in the nucleus (**Figure 3.12A**, right). Analysis of cytoplasmic: nuclear fluorescence confirmed the nuclear accumulation of pY701-STAT1 (**Figure 3.12B**).

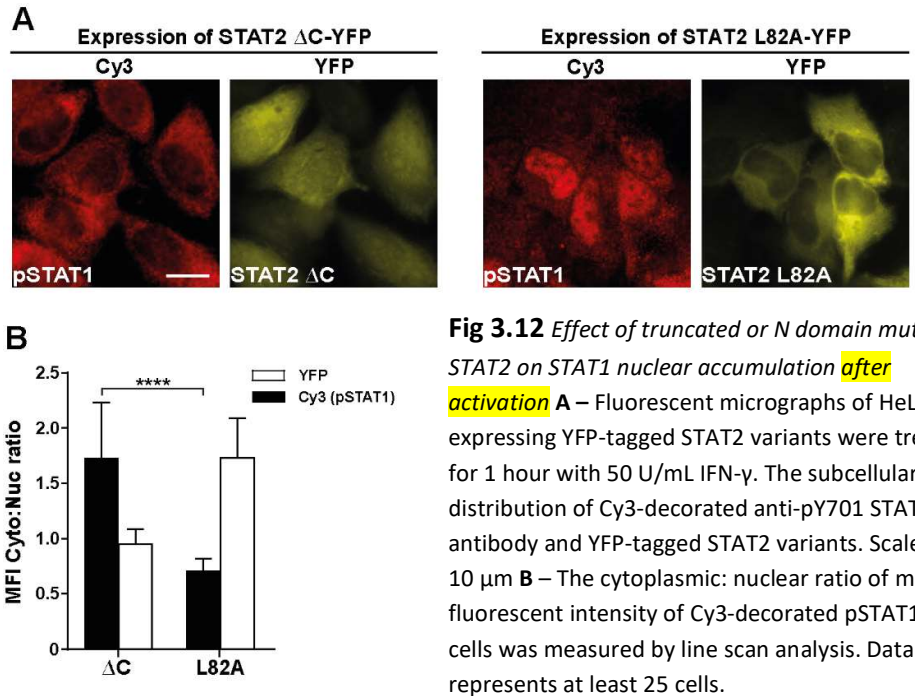

Fig 3.12 *Effect of truncated or N domain mutant STAT2 on STAT1 nuclear accumulation after activation* **A –** Fluorescent micrographs of HeLa cells expressing YFP-tagged STAT2 variants were treated for 1 hour with 50 U/mL IFN-γ. The subcellular distribution of Cy3-decorated anti-pY701 STAT1 antibody and YFP-tagged STAT2 variants. Scale bar = 10 µm **B** – The cytoplasmic: nuclear ratio of mean fluorescent intensity of Cy3-decorated pSTAT1 in cells was measured by line scan analysis. Data represents at least 25 cells.

3.3.4. STAT1 and STAT2 form semi-phosphorylated heterodimers through N domain - interactions.

The co-localisation of STAT1 and STAT2 during IFN-γ signalling suggested that phosphorylation of STAT1 did not prevent the formation of heterodimers through N domain mediated interactions. To confirm the formation of this as yet unknown species, immunoprecipitation studies were performed. STAT dimerisation can occur either via N domain or SH2-phosphotyrosine interactions. Results described in the previous subchapters demonstrated that the point mutation F77A in STAT1 disrupted N domain mediated interactions with STAT2. A point mutation of the tyrosine residue at position 701 to phenylalanine (Y701F) prevents activation of STAT1 and thus abolishes the SH2-phosphotyrosine interaction. As such, a STAT1 containing both the F77A and Y701F mutations was expected to lose the ability to dimerise with STAT2 altogether. To that end, the ability of FLAG-tagged STAT1 constructs, with the relevant mutations to co-precipitate with STAT2, was investigated (**Figure 3.13A**).

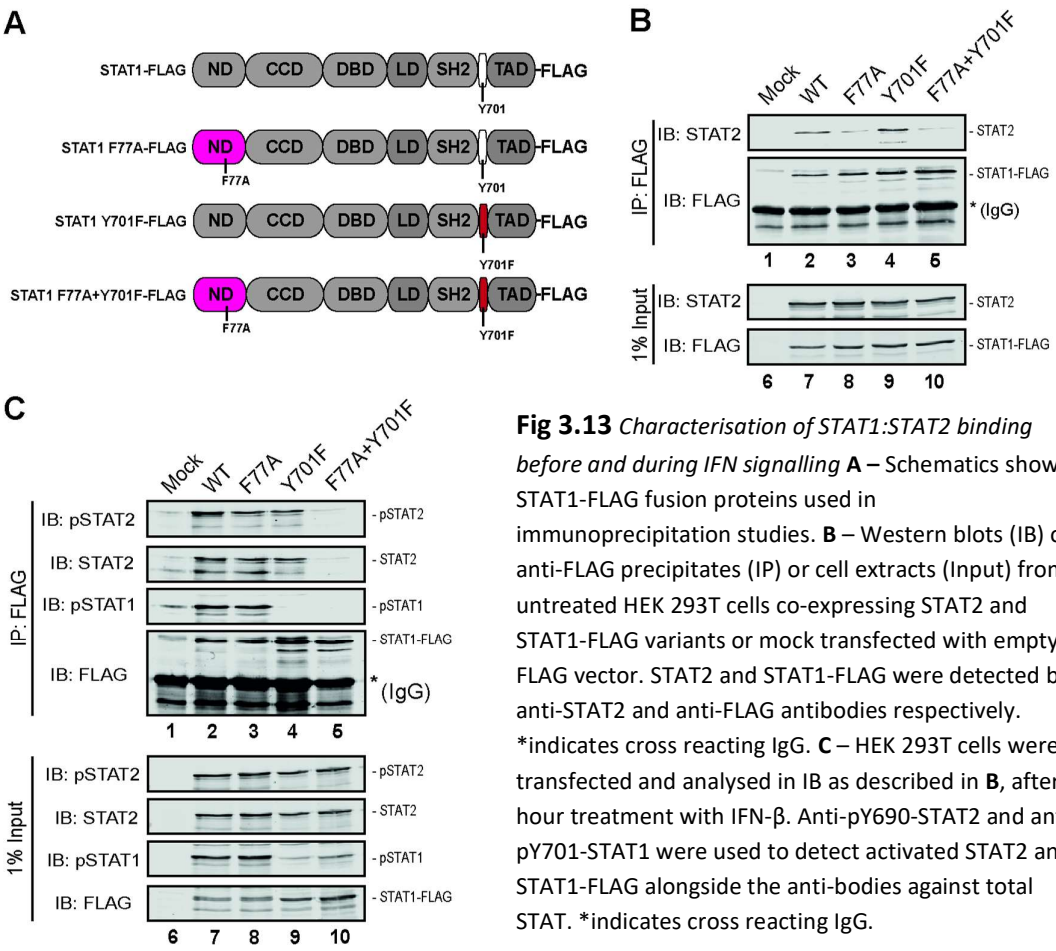

Fig 3.13 *Characterisation of STAT1:STAT2 binding before and during IFN signalling* **A –** Schematics showing STAT1-FLAG fusion proteins used in immunoprecipitation studies. **B** – Western blots (IB) of anti-FLAG precipitates (IP) or cell extracts (Input) from untreated HEK 293T cells co-expressing STAT2 and STAT1-FLAG variants or mock transfected with empty FLAG vector. STAT2 and STAT1-FLAG were detected by anti-STAT2 and anti-FLAG antibodies respectively. *indicates cross reacting IgG. **C** – HEK 293T cells were transfected and analysed in IB as described in **B**, after 1 hour treatment with IFN-β. Anti-pY690-STAT2 and anti-pY701-STAT1 were used to detect activated STAT2 and STAT1-FLAG alongside the anti-bodies against total STAT. *indicates cross reacting IgG.

To confirm that the results suggesting anti-parallel heterodimers of STAT1 and STAT2 exist independently of IFN could be reproduced with immunoprecipitation experiments, HEK 293T cells were transiently co-transfected with STAT2 in conjunction with FLAG-tagged STAT1 variants. Extraction of proteins and subsequent precipitation of FLAG-STAT1 with magnetic beads conjugated to anti-FLAG antibody was performed. STAT1 and co-precipitating proteins were subsequently identified by western blot analysis and compared to whole cell extracts (**Figure 3.13B**). As expected STAT2 co-precipitated with wild-type STAT1 and STAT1 Y701F which both have a functional N domain interface and thus are capable of anti-parallel heterodimerisation (**Figure 3.13B,** lanes 2 and 4). Disruption of the N domain interaction by the F77A mutation prevented STAT2 co-precipitation, confirming that this interaction is responsible for IFN-independent heterodimer formation (**Figure 3.13B,** lanes 3 and 5). Having demonstrated that the N-domain interaction of STAT1 and STAT2 could be observed in this assay, the experiment was repeated following a treatment with

500 U/mL IFN-β for 1 hour which resulted in co-precipitation and phosphorylation of both wild type STAT1 and STAT2 (**Figure 3.13C,** lanes 2 and 7). Consequently, the nature of STAT1:STAT2 heterodimers could be extrapolated by the ability of the STAT1 mutants to precipitate STAT2. In contrast to the untreated situation, both FLAG-tagged STAT1 F77A and STAT2 were detected following FLAG-antibody precipitation (**Figure 3.13C**, lanes 3 and 8). This was attributed to the formation of the parallel heterodimer stabilised by reciprocal SH2-phosphotyrosine interactions. Mutation of the key tyrosine in STAT1 Y701F prevented STAT1 activation by IFN but not co-precipitation with tyrosine phosphorylated STAT2 (**Figure 3.13C**, lane 4). This was attributed to the formation of semi-phosphorylated heterodimers supported by N domain interaction due to the loss of co-precipitation of STAT2 with the STAT1 F77A, Y701F double mutant which supports neither parallel nor anti-parallel dimerisation (**Figure 3.13C**, compare lanes 4 and 5).

3.3.5. A chimeric STAT2 protein with the SH2 domain of STAT1 does not inhibit the nuclear translocation of STAT1

Whilst a semi-phosphorylated heterodimer of STAT1 and STAT2 appeared to be stable, fluorescence microscopy suggested that it was incapable of accumulating in the nucleus (**Figure 3.10**). The likely cause of this was predicted to be due to impaired nuclear import as the removal of the NES within STAT2 did not enable STAT1 nuclear accumulation. Nuclear import of activated STAT1 homodimers and heterodimers with STAT2 is dependent on an interaction with importin α5, which is facilitated by parallel STAT dimerisation. Therefore, an IFN-γ responsive STAT2 was presumed to allow nuclear import and thus accumulation of STAT1.

Substitution of the STAT2 SH2 domain and tyrosine 690, for that of STAT1, has previously been shown to confer IFNGR recruitment and subsequent activation in response to type-2 interferon (Heim et al, 1995; **Figure 3.14A**). HeLa cells expressing this chimeric STAT2 tagged with YFP were left either untreated or treated for 1 hour with IFN-γ. Detection of STAT1 distribution within the cell was achieved using a Cy3-decorated antibody against the C terminal domain of STAT1 in order to discriminate between the chimera and endogenous STAT1 (**Figure 3.14B**). Prior to activation, STAT1 and the chimeric STAT2 co-localised within

the cytoplasm similar to the case with STAT2 WT (**Figure 3.14B**, upper panels). In contrast, treatment with IFN-γ not only resulted in the nuclear accumulation of STAT1 but also an increased nuclear presence of the STAT2 chimera (**Figure 3.14B**, middle panels). The point mutation Arg602Leu (R602L) within the SH2 domain of STAT1 disrupts its recruitment to the IFNGR receptor and thus activation in response to IFN (Shuai et al, 1993). This mutated STAT1 SH2 domain was introduced to YFP-tagged STAT2. This chimeric STAT2 R602L inhibited the nuclear accumulation of STAT1, recapitulating the phenomenon seen with wild type STAT2 (**Figure 3.14B**, lower panels). This result suggested that the inability to form parallel heterodimers in response to IFN-γ could explain why STAT2 and activated STAT1 fail to accumulate within the nucleus.

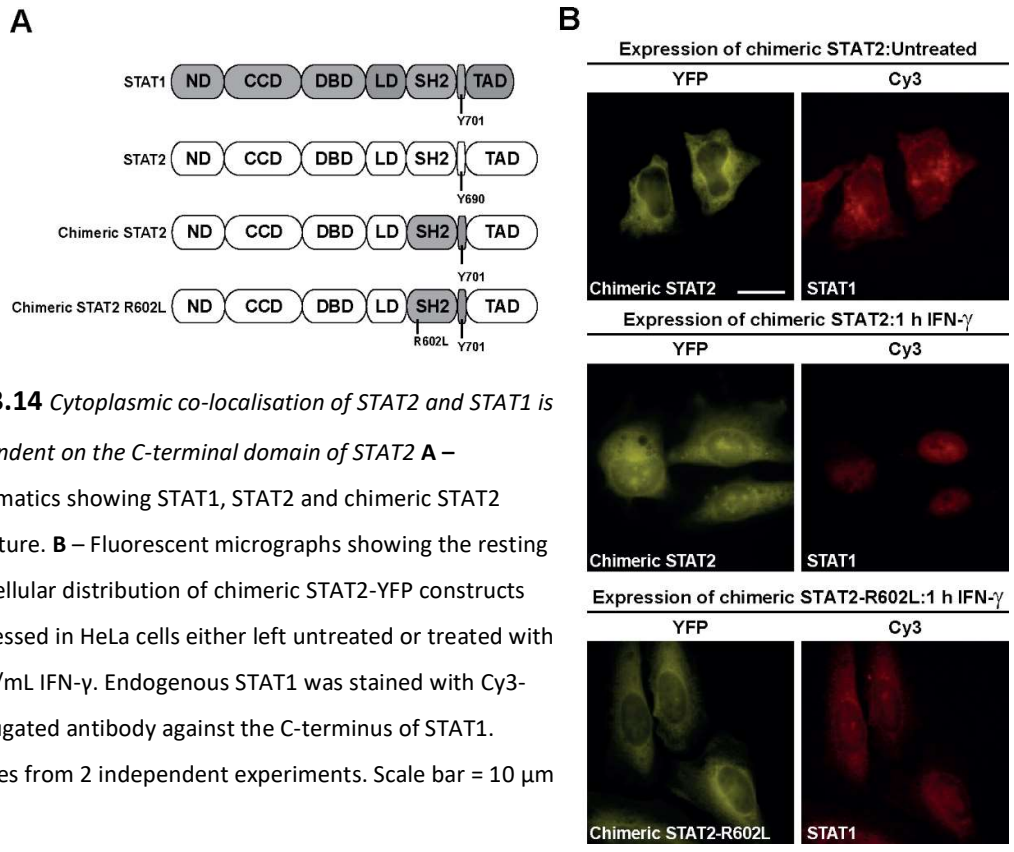

Fig 3.14 *Cytoplasmic co-localisation of STAT2 and STAT1 is dependent on the C-terminal domain of STAT2* **A –** Schematics showing STAT1, STAT2 and chimeric STAT2 structure. **B** – Fluorescent micrographs showing the resting subcellular distribution of chimeric STAT2-YFP constructs expressed in HeLa cells either left untreated or treated with 50 U/mL IFN-γ. Endogenous STAT1 was stained with Cy3-conjugated antibody against the C-terminus of STAT1. Images from 2 independent experiments. Scale bar = 10 µm

3.4. Chapter Summary

A previously uncharacterised interaction between STAT1 and STAT2 was observed and characterised. In the absence of interferon STAT1 and STAT2 co-localised within the cytoplasm of cells. The cause of this subcellular distribution was identified as result of CRM1-dependent export of STAT2 in combination with a stable interaction between STAT1 and STAT2 that required the N domain interface. In addition, the identification of a hitherto unknown interaction interface within the STAT2 N domain was discovered. In light of these results, the ability of the NES contained within the STAT1 coiled-coil domain to affect its own subcellular distribution independent of STAT2 was investigated and confirmed.

The consequences of this interaction, following type-2 IFN, was investigated. In this case phosphorylated STAT1 can co-localise with STAT2 within the cytoplasm, as opposed to accumulating within the nucleus. As with the unphosphorylated STAT1, this phenomenon was dependent on the interactions of the respective STAT N domains. In contrast to resting cells, this cytoplasmic distribution was not due to the active nuclear export of STAT2 but instead due to impaired import of a semi-phosphorylated STAT1:STAT2 complex. Furthermore, the nuclear translocation of activated STAT1 in response to IFN-γ was enhanced in cells lacking STAT2.

4. Results

STAT2 is an inhibitor of several IFN-γ dependent biological responses.

4.1. Introduction

In the previous chapter, a hitherto uncharacterised interaction between STAT1 and STAT2, distinct from the classical parallel heterodimer, was described. Furthermore, this interaction facilitated the inhibition of STAT1 nuclear accumulation in response to the lone type-2 interferon, IFN-γ. Consequently, this interaction was predicated to have implications for the biological response to IFN-γ.

Interferon γ has been identified as an integral modulator of the immune response, governing functions as wide ranging as cellular maturation, tumour killing and anti-bacterial immunity. The response to IFN-γ is mediated primarily by STAT1 homodimers, which translocate to the nucleus and act as transcription factors at the promoter regions of target genes. Preventing the nuclear translocation of STAT1 should result in an inhibition of its function as a transcription factor. Thus, in the context of the results presented in **chapter 3**, STAT2 was identified as a possible inhibitor of IFN-γ responsiveness.

To investigate this, cell lines that were deficient in STAT2 expression were tested for various biological functions in response to IFN-γ. These cells included the human fibrosarcoma cell line U6A and immortalised macrophages that were derived from transgenic mice lacking STAT2 expression. During the course of this work, U6A cells were reconstituted with wild type and the L82A STAT2 mutant described in **chapter 3**. These cells were characterised for IFN responsiveness including STAT activation, gene expression, parasite resistance and major histocompatibility complex upregulation.

4.2. Characterisation of STAT2 deficient and reconstituted cell lines

A transgenic mouse line that lacks STAT2 expression has been available for over a decade (Park et al, 2000). Despite this, little, if any, attention has focused on the IFN-γ functionality of this mouse model due to the presumption that STAT2 plays no role in type-2 interferon responses. An immortalised macrophage cell line, derived from the bone marrow of these mice, was available (Alazawi et al, 2013). Biochemical characterisation of these cells, in the context of type-1 and type-2, interferon was performed. Similarly, the STAT2 deficient U6A cell line was recently reconstituted with YFP-tagged wild-type STAT2, or the STAT2 L82A mutant, in our lab (work of the author in collaboration with Andreas Begitt and Maureen Mee. Ho et al, 2016). The biochemical IFN response of these cell lines was subsequently characterised during this work.

4.2.1. STAT2 deficient mouse macrophages show reduced STAT1 expression but not activation

In order to compare STAT2 deficient (S2 -/-) macrophages to the wild type, the expression and activation of STAT1 in response to IFN was verified. Macrophages were left untreated or treated for 1 hour with either 500 U/mL IFN-β or 50 U/mL IFN-γ. Whole cell extracts were prepared and analysed by western blot for both expression and activation of STAT1 and STAT2 (**Figure 4.1A**). The expression of STAT1 was reduced in STAT2 deficient macrophages (**Figure 4.1A**, compare lanes 1-3 with 4-6). Quantitative analysis of STAT1 expression normalised to β-Actin confirmed this phenotype, with around 50% less STAT1 detected in STAT2 deficient cells compared to wild type (**Figure 4.1B**).

In order to compare STAT1 activation at the IFN receptor, STAT1 phosphorylation was concurrently detected with anti-pY701 STAT1 antibody (**Figure 4.1A**). The band intensity of pSTAT1 was normalised by STAT1 expression in order to compare WT and S2 -/- macrophages. In response to IFN-γ, both WT and S2 -/- were capable of activating STAT1 to a similar degree (**Figure 4.1C**). In contrast, the activation of STAT1 in response to IFN-β, which results in simultaneous phosphorylation of both STAT1 and STAT2, was reduced in the S2 -/- macrophages (**Figure 4.1C**). These results suggested that, whilst STAT1 expression was reduced in S2 -/- cells, STAT1 phosphorylation in response to type-2 IFN was not impaired; although it was significantly reduced in the case of type-1 IFN.

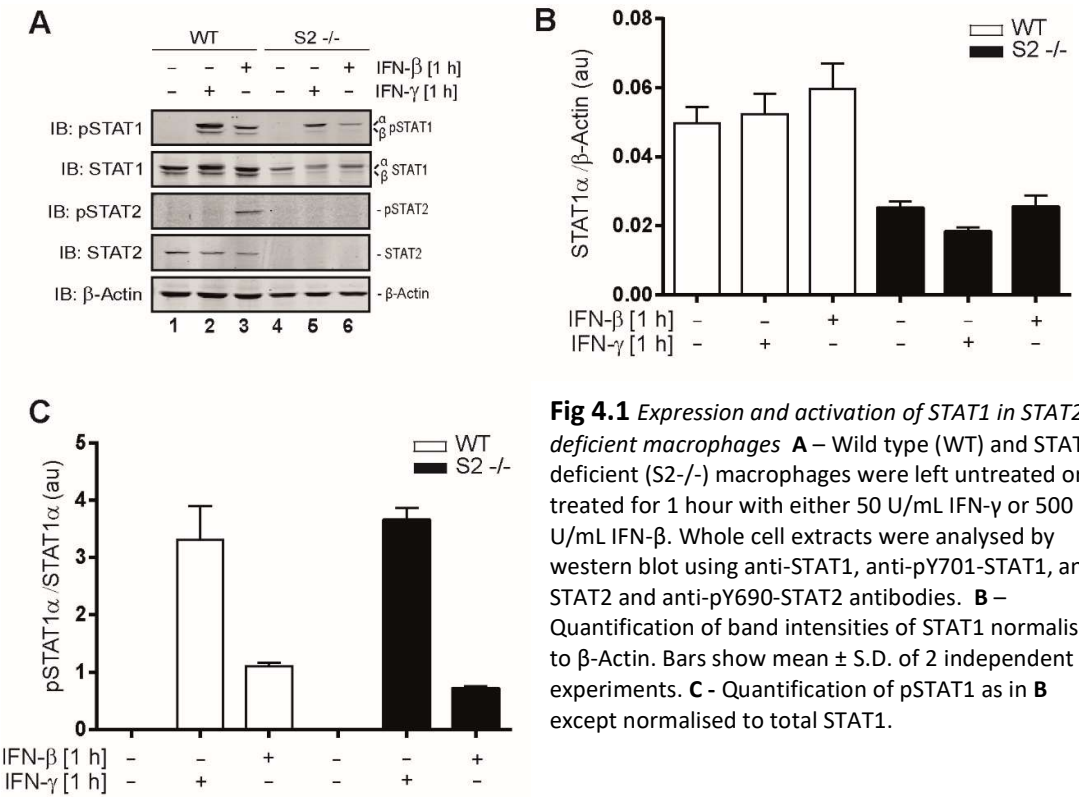

Fig 4.1 *Expression and activation of STAT1 in STAT2 deficient macrophages* **A** – Wild type (WT) and STAT2 deficient (S2-/-) macrophages were left untreated or treated for 1 hour with either 50 U/mL IFN-γ or 500 U/mL IFN-β. Whole cell extracts were analysed by western blot using anti-STAT1, anti-pY701-STAT1, anti-STAT2 and anti-pY690-STAT2 antibodies. **B** – Quantification of band intensities of STAT1 normalised to β-Actin. Bars show mean ± S.D. of 2 independent experiments. **C** - Quantification of pSTAT1 as in **B** except normalised to total STAT1.

4.2.2. IFN priming of macrophages lacking STAT2

The expression of STAT1 and STAT2 in cells can be increased by incubation with low concentrations of IFN, a process known as priming (Hu et al, 2002). The ability of STAT2 deficient macrophages to undergo priming was investigated. Cells were primed for 48 hours with either IFN-γ or IFN-β at a concentration 50 times less than used for acute activation, i.e., 1 U/mL IFN-γ or 10 U/mL IFN-β. After priming, cells were washed and treated with normal medium or medium containing 50 U/mL IFN-γ or 500 U/mL IFN-β for 1 hour. Whole cell extracts were prepared and analysed by western blot (**Figure 4.2A**). A dramatic upregulation of STAT1 protein expression was observed in both wild type (~12-fold increase) and STAT2 deficient (~45-fold increase) macrophages following priming with IFN-γ (**Figure 4.2B**). Moreover, STAT1 expression in STAT2 deficient cells was higher compared to wild type after type-2 IFN priming. This was also the case with unprimed cells, the 1 hour treatment with either IFN-γ or IFN-β did not significantly alter STAT expression but did induce STAT phosphorylation (**Figure 4.2A**, lanes 8, 9, 11, 12, 14, 15 17 and 18).

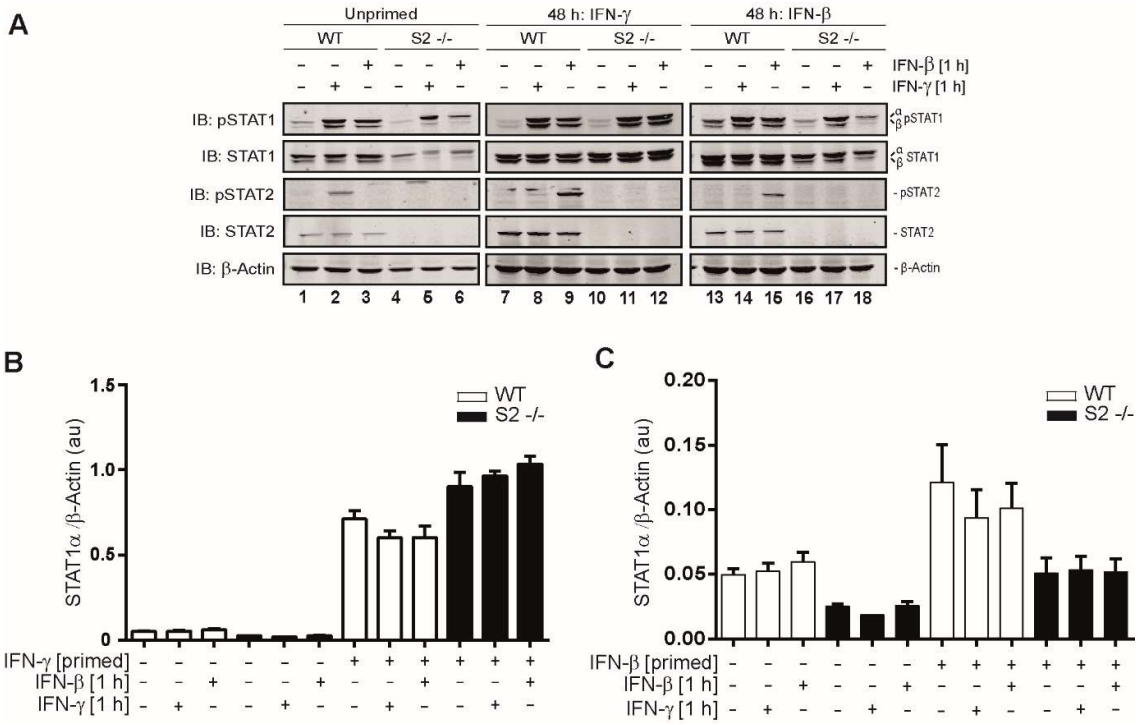

Fig 4.2 *Effect of IFN priming on STAT1 expression in STAT2-deficient macrophages* **A** – Wild type (WT) and STAT2 deficient (S2-/-) macrophages were primed for 48 hours in the presence of either 1 U/mL IFN-γ or 10 U/mL IFN-β. Cells were subsequently left untreated or treated for 1 hour with either 50 U/mL IFN-γ or 500 U/mL IFN-β. Whole cell extracts were analysed by western blot using anti-STAT1, anti-pY701-STAT1, anti-STAT2 and anti-pY690-STAT2 antibodies. **B** – Comparison between unprimed cells and cells primed with IFN-γ of band intensities of STAT1 normalised to β-Actin. Bars show mean ± S.D. of 2 independent experiments. **C -** Quantification of pSTAT1 as in **B** except normalised to total STAT1.

Priming with type-1 interferon also resulted in an increased STAT1 expression (**Figure 4.2C**) although not to the same degree as with IFN-γ. STAT1 expression increased ~2-fold in both wild type and STAT2 deficient cells, which mirrored the situation seen in naïve cells that STAT1 was expressed to higher degree in the wild type. These results suggested that the priming with IFN-γ, but not IFN-β, could be triggered to a different degree between wild type and STAT2 knockout macrophages. Type-2 IFN was tested at various concentrations to determine whether priming with IFN-γ could normalise the expression of STAT1 between the genotypes.

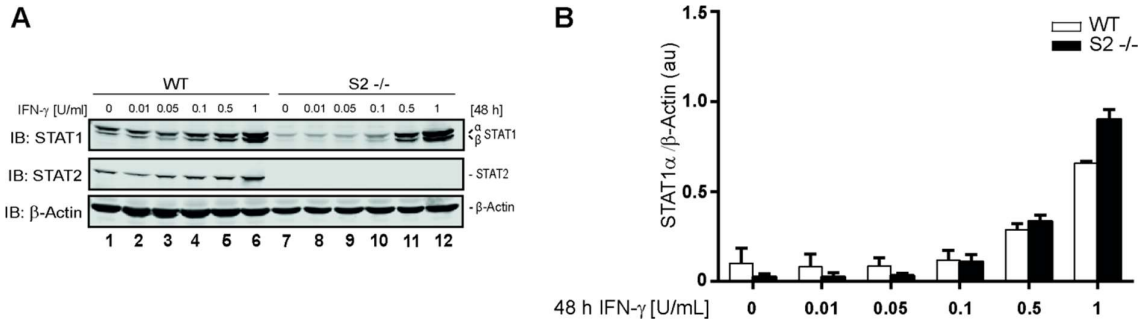

Fig 4.3 *IFN-γ priming can normalise STAT1 expression between wild type and STAT2-deficient macrophages* **A** – Wild type (WT) and STAT2 deficient (S2-/-) macrophages were primed for 48 hours in the presence of increasing concentrations of IFN-γ. Whole cell extracts were analysed by western blot using anti-STAT1 and anti-β-Actin antibodies. **B** – Quantification of band intensities of STAT1 normalised to β-Actin in response to IFN priming. Bars show mean ± S.D. of 2 independent experiments.

Macrophages were incubated with various concentrations of IFN-γ for 48 hours before whole cell extraction and analysis of STAT1 expression by western blot (**Figure 4.3A**). As seen in **Figure 4.2**, unprimed (0) STAT2 deficient cells showed less STAT1 expression compared to the wild type, a phenotype that could be reversed following 48 hour treatment with 1 U/mL of IFN-γ (**Figure 4.3B**). Priming with 0.1 U/mL of IFN-γ appeared to increase the STAT1 expression in STAT2 knockout cells but not the wild type (**Figure 4.2A**, compare lanes 3-4 to 9-10), whilst lower IFN-γ concentrations did not appear to alter the STAT1 expression in either genotype. STAT1 expression was increased in both genotypes in response to 0.5 U/mL of IFN-γ, resulting in a similar expression of this protein. Thus, priming with a concentration of IFN-γ between 0.1 and 0.5 U/mL was determined to normalise the expression of STAT1 in STAT2 knockout and wild type macrophages.

4.2.3. Characterisation of STAT2 reconstituted cell lines.

The STAT2 deficient cells were a useful initial tool in observing the effects of STAT2 on type-2 interferon signalling. As observed during the course of this work, the point mutation Leu82Ala in the N domain of STAT2 was sufficient to abrogate the inhibition of STAT1 nuclear accumulation by STAT2. Thus the establishment of a cell line that expressed STAT2 with this point mutation was determined to be an even more suitable reagent for dissecting the consequences of STAT1:STAT2 N domain interactions.

The STAT2 deficient human sarcoma cell line, U6A, was transfected with YFP-tagged wild type STAT2 or STAT2 L82A and a stable transfection was established by antibiotic selection (Ho et al, 2016). The biochemical response to IFN of these cells was subsequently determined by western blot analysis (**Figure 4.4A**). U6A and reconstituted cells were left untreated or treated for 1 hour, with either 50 U/mL IFN-γ or 500 U/mL IFN-β, prior to preparation of whole cell extracts.

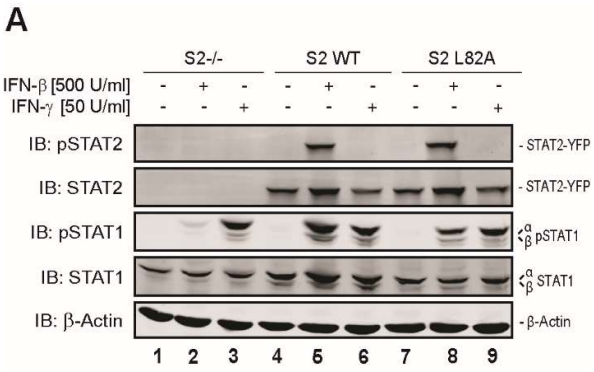

Fig 4.4 *Characterisation of reconstituted U6A cells* **A** – U6A (S2-/-) and STAT2 wild type (S2 WT) and L82A (S2 L82A) reconstituted cells were left untreated or treated for 1 hour with either 50 U/mL IFN-γ or 500 U/mL IFN-β. Whole cell extracts were analysed by western blot using anti-STAT1, anti-pY701-STAT1, anti-STAT2 and anti-pY690-STAT2 antibodies. (The experiments in this figure are courtesy of Dr Andreas Begitt and form part of Ho et al, 2016).

Western blot analysis revealed that STAT2 WT and L82A were stably expressed to a similar degree in cells (**Figure 4.4A**, compare lanes 4-6 with 7-9). Moreover, both the STAT2 variants were activated in response to type-1 IFN but not type 2 (**Figure 4.4A**, compare lanes 5, 6 with 8 and 9). Finally, it was established that STAT1 expression and activation was comparable between these cell lines (**Figure 4.4A**). These results confirmed the reconstituted U6A cells as a suitable tool for investigating the STAT2 role in IFN-γ signalling, without the need for normalisation via priming.

4.2.4. Gene expression in STAT2 deficient macrophages and reconstituted U6A cells.

STAT1 is an activator of transcription for hundreds of target genes in response to IFN-γ. Following the biochemical characterisation of the STAT2 deficient and reconstituted cells, a reverse transcription polymerase chain reaction (RT-PCR) assay was used to analyse the response to IFN-γ at the transcriptional level. RT-PCR is a powerful technique that allows the relative quantification of specific gene activity in response to a stimulus. Macrophages are key IFN-γ targets that are driven by this cytokine to accumulate within an area of infection,

seeking out and destroying pathogens. The upregulation of several key IFN-γ-induced genes was analysed in macrophages from wild type and STAT2 knockout mice that were treated for 4 hours with 50 U/mL IFN-γ. Several genes, including *Cxcl10, Mx1, Irf1* and *Il1β*, were significantly better induced in STAT2 -/- cells compared to the wild type (**Figure 4.5A**). Moreover, priming with IFN to normalise STAT1 expression, as seen in **Figure 4.3**, further accentuated the enhanced response of STAT2 deficient cells. However, not all IFN induced genes were better upregulated. Neither *Socs1* nor *Isg15,* key downstream regulators of IFN-γ signalling, were significantly better induced in STAT2 deficient cells; even following IFN-γ priming. These genes are known to have rapid turnover during interferon signalling and thus may not have been captured for this reason

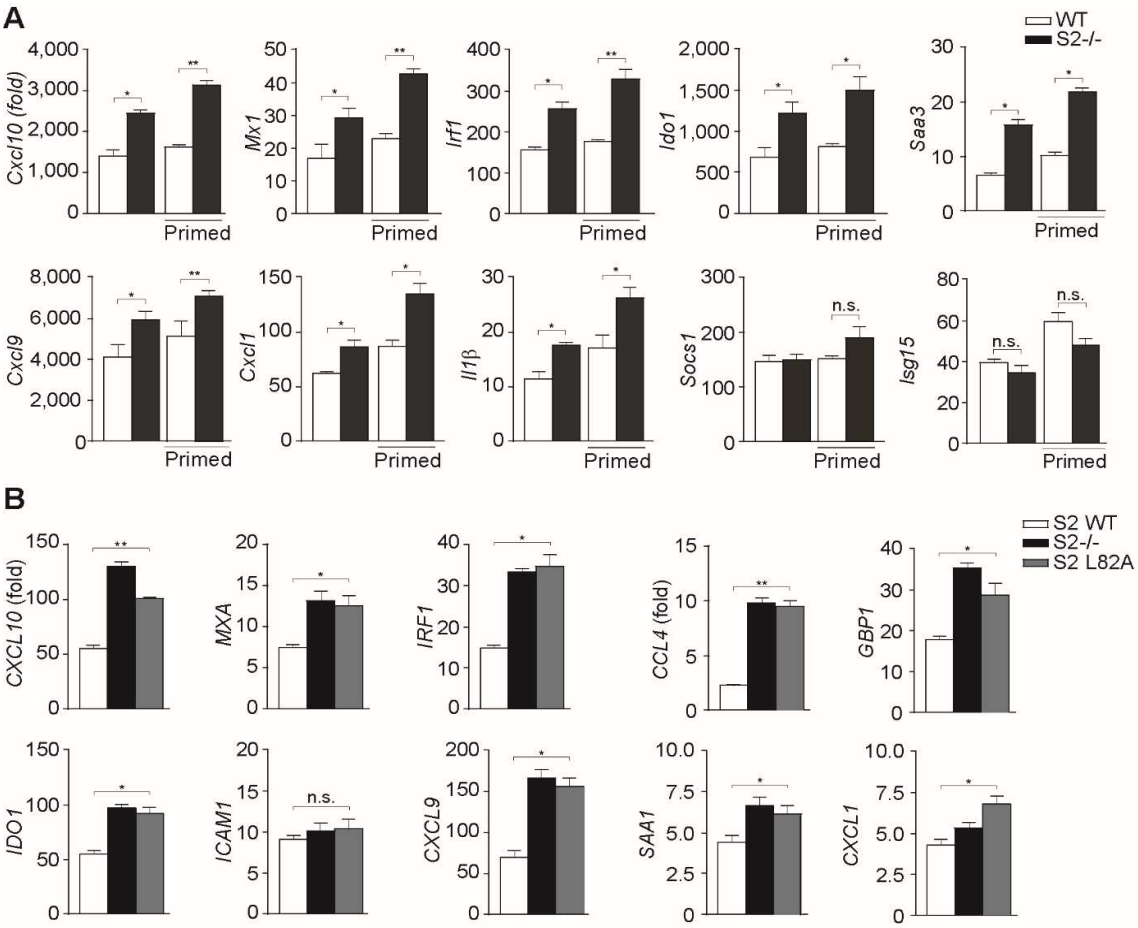

Figure 4.5 *IFN-γ gene induction in STAT2 deficient macrophage and reconstituted fibrosarcoma cells.* **A** – Quantitative RT-PCR analyses of wild type (WT) and STAT2 deficient (S2 -/-) immortalised mouse macrophages. Cells were either left unprimed or primed for 48 h with 0.5 U/mL of IFN-γ. Cells were subsequently treated for 4 hours with IFN-γ at a concentration of 50 U/mL. **B** – Quantitative RT-PCR of human STAT2 deficient U6A cells (S2-/-) and U6A cells reconstituted with either wild type (S2 WT) or L82A (S2 L82A) STAT2. Cells were treated for 4 hours with 50 U/mL IFN-γ. (The experiments in this figure are courtesy of Dr Andreas Begitt and form part of Ho et al, 2016).

IFN-γ induced gene expression in STAT2 deficient and reconstituted U6A cells was investigated by RT-PCR analysis. As was the case with the murine macrophages, several genes such as *CXCL10, MXA, IRF1* and *GBP1* were upregulated to a higher degree in cells lacking STAT2 compared to cells reconstituted with wild type STAT2 (**Figure 4.5B**). However, reconstitution of cells with the STAT2 L82A mutant resulted in gene induction similar to that seen in cells where STAT2 was absent. One of the genes tested, *ICAM1*, was similarly upregulated in response to IFN-γ regardless of the absence or presence of either wild type or mutant STAT2. These results supported the suggestion that inhibition of STAT1 nuclear accumulation by STAT2 could inhibit type-2 IFN gene induction and that the L82A mutation in STAT2 disrupted this effect.

4.3. Effect of STAT2 on nitric oxide production and parasite killing.

Having confirmed that the inhibition of STAT1 nuclear accumulation by STAT2 resulted in the reduced upregulation of several IFN-γ target genes, an investigation into the effect of STAT2 on cellular response to type-2 IFN was performed. A cardinal role of IFN-γ signalling is to facilitate the immune response to intracellular pathogens such as bacteria and protozoa. Phagocytes such as macrophages are an essential part of this response. These specialised immune cells are capable of engulfing pathogens or infected cells, and then destroying them by utilising free radical production. IFN-γ is highly involved in activating these microbicidal pathways and as such is crucial for the defence against classic intracellular parasites such as *Toxoplasma gondii*. Macrophages are also capable of microbial killing independent of phagocytosis by producing and releasing nitric oxide. Nitric oxide production by macrophages is highly dependent on IFN-γ, often in conjunction with detection of bacterial lipopolysaccharide (LPS).

4.3.1. NO production in macrophages before and after IFN-γ priming.

Detection of nitric oxide release by cells can be achieved by a simple spectrophotometric technique known as the Griess assay. This technique involves the use of two reagents, sulphanilamide and N-1-napthylethylenediamine (NED) which react to form a red azo compound in the presence of NO. Immortalised macrophage cell lines from wild type and STAT2 deficient mice were either left untreated or treated with 1 u/mL IFN-γ and/or 1

ng/mL LPS for 36 hours (**Figure 4.6**). Triplicate supernatant samples from each culture were acquired and treated with Griess reagent. The subsequent detection of azo compound was performed using a photospectrometer and concentrations of NO were calculated with the use of a nitrite standard.

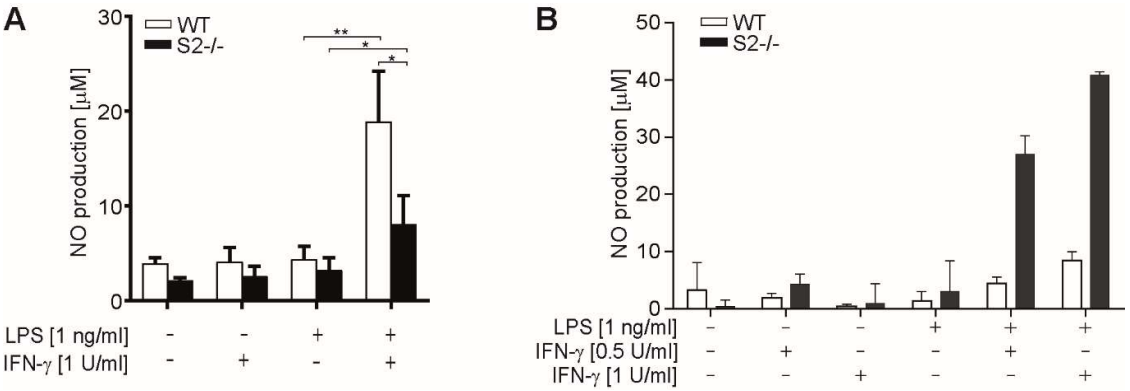

Figure 4.6 *NO production in STAT2 deficient and wild type macrophages in response to IFN-γ and LPS.* **A** – Griess assay results from wild type (WT) and STAT2 deficient (S2 -/-) immortalised mouse macrophages. Cells were left untreated or treated for 36 hours with 1 U/mL IFN-γ and/or 1 ng/mL LPS. Supernatant samples were treated with Griess reagent and analysed by spectrophotometry. NO concentration was subsequently calculated with a nitrite standard curve. *, $p<0.05$, ** $p<0.01$. **B** – Nitric oxide assay was performed as in **A**, but in macrophages that had been primed for 48 hours with 0.5 U/ml IFN-γ prior to treatment.

Treatment of macrophages with either LPS or IFN-γ separately failed to induce an increase in NO production, in line with previous literature suggesting the need for synergistic action (Lorsbach et al, 1993). Simultaneous exposure to both IFN-γ and LPS caused a significant increase in NO production in both genotypes, however, wild type macrophages produced significantly more NO compared to the wild type (**Figure 4.6A**). This was contrary to the increased IFN-γ sensitivity seen in gene expression assays (**Figure 4.5A**).

As seen in **Figure 4.2**, wild type macrophages inherently express more STAT1 than STAT2 knockout cells, an effect which can be normalised by priming with a low dose of IFN-γ. As such, nitric oxide production in response to IFN and LPS was analysed in cells that had been primed with a normalising concentration (0.5 U/mL) of IFN-γ for 48 hours (**Figure 4.6B**). Cells were subsequently washed and incubated with growth medium containing the indicated concentrations of LPS and/or IFN. As seen in unprimed cells, the application of either IFN or LPS alone did not induce secretion of NO in either genotype. Similarly, continued incubation with the priming concentration of IFN-γ did not increase NO concentration. A remarkable increase in NO production was seen in primed STAT2 knockout macrophages treated with

both IFN-γ and LPS, significantly more so than that seen in the wild type cells, reversing the previously observed phenomenon. In fact, the primed STAT2 deficient cells released more than double the NO detected by unprimed wild type cells (Compare **Figure 4.6A** to **B**). This indicated that induction of nitric oxide, a key IFN-γ regulated process, in primed STAT2 deficient macrophages was much more efficient than in the wild type although the opposite was true in the unprimed state.

4.3.2. Lack of STAT2 enhances suppression of *T.gondii* by immortalised macrophages.

The protozoan, *Toxoplasma gondii,* is an obligate parasite that is amongst the most common parasite of humans and other mammals, such as cats. The immune response to this parasite is well developed in order to minimise the pathogenicity of this species, and the result is an often benign infection that causes complications almost exclusively in pregnancy. The immune response to this parasite is highly IFN-γ dependent (Suzuki et al, 1988). As such, it was considered a suitable model to investigate the effects of STAT2 deficiency on type-2 IFN-mediated immune responses. In humans, *T. gondii* undergo the lytic cycle (reviewed in Blader et al, 2015), which involves penetration into the host cell, the formation of cytoplasmic cysts within which replication takes place, and finally emergence from the cell (**Figure 4.7**).

The ability of *T. gondii* to replicate in immortalised wild type or STAT2 knockout macrophages was investigated. Macrophages were grown for 48 hours in the absence or presence of various IFN-γ concentrations. Cultures were subsequently seeded with parasites at a multiplicity of infection (MOI) of 3. After 5 hours for parasite entry, extracellular parasites were washed away and cells were incubated for up to 5 days in a medium containing IFN-γ at the concentration they had been exposed to previously. Samples of supernatant were taken 24, 48, 72 and 150 hours post infection and the proliferation of parasite was determined by counting in a haemocytometer (**Figure 4.8**).

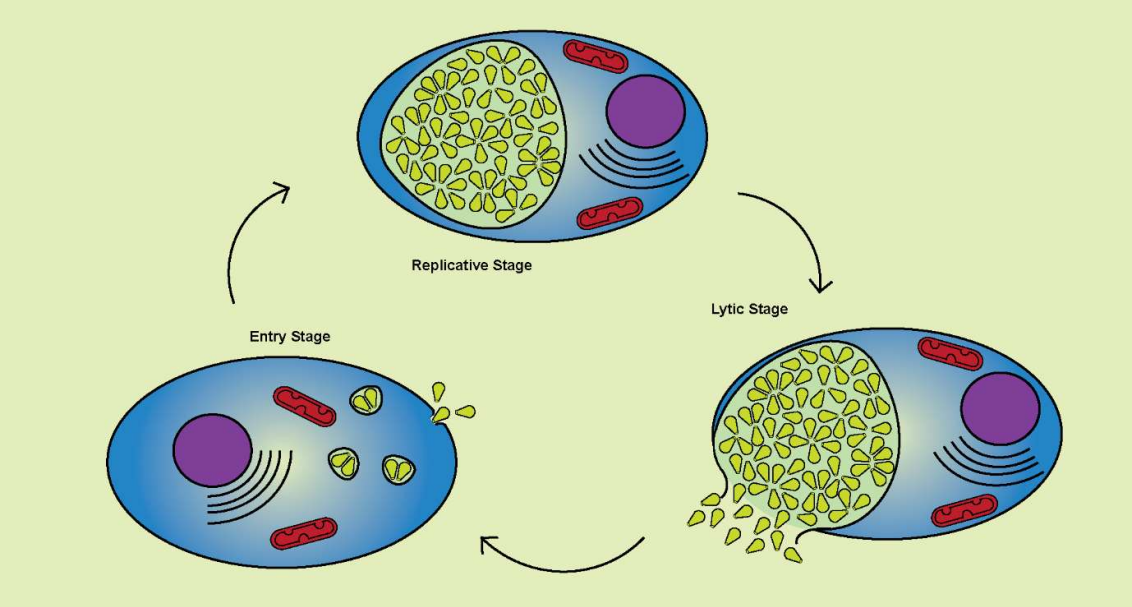

Figure 4.7 *Lytic cycle of the protozoan parasite, Toxoplasma gondii, in non-feline mammalian cells***.** When infecting non-feline mammals the parasite exists in a tear-drop shaped tachyzoite form. During the ***entry stage*** the parasite attaches to the host cell membrane and usually gains entry within 5 hours. Once inside the host the parasite maintains itself within a vacuole structure. Within this structure the parasite enters the ***replicative stage*** and begins asexual reproduction by a process known as endodyogeny. This process typically takes around 8 hours to complete after which the ***lytic stage*** begins. In keeping with its name, this stage usually involves the destruction of the host cell and releases the parasites into the extracellular matrix where they can infect neighbouring cells.

Macrophages infected with *T. gondii* in the absence of IFN-γ were unable to prevent the proliferation of the parasite, which increased exponentially over time regardless of genotype (**Figure 4.8**, top left). Treatment of macrophages with 50 U/mL of IFN-γ, however, was sufficient to protect both genotypes of macrophages from parasite growth (**Figure 4.8**, top right). This confirmed the essential role of IFN-γ in the immune response to *T. gondii* whilst also demonstrating the ability of immortalised macrophages to contain the parasite load. A 50-fold reduction in IFN-γ concentration (**Figure 4.8**, bottom left) was sufficient to protect the STAT2 deficient cells but the parasite managed to proliferate in the wild type macrophages, albeit not to the same extent as the untreated case. Under a very low IFN-γ treatment of just 0.1 U/mL, STAT2 deficient macrophages still controlled *T. gondii* growth, however, the parasite was able to proliferate in wild type to a similar level seen without IFN.

This indicated that enhanced IFN-γ responsiveness in STAT2 deficient cells extended to anti-parasitic immunity.

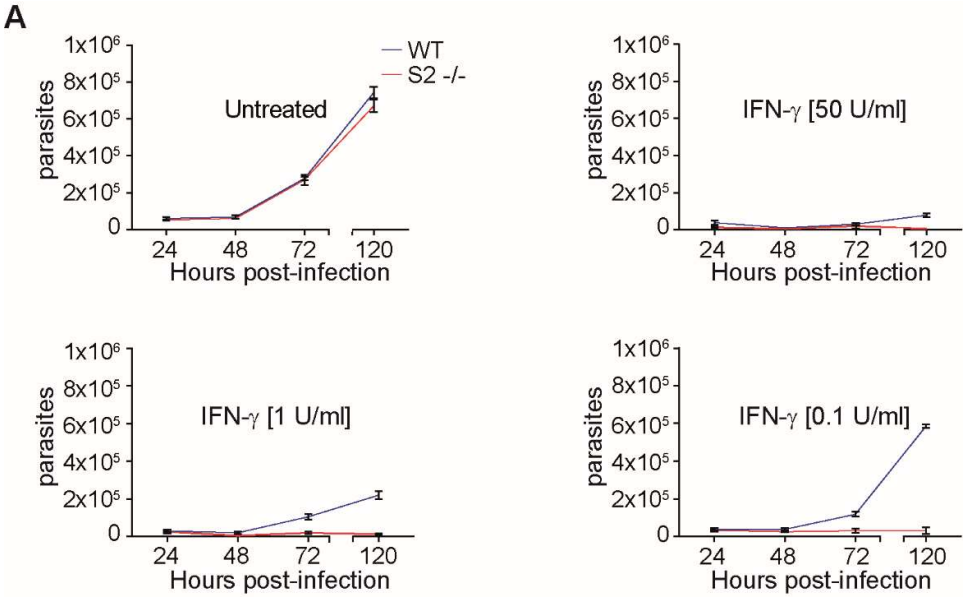

Figure 4.8 *STAT2 deficient cells are more responsive to anti-parasitic effect of IFN-γ* **A** – Parasite proliferation assay results from wild type (WT) and STAT2 deficient (S2 -/-) immortalised mouse macrophages. Cells were treated with the indicated concentrations of IFN-γ 48 h prior to infection with *T. gondii* at an MOI of 3. Extracellular parasites 5 h after infection were removed and cells were grown for a further 120 h in the presence of the indicated IFN-γ. Extracellular parasite numbers at 24, 48, 72 and 120 h were counted in an improved Neubauer chamber. Results are representative of triplicate samples from two independent experiments.

To specifically investigate the role of STAT2 L82A in terms of IFN-γ mediated anti-parasitic immunity, the infection experiments were repeated using human fibrosarcoma cells either lacking STAT2 (U6A) or reconstituted with wild type (U6A-S2WT) or L82A (U6A-S2L82A) STAT2 (**Figure 4.9**). In the absence of IFN-γ, *T. gondii* proliferated exponentially over the course of the experiment (**Figure 4.9**, top left). Treatment with 50 U/mL of IFN-γ was capable of providing incomplete protection to all cells, however the STAT2 deficient and L82A mutant cell lines were better protected than the wild type expressing cells (**Figure 4.9**, top right). This was also the case with lower concentrations of IFN, with STAT2 L82A and STAT2 deficient cells responding equally better than the cells expressing wild type STAT2

(**Figure 4.9**, bottom panels). Taken together, this experiment confirmed that the mutation of STAT2 at residue 82 was capable of enhancing anti-parasitic activities in response to IFN-γ.

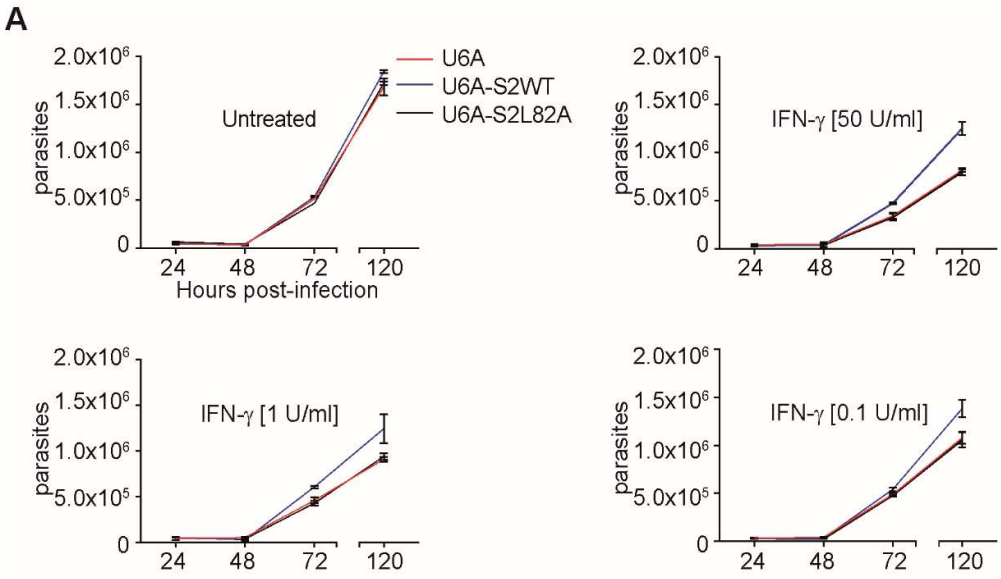

Figure 4.9 *STAT2 L82A mutation enhances the anti-parasitic effect of IFN-γ* **A** – Parasite proliferation assay results using human cells deficient in STAT2 (U6A) or reconstituted with wild type (U6A-S2WT) and STAT2 L82A (U6A-S2L82A). Cells were treated with the indicated concentrations of IFN-γ 48 h prior to infection with *T. gondii* at an MOI of 3. Extracellular parasites 5 h after infection were removed and cells were grown for a further 120 h in the presence of the indicated IFN-γ. Extracellular parasite numbers at 24, 48, 72 and 120 h were counted in an improved Neubauer chamber. Results are representative of triplicate samples from two independent experiments.

Having confirmed that STAT2 has an inhibitory role in IFN-γ anti-parasitic immunity *in vitro*, the ability of peritoneal macrophages from IFN-γ treated mice to combat the immune response was investigated. Wild type and STAT2 deficient mice (8 of each genotype) were treated with 5 µg of carrier free IFN-γ by intraperitoneal injection on two consecutive days. As a control, 5 mice of each genotype were injected with PBS instead of IFN-γ. The mice were sacrificed 24 hours after the second injection and peritoneal leucocytes were collected. Macrophages can be isolated from peritoneal samples via their adhesion to tissue culture dishes (McLeod and Remington, 1977). Isolated macrophages were inoculated with *T. gondii* at an MOI of 3 and incubated in the absence of IFN or with 1 U/mL IFN-γ for 120

hours (**Figure 4.10**). As before, parasite egress into the extracellular supernatant was quantified via use of a haemocytometer.

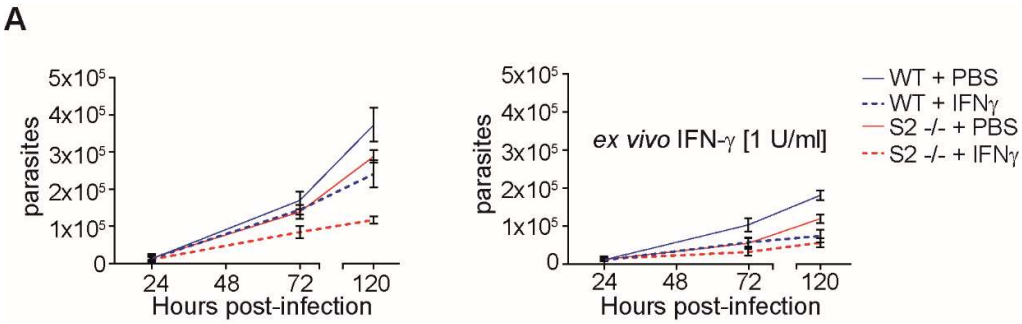

Figure 4.10 *Peritoneal macrophages from STAT2 deficient mice show enhanced anti-parasitic activity mediated by IFN-γ* **A** – Parasite proliferation assay results using peritoneal macrophages isolated from wild type (WT) and STAT2 deficient (S2 -/-) mice. Mice were injected *i.p* with 5 µg IFN-γ (n=8 per genotype) or PBS (n=5 per genotype) on two consecutive days prior to isolation of peritoneal macrophages. Macrophages were subsequently infected with *T. gondii* at an MOI of 3. Extracellular parasites 5 h after infection were removed and cells were grown for a further 120 h in the absence or presence of 1 U/mL of IFN-γ. Extracellular parasite numbers at 24, 48, 72 and 120 h were counted in an improved Neubauer chamber. Results are representative of duplicate samples from each mouse.

Unlike the immortalised macrophage cell lines the control conditions suggested inherent differential anti-parasitic immunity between wild type and STAT2 knockout mice, perhaps due to reduced STAT1 expression. Under these conditions (PBS injections), parasite proliferation after 120 hours was higher in the presence of wild type macrophages compared to STAT2 deficient cells (**Figure 4.10**, left panel). Regardless of genotype, mice injected with IFN-γ showed better resistance to parasite proliferation compared to their respective controls. However, once again, the cells derived from STAT2 deficient were better protected than the wild type. The infection experiment was also performed in the presence of a low dose (1 U/mL) of IFN-γ present in the culture medium (**Figure 4.10**, right panel). Under these conditions, parasite proliferation was reduced, however the discrepancy between PBS injected wild type and knockout cells remained. In contrast, parasite growth was lowest in cells from mice injected with IFN-γ that were subsequently maintained in medium also containing IFN. In these conditions, wild type and STAT2-deficient cells were equally well protected. These results confirmed that an *in vivo* lack of

STAT2, contributed to better protection against *T. gondii* similar to that observed in the immortalised cells.

4.4. Expression of the major histocompatibility complex in STAT2-deficient cells

The presentation of intra- and extracellular proteins to highly specialised immune cells is fundamentally important to enable the cell-based immune response to infection. Macrophages are included within a group of immune cells described as professional antigen presenting cells. This group of cells have an important function presenting protein fragments called antigens by utilising a group of proteins collectively called the major histocompatibility complex (MHC). These complexes allow the display of either intracellular proteins (MHC Class I) or proteins from extracellular sources such as bacteria (MHC Class II). Type-2 interferon plays a key role in the regulation of the MHC system, especially in upregulating presentation of class II complexes (Schroder et al, 2004).

4.4.1. IFN-γ induction of MHC class II is enhanced in the absence of STAT2

The immortalised macrophage cell lines were utilised to investigate the expression of MHC class II. The expression of cell surface molecules can be quantified by fluorescent assisted cell sorting (FACS) assays. Cells can be decorated with fluorophore-conjugated antibodies against specific surface proteins prior to analysis of each individual cell in a capillary flow system, allowing the collation data from tens of thousands of cells in a single experiment. This approach was utilised with immortalised wild type or STAT2 deficient macrophages. Cells were either left untreated or treated for 72 hours with different concentrations of IFN-γ, prior to detection of cell surface MHC class II using an AlexaFluor-488 conjugated antibody (**Figure 4.11**). Cells were simultaneously stained with propidium iodide, which allowed the identification and subsequent removal of dead cells from the final analysis.

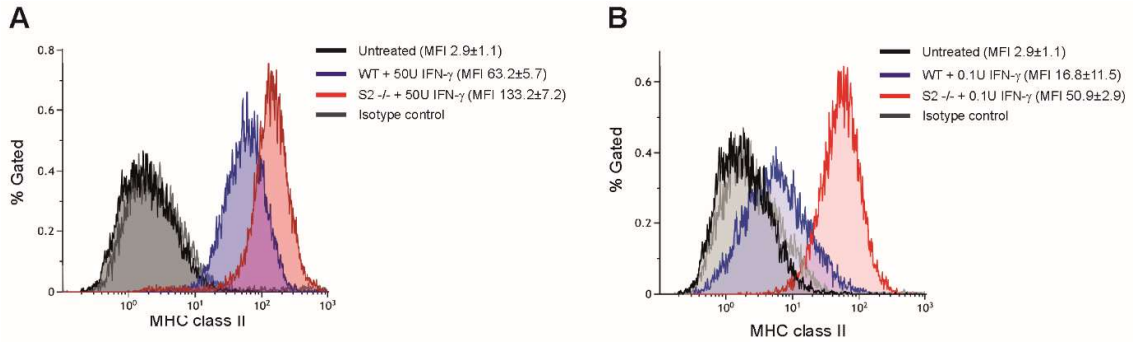

Figure 4.11 *STAT2 deficient immortalised macrophages show enhanced MHC class II induction by IFN-γ* **A** – Wild-type (WT) and STAT2 deficient (S2-/-) immortalised macrophages were left untreated or treated for 72 hours with 50 U/mL IFN-γ. Shown are histograms indicating MHC class II expression detected using fluorescence-assisted cell sorting (FACS) in combination with a specific AlexaFluor488- conjugated antibody. Shown are the median fluorescence intensities (MdFI) ± s.d. of two independent experiments. An isotype control antibody was used to indicate the non-specific background level of AlexaFluor488 detection, represented here by the resulting histogram from IFN-γ treated WT macrophages. **B** – Representative histograms from experiments performed as in **A** but with macrophages treated for 72 hours with IFN-γ at a concentration of 0.1 U/mL.

Upon treatment with 50 U/mL IFN-γ, cell surface expression of MHC class II increased considerably compared to untreated cells regardless of genotype, confirming the ability of IFN-γ to induce expression (**Figure 4.11A)**. However, STAT2 deficient macrophages expressed over double the amount of MHC class II than the wild type cells (**Figure 4.11A**, MFI of 133.2 compared to 63.2). This difference in IFN-γ sensitivity was even more pronounced at a much lower concentration of 0.1 U/mL, which resulted in three-fold more MHC class II in STAT2 knockout cells than in wild type (**Figure 4.11B**). These results demonstrated, *in vitro*, the regulation of MHC class II expression by STAT2.

Having observed a considerably enhanced IFN-γ response by immortalised macrophages, the ability of STAT2 to affect the *in vivo* MHC response to IFN was investigated. The peritoneal space of wild type and STAT2 deficient mice were injected with either PBS or 5 µg IFN-γ on consecutive days and sacrificed the following day. Peritoneal leukocytes were extracted and simultaneously decorated with PerCP-conjugated anti-MHC class II and AlexaFluor 488-bound anti-F4/80 antibodies before analysis by FACS. F4/80 is a cell surface marker that can discriminate murine macrophages from other cell types and thus was used to gate samples, allowing comparison of MHC expression between F4/80 positive macrophages of wild type and STAT2 knockout mice (**Figure 4.12**).

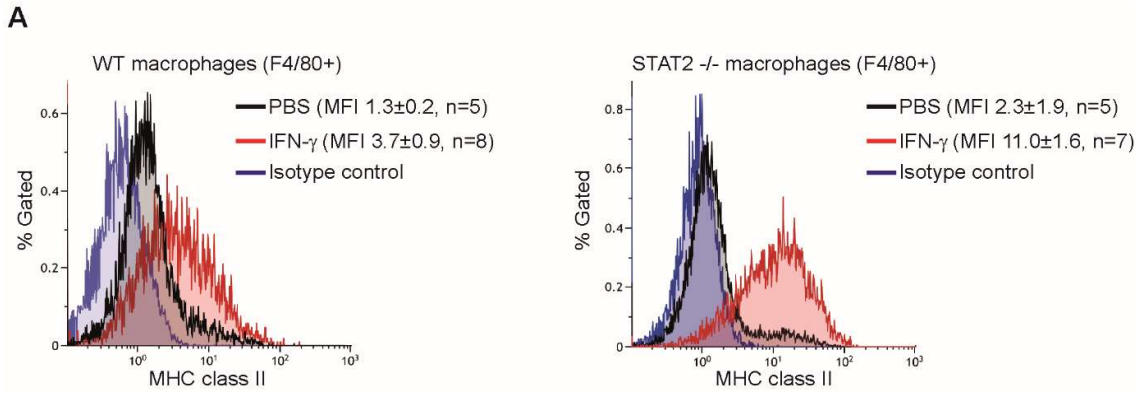

Figure 4.12 *Peritoneal macrophages from STAT2 deficient mice show enhanced MHC class II expression mediated by IFN-γ* **A** – Representative histograms of MHC class II expression of F4/80+ peritoneal leukocytes isolated from wild-type (WT) mice injected with either PBS (n=5) or 5 µg IFN-γ (n=8) on consecutive days. MHC class II expression was detected using fluorescence-assisted cell sorting (FACS) in combination with a specific PerCP- conjugated antibody. An isotype control antibody was used to indicate the non-specific background level of PerCP detection, represented here by inclusion of a representative histogram from IFN-γ injected WT mice. F4/80+ cells were identified using an AlexaFluor488-conjugated anti-F4/80 antibody. Shown are the median fluorescence intensities (MdFI) ± s. d. **B** – Representative histograms from experiments performed as in **A** but with STAT2 deficient (S2-/-) mice receiving injections of either PBS (n=5) or 5 µg IFN-γ on 2 consecutive days. The isotype control is representative of background PerCP detection in cells isolated from IFN-γ injected S2 -/- mice. Shown are the median fluorescence intensities (MdFI) ± s. d.

In PBS-injected control animals (n=5 per genotype), similar levels of MHC class II expression were observed between the strains (**Figure 4.12**, compare MFI of 1.3±0.2 to 2.3±1.9). In agreement with the *in vitro* findings, macrophages from STAT2 deficient mice injected with IFN-γ showed a higher MHC class II expression than the similarly treated wild types. To this end the STAT2 deficient cells expressed approximately 3-fold more MHC than the wild type (**Figure 4.12**, compare MFI of 3.7±0.9 to 11.0±1.6), despite expressing less MHC in the PBS control setting. The results of both the *in vitro* and *in vivo* FACS experiments suggested that the absence of STAT2 increases the sensitivity of the MHC class II system to IFN-γ.

4.4.2. Abolishing the interaction between STAT2 and STAT1 increases IFN-γ mediated MHC class I expression.

The previous results supported the position that STAT2 played a regulatory role in the induction of MHC expression by IFN. Consequently, the role of the N domain interaction of STAT1 and STAT2 in explaining this phenomenon was investigated using the human U6A cells lacking or reconstituted with wild type or STAT2 L82A. The ability to express MHC class II is restricted to professional antigen presenting cells, thus the U6A fibrosarcoma lines were deemed unsuitable to test regulation of these complexes. The MHC class I system is much more widespread and thus the ability of IFN-γ to induce cell surface expression of this complex was investigated in cells. The native and reconstituted U6A cell lines were treated with different concentrations of IFN-γ for 72 hours or left untreated, prior to suspension and decoration with APC-conjugated anti-MHC class I antibodies. Cells were also incubated with propidium iodide in order to exclude dead cells from the final analysis. The expression of MHC class I on the surface of living cells was subsequently analysed by FACS (**Figure 4.13**). U6A cells reconstituted with wild type STAT2 showed an expression of MHC class I on the cell surface that increased in the presence of IFN-γ in a concentration dependent manner (**Figure 4.13A**). The fold increase of MHC class I in response to 1 U/mL IFN-γ was ~1.3, increasing to ~1.5 in cells exposed to 5 U/mL and approximately 3-fold in response to 50 U/mL, the highest concentration used. This pattern was also observed in STAT2 deficient U6A cells, however, the expression of MHC class I in these cell lines was not only constitutively higher but the fold increase induced by IFN-γ was also enhanced (**Figure 4.13B**). In U6A cells, IFN-γ concentrations of 1, 5 and 50 U/mL resulted in roughly 1.6-, 2- and 3.4-fold increases in MHC detection respectively. Interestingly, the U6A cells reconstituted with the L82A mutant of STAT2 displayed a yet higher IFN-γ response (**Figure 4.13C**). At the lowest concentration of IFN-γ, a 2-fold increase in MHC was already detected, whilst cells treated with 5 and 50 U/mL exhibited 2.8- and 4.7-fold increases. The differential IFN-γ sensitivity, between the STAT2 deficient and STAT2 L82A reconstituted cells in particular, supported the hypothesis that the N domain interactions between STAT1 and STAT2 played a key role in regulating this cardinal function of type 2 interferon.

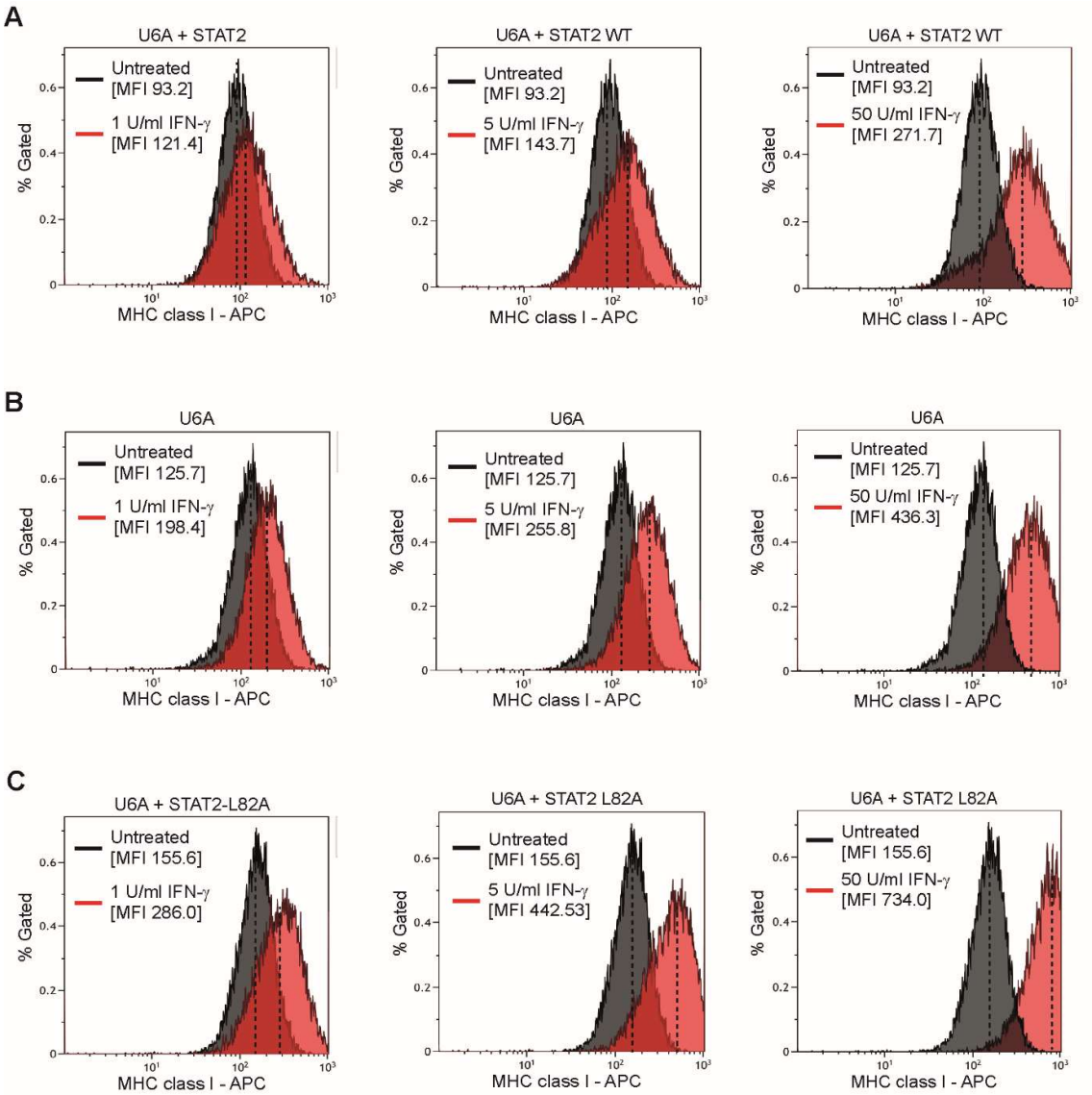

Figure 4.13 *The lack of STAT2 and presence of STAT2 L82A are both sufficient to improve the IFN-γ sensitivity of fibrosarcoma in terms of MHC class I expression* **A** – Human U6A fibrosarcoma cells reconstituted with STAT2 were either left untreated or treated for 72 hours with 1, 5 or 50 U/mL IFN-γ. MHC class I expression was detected by FACS in combination with a specific allophycocyanin (APC) - conjugated antibody. Shown are the median fluorescence intensities (MdFI), with histogram peaks (mode) identified by dotted lines for clarity. Gating for cells was done by forward and side scatter plots and kept the same throughout **B** – Histograms from experiments performed as in **A** but with U6A cells deficient in STAT2 **C** – Histograms from experiments performed as in **A** but with U6A cells stably reconstituted with STAT2 L82A.

4.5. Anti-proliferative effects of IFN-γ in STAT2-deficient cells

Interferon is intimately linked to the management of cell growth and death. Cells infected with viruses, for example, are driven to apoptosis by interferon in order to prevent viral replication and spread. In addition, damaged or tumorigenic cells can be encouraged into cell cycle arrest by interferon secreting immune cells. Whilst all types of IFN are capable of inducing cell death, interferon-γ has a unique function as a cytokine secreted by tumour-sensing lymphocytes such as cytotoxic T-cells. The arrest of cell growth in response to IFN was investigated in macrophages by analysing known markers for senescence and apoptosis.

4.5.1. Enhanced IFN-γ induced heterochromatin formation in STAT2-deficient cells

Senescence is the process by which cells irreversibly cease to divide, instead remaining in an inert state. This mechanism of cell growth arrest is an important tool utilised by the immune system in preventing the proliferation of mutated and potentially tumorigenic cells. Interferon-γ has been implicated in driving cancer cells into senescence (Braümuller et al, 2013; Wang et al, 2014). The primary facilitator of IFN-γ signalling, STAT1, has been shown to drive the expression of cyclin dependent kinase (CDK) inhibitors in order to prevent cell cycle progression (Chin et al, 1996). Whilst the identification of senescent cells by their secretome remains a developing field (Matjusaitis et al, 2016), one established feature of senescent cells is the formation of senescence-associated heterochromatin foci (SAHF) within the nucleus (Aird and Zhang, 2013).

The role of SAHF appears to be a physical remodelling of the chromatin structure that prevents access to genes that promote proliferation. The proteins which maintain these structures can be used to identify them and include members of the heterochromatin protein 1 (HP1) family. The detection of HP1γ that has been phosphorylated at a key serine residue, Ser83, has been successfully utilised as an assay to identify SAHF and subsequently detect senescent cells (Braumüller et al, 2013). In order to assess the role of STAT2 in the regulation of cell proliferation, immortalised macrophages derived from wild type and

STAT2 knockout mice were treated with IFN-γ at concentrations of 0.1, 10 and 50 U/mL for 72 hours. Untreated cells of each genotype were included as negative controls. Cells were fixed and stained with anti-phospho-S83 HP1γ antibody subsequently decorated with Cy3. Nuclei were counterstained with Hoechst and cells were analysed by fluorescent microscopy (**Figure 4.14**).

In the absence of IFN-γ, phosphorylated HP1γ was not detected in any cells, regardless of genotype, in line with their immortalised state (**Figure 4.14**, top row). The detection of phospho-S83 HP1γ was observed in both wild type and STAT2 deficient cells treated with the highest concentration of IFN-γ (**Figure 4.14**, second row). The phospho-HP1γ was located within the nuclei as punctate structures, previously identified as SAHF (Braümuller et al, 2013), and this indicated the ability of IFN to drive both cell lines into senescence. At lower concentrations, IFN-γ treatment failed to drive detectable SAHF formation in wild type macrophages as opposed to the STAT2 deficient macrophages which displayed phospho-HP1γ containing structures following treatment with as little as 0.1 U/mL IFN-γ (**Figure 4.14**, third and fourth rows). These results supported previous findings that IFN-γ can induce SAHF formation, whilst highlighting an increased sensitivity to form SAHF in STAT2 knockout cells compared to their wild type counterparts.

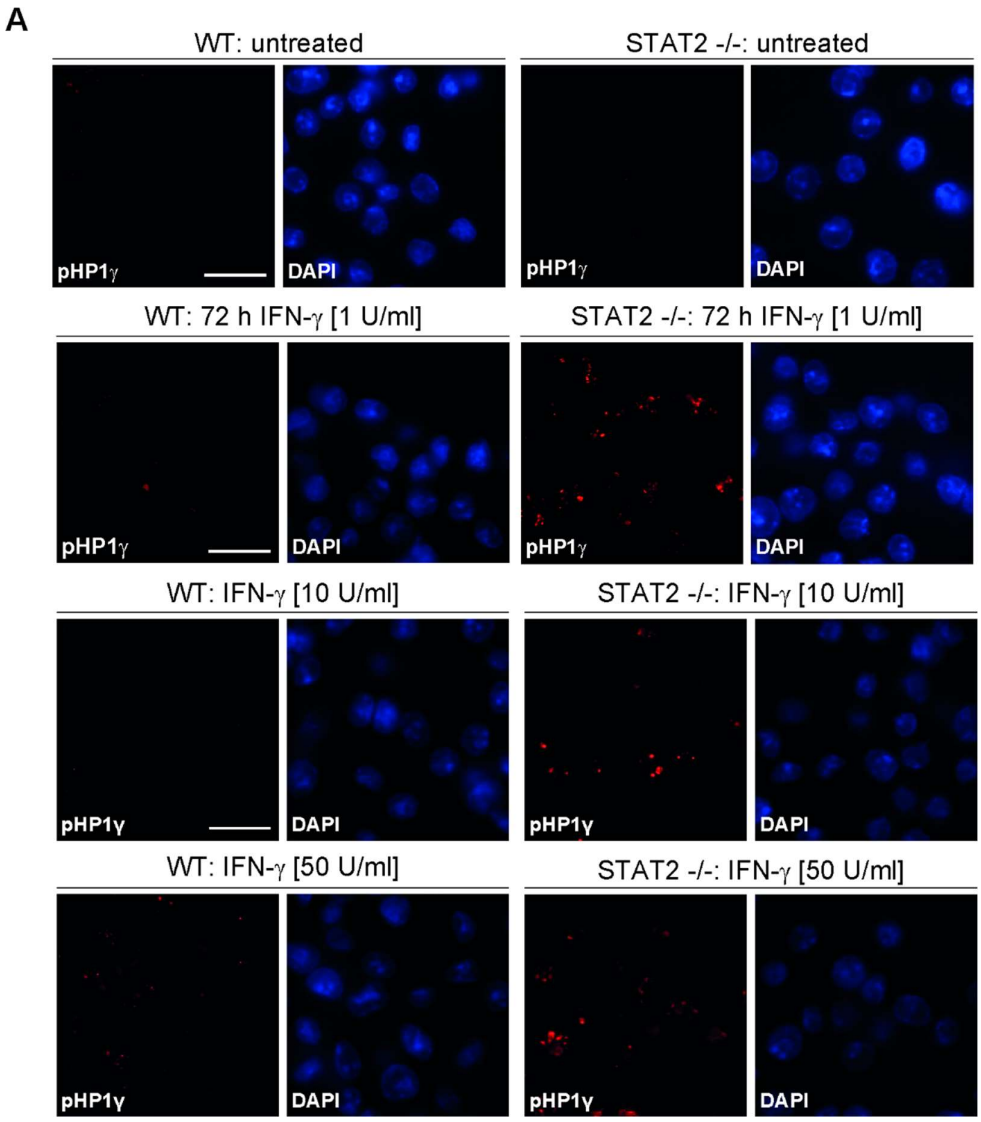

Figure 4.14 *Formation of senescence –associated heterochromatin foci (SAHF) can be induced by IFN-γ at lower concentrations in immortalised macrophages from STAT2 deficient mice.* **A** – Fluorescent micrographs of immortalised macrophages from wild type (WT) and STAT2 knockout (S2 -/-) mice left untreated or treated for 72 hours with indicated concentrations of IFN-γ. The formation of SAHF was detected using a Cy3-decorated antibody against phospho-S83 HP1γ, nuclei were counterstained with Hoechst. Images represent 3 independent experiments. Scale bar = 15 µm

4.5.2. IFN-γ triggers higher apoptotic marker presentation in the absence of STAT2

Upon infection or DNA damage, many cells undergo apoptosis. In contrast to senescence, apoptosis is a form of programmed cell death that results in the removal of the cell. Apoptosis can be triggered by internal stress such as DNA damage or by external stimuli such as cytokine or pathogen recognition. The ability to induce apoptosis is an important tool available to the immune response as it can prevent the spread of intracellular pathogens and the proliferation of potential cancer cells. The initiation of apoptosis is another function of IFN signalling. Type-1 IFNs are well established apoptotic signalling molecules whilst type-2 IFN has been demonstrated to both drive (Herbst et al, 2011; Barthson et al, 2011) and inhibit apoptosis (Buschle et al, 1993), depending on the target cell.

Unlike senescence, which results in a specific set of permanent changes to a living cell, apoptosis must be differentiated from other forms of cell death such as necrosis and autophagy. One defining aspect of apoptosis is an unstable cell membrane that results in the extracellular exposure of phosphatidylserines, a process that is believed to enable the detection and clearance of apoptotic cells by macrophages (Martin et al, 1995). This process can be detected by the binding of annexin V-conjugated fluorophores which can subsequently be analysed by FACS (Koopman et al, 1994). When used in conjunction with propidium iodide, which fluoresces when bound to DNA of dead cells, cells in the early stages of apoptosis can be isolated. This assay was used to investigate the induction of apoptosis in macrophages by IFN-γ (**Figure 4.15**).

Wild type and STAT2 deficient macrophages were either left untreated or treated for 48 hours with IFN-γ at concentrations of 1, 5 and 50 U/mL. Cells were then simultaneously labelled with FITC-conjugated annexin V and propidium iodide prior to analysis by FACS. In untreated cells, a similar proportion of living (98.76% of wild type and 99.01% of STAT2 -/-) and early apoptotic (wildtype: 0.66% vs STAT2 -/-: 0.7%) was observed between the genotypes (**Figure 4.15**, upper panels). Treatment of wild type cells with 1 U/mL IFN-γ resulted in detection of a small population (1.35% of total) of apoptotic cells that increased only slightly with higher concentrations (**Figure 4.15**, left column). In contrast, the lowest

dose of IFN-γ drove a higher proportion of STAT2 -/- cells (2.61% of total after 1 U/mL IFN-γ) into apoptosis than the highest dose, 50 U/mL, did in the wild type cells (1.79%). In addition, increased concentrations of IFN-γ resulted in a higher proportion (up to 7.09% of total) of apoptotic STAT2 -/- cells (**Figure 4.15**, right column). This confirmed that whilst IFN-γ has a weak ability to drive immortalised macrophages into apoptosis, this is increased in macrophages lacking STAT2 expression.

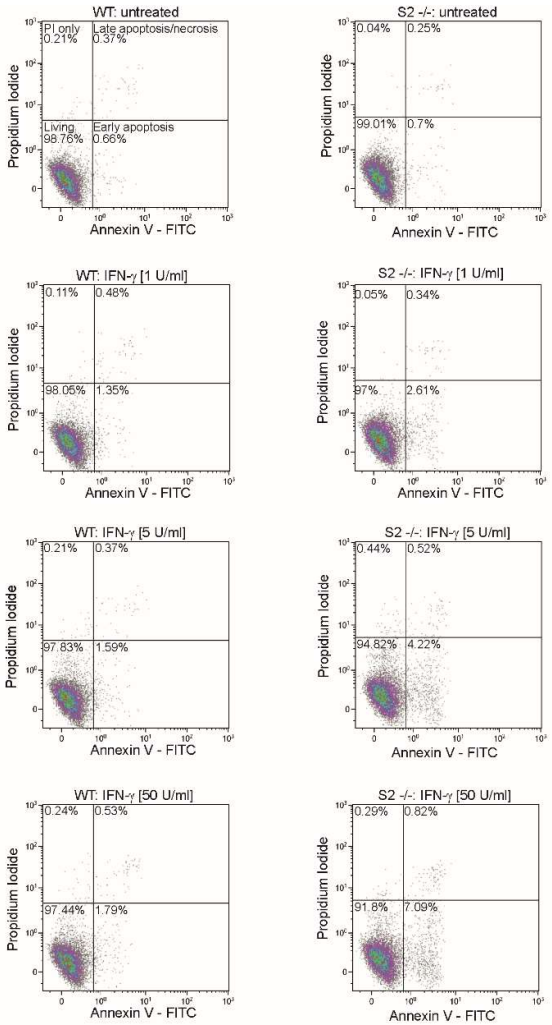

Figure 4.15 *Increased IFN-γ induced apoptosis in STAT2 deficient macrophages* **A** – Contour plots showing detection of early apoptotic cells by simultaneous annexin V and propidium iodide staining. Immortalised macrophages from wild type (WT) and STAT2 knockout (S2 -/-) mice were left untreated or treated for 72 hours with IFN-γ at 1 , 5 or 50 U/mL, prior to suspension and subsequent staining with FITC-conjugated annexin V and propidium iodide. Cells were gated as living (double negative, bottom left), early apoptotic (annexin V only, bottom right), dead (double positive, top right) and non-apoptotic dead (PI only, top left). Results represent 2 independent experiments.

4.6. Chapter Summary

In **chapter 3** a novel behaviour of STAT2, namely to inhibit nuclear accumulation of activated STAT1 was described. In order to investigate further, **chapter 4** detailed the characterisation of cell lines lacking STAT2 or expressing the L82A mutant form of STAT2. This facilitated investigation into the role of STAT2 in several IFN-γ driven biological responses.

The induction of several genes by IFN-γ was found to be increased in the absence of STAT2, which corroborated the hypothesis that increased nuclear access to activated STAT1 facilitated transcription of target genes. This was in spite of the fact that cells lacking STAT2 appeared to show reduced innate STAT1 expression, although this could be overcome by priming with low concentrations of IFN.

Several cardinal functions of IFN-γ were enhanced in cells either lacking STAT2 or expressing a STAT2 mutant that did not inhibit STAT1 nuclear accumulation. These included the secretion of nitric oxide and control of the proliferation of an intracellular protozoa. The regulation of MHC expression by IFN-γ was also investigated in the context of STAT2 absence or mutation. Nitric oxide production was found to be enhanced in macrophages lacking STAT2, but only once STAT1 expression had been normalised by IFN priming. The ability of IFN-γ signalling to limit *T. gondii* proliferation in cells was found to be superior in cells either lacking STAT2 entirely or expressing the L82A mutant of STAT2. Abolishing the inhibition of STAT1 by STAT2 also facilitated improved MHC expression in macrophage and fibrosarcoma cell lines. Finally, the regulation of cell proliferation by STAT2 was investigated. In the absence of STAT2, cells could be driven into both senescence and apoptosis by lower concentrations of IFN-γ than the wild type.

The expression of MHC and the anti-parasitic activity regulated by IFN was also investigated in an *in vivo* model of STAT2 deficiency. Macrophages derived from IFN-γ injected STAT2 -/- mice showed a substantially higher MHC class II expression than wild type, in agreement with *in vitro* results. Additionally, primary macrophages from STAT2 -/- mice were better protected against *T. gondii* infection.

5. Discussion

Cytokine signalling is integral to the organisation of the immune response and maintaining the balance between effective pathogen destruction and avoiding self-damaging autoimmunity. In turn, cellular responses to cytokines are dependent on tight regulation of the JAK-STAT pathway. This is particularly important when considering that over 50 distinct cytokines converge on a family of 7 STAT proteins. Since the discovery of the JAK-STAT pathway in the early 1990's, a wide range of regulatory mechanisms have been described – from negative feedback loops involving target genes to antagonism between the individual STAT family members. STAT1 and STAT3 are an example of antagonism between STAT proteins; they compete directly for DNA binding sites (Hirahara et al, 2015) and also indirectly affect the activity of one another through target genes (Dimberg et al, 2012). In stark contrast, STAT1 and STAT2 are viewed as highly synergistic members of this family which contribute to the innate immune response through their role as interferon signal transducers.

Interferon signalling primarily functions through one of two dimeric species, STAT1 homodimers and STAT1-STAT2 heterodimers, which have both overlapping and exclusive target genes. At a simplistic level this allows for the distinction between type-1 (heterodimer) and type-2 interferon (homodimer) signalling. In reality, interferon signalling is more complex as type-1 interferon also induces the formation of STAT1 homodimers, albeit as a minority (Au-Yeung et al, 2013; Begitt et al, 2014). The production of either homodimer or heterodimer was once believed to be a result of events at the IFN receptor, due to latent STATs existing as monomers. However, it is now acknowledged that STAT1 can form homodimers and heterodimers with STAT2 or STAT3 dimers prior to activation (Stancato et al., 1996; Ho et al, 2006). Mounting evidence suggests a variety of biological roles for these unphosphorylated STAT interactions, from perpetuation of interferon signalling by the formation of macromolecules (Droescher et al., 2011) to the activation of DNA damage resistance genes in certain cancer cells (Cheon et al, 2014). With this in mind the function of unphosphorylated STAT1-STAT2 heterodimers was investigated.

5.1. The association of STAT1 and STAT2 via amino-terminal domain interactions

Research has thus far demonstrated that STAT2 is unique amongst its protein family in that it fulfils its canonical role as a transcription factor not as a homodimer but as a heterodimer with STAT1 (Steen and Gamero, 2013). Whilst this is certainly not the only case in which STAT hetero-dimerisation is observed, the vast majority of cytokines appear to primarily induce STAT homodimers with some heterodimeric species produced in addition. STAT2 also stands out as having a much narrower range of activating cytokines than other STATs, being restricted mostly to type-1 and 3 interferon signalling (Steen and Gamero, 2013). It is possibly because of this relatively restricted role that the majority of recent studies into STAT2 focus on its nature as a target of several viruses (Parisien et al, 2002; Xu et al, 2014; Grant et al, 2016) as opposed to further understanding its physiological roles. Although important in establishing the critical nature of STAT2 in anti-viral immunity, focus on this area of research gives the impression that the functional aspect of STAT2 is sufficiently well understood. However, in light of the work within this thesis, there is clearly much more scope for improvement than previously thought.

Another aspect of STAT biology that has, until recently, proven somewhat underappreciated is the ability to dimerise independent of activation. The existence of phosphorylation independent dimers was first suggested not too long after the discovery of STATs (Stancato at el., 1996). Two decades on and, at least in the case of STAT1, both the existence and molecular interactions which underpin these structures have now been characterised. Yet, despite these advances appreciation our understanding of their physiological functions has only just begun to be realised.

The first discovered, and arguably most important, function to be discovered is the facilitation of STAT protein dephosphorylation. By transitioning into an anti-parallel conformation activated STAT proteins allow TC45 phosphatases access to their critical tyrosine residues which in turn results in STAT inactivation (Meyer et al, 2004). Within this context, it is not surprising that anti-parallel heterodimerisation of STAT1 and STAT2 also occurs. As part of the ISGF3 complex activated STAT1-STAT2 heterodimers translocate to the nucleus and bind DNA in the same manner as STAT1 homodimers, therefore it is reasonable to predict that they are subject to a similar mechanism of inactivation. Whilst this thesis'

work does not investigate the mechanism of ISFG3 inactivation, the evidence it provides of STAT1-STAT2 anti-parallel dimerisation does support the plausibility of such a hypothesis.

Work by Droescher et al. (2011) uncovered another functional aspect of these dimers, namely, the regulation of STAT1 signalling via the formation of paracrystalline reservoirs within the nucleus. These STAT macrostructures serve to both prolong IFN-γ signalling and allow its subsequent regulation by another unrelated protein, SUMO (Begitt et al, 2011). The ability of STAT1 and STAT2 to dimerise via their amino-terminal domains raises the question of whether such macrostructures are seen in IFN-α/β, and to what extent this exposes type-I interferon to the influence of SUMOylation. The relevance of this question is all the more apparent, as IFN signalling has recently been shown to substantially alter the expression of genes that regulate SUMOylation itself (Maarifi e al, 2015).

5.2. The role of the N-domain in phosphorylation independent STAT interactions

The interaction of STAT1 and STAT2 was first observed in the absence of interferon (**Figure 3.2**) and thus, its relevance within this context was explored first. The clearest result of this interaction was the change in STAT1 cellular distribution in cells overexpressing STAT2, compared to those that did not. The strong nuclear export signal within STAT2 results in a resting distribution that appears almost entirely outside the nucleus, whilst STAT1 can be detected throughout the cell. The subsequent shift in STAT1 subcellular distribution in the presence of overexpressed STAT2 supported two conclusions. The first was that, as previously mentioned, STAT1 and STAT2 can interact in the absence of interferon signalling. In the context of the current literature this is not an unheralded finding; a prior study also noticed a change in STAT1 distribution in cells overexpressing STAT2 (Melen et al, 2003) however this was not explored further at the time. Additionally, the homodimerisation of STAT1 independent of interferon signalling has been conclusively shown in recent years (Mao et al, 2005) and, given the structural similarity within the STAT family, the extension of this interaction to other members builds upon, rather than rewrites, the currently accepted model. Yet despite this finding representing a modest step forward in our understanding of STAT behaviour, it may well prove to be the basis of an altogether larger shift in interferon regulation of which more will be discussed later in this chapter.

The second conclusion from these initial investigations, was that this interaction did not significantly affect the rate of nuclear export of STAT2, as the line scan analysis showed the nucleocytoplasmic ratio of STAT2 remained almost identical in the presence or absence of concurrently overexpressed STAT1 (**Figure 3.2**). This was an important, albeit not conclusive, observation that supported the hypothesis that these were antiparallel heterodimers. The basis for this support is in the current model of type-I interferon signalling, where a parallel STAT1-STAT2 heterodimer produces a bipartite NLS (Melen et al, 2003) that facilitates the entry of both into the nucleus. In fact, recent research has identified a factor termed u-ISGF3 that includes unphosphorylated STAT1, STAT2 and IRF9 that enters the nucleus and upregulates a specific set of IFN target genes (Cheon et al, 2013). Such a model would suggest that if the colocalization of latent STAT1 and STAT2 were to predominantly be in the parallel conformation, the subcellular distribution of both STAT1 and STAT2 would not be localised to the cytoplasm as strongly as it was observed in **Figure 3.2**.

In light of these investigations, some questions were raised regarding the previous literature. STAT1 has been shown to contain a weak NES within the coiled coil domain, which contributes to a distribution that is often more prominent in the cytoplasm but to a much lesser degree than STAT2 (Begitt et al, 2000). However, given that STAT2 clearly can interact with and influence the STAT1 distribution within cells, this weak STAT1 nuclear export activity in cells required re-examination. The distribution of STAT1 in cells deficient of STAT2 was analysed by line scan and still found to be slightly cytoplasmic (**Figure 3.8**). However, a STAT1 with a deletion mutation within the NES was found to have an even distribution between cytoplasm and nucleus. Similarly, the wild type STAT1 could be redistributed throughout the cell when active nuclear export was inhibited. These results confirmed that the NES within STAT1 has an influence on its subcellular distribution, but that its relevance in the context of the effect of STAT2 requires further investigation.

It is fair to assume that the N-domain interaction between STAT1 and STAT2 has an important biological function as it is highly conserved yet susceptible to a single point mutation. In this sense, it is similar to the corresponding interaction between STAT1 homodimers, which has been shown to provide the basis of both a mechanism to prolong IFN signalling (Droescher et al, 2011; Begitt et al, 2011) and terminate it (Meyer et al, 2004). Furthermore, the N-domain of both STAT1 and STAT2 have been found to be required for

their protein degradation by a variety mechanisms of viral immune evasion (Parisien et al, 2002). With the evidence of STAT1-STAT2 N-domain interactions presented in this thesis, further studies into the role of this interferon independent dimer species is warranted. Furthermore, the participation of IRF9 in this dimer was not investigated during this work and is a factor that one must consider when drawing conclusions, particularly in light of research suggesting the ability of latent STAT1 and STAT2 to bind IRF9 to form a complex U-ISGF3 that is proposed to drive gen selection of a small cohort of IFN target genes (Cheon et al, 2013).

5.3. The effect of STAT2 on nuclear translocation of phosphorylated STAT1

The accumulation of phosphorylated STAT proteins within the nucleus is a hallmark of cytokine signalling. In contrast to the rest of the interferons, IFN-γ signalling utilises STAT1 as the sole signal transducer. In light of the revelation that STAT1 and STAT2 do indeed interact independently of phosphorylation, the existence and effect of this contact during IFN-γ signalling was investigated. Strikingly, the co-localisation between STAT1 and STAT2 is not only maintained during IFN-γ signalling but is localised to the cytoplasm (**Figure 3.10**), despite no inhibition of STAT1 activation observed (**Figure 3.11**) The nature of STAT signal transduction requires translocation of the protein to nucleus and thus inhibition of this process is likely to have a significant impact on the cellular response. Furthermore, contrary to the situation between the latent STAT proteins, this cytoplasmic co-localisation is not caused by active nuclear export as the STAT2-ΔC mutant exhibit the same inhibition of pSTAT1 nuclear accumulation as wild-type (**Figure 3.5 and 3.12**).

These results represent the first example of an inactivated STAT protein inhibiting the nuclear accumulation of another. In addition, the basis for this effect is localised to the N-domain interaction as both the STAT1 F77A and STAT2 L82A mutations abrogate it. This provides initial evidence that inactive STAT2 may be an inherent negative regulator of STAT1 activity, a significant finding as STAT1 is activated in response to a far wider range of cytokines that STAT2. These results prompted two lines of further investigation; the

mechanism by which STAT2 inhibited STAT1 nuclear accumulation, and the biological effects of this inhibition.

During the course of this thesis, the characterisation of STAT1-STAT2 heterodimers in various states of activation was performed (**Figure 3.13**). This provided evidence that STAT1 and STAT2 are bound in an N-domain dependent manner even when one is phosphorylated and the other is not, producing a species termed a semi-phosphorylated dimer. A concurrent investigation detailed in (Ho et al, 2016), showed how this dimer species is unable to bind to the importin structures of the nuclear membrane and thus was excluded from entry into the nucleus.

Although these results together show an example of the mechanism by which STAT2 may inhibit STAT1 nuclear accumulation, it is not a direct observation of the mechanism itself. These studies used IFN-β, a type-I interferon, rather than IFN-γ in order to provide a positive control for the experiments. However, further evidence of the relevance of this semi-phosphorylated species was observed using a chimeric STAT2 molecule which had been previously shown to become activated by IFN-γ, due to incorporation of the SH2 domain of STAT1 (Heim et al, 1995). The expression of this hybrid molecule did not inhibit the nuclear accumulation of STAT1 unless an additional mutation, R602L, was incorporated which rendered the chimera unresponsive to IFN-γ once again (**Figure 3.14**).

In addition, a recent paper (Majoros et al, 2016) observed a reciprocal effect of STAT1 Y701F, incapable of activation, on the nuclear accumulation of STAT2 in response to type-I interferon. Thus the mechanism directly observed in this thesis, has been shown to result in a phenomenon that is very similar to the ability of STAT2 to inhibit STAT1 nuclear accumulation. That being said, the ability of STAT2 to inhibit STAT1 nuclear accumulation described in this thesis, is more biologically relevant than the reciprocal effect as it occurs within the natural setting as opposed to one in which STAT1 is mutated.

This thesis primarily investigates the impact of STAT2 on STAT1 nuclear accumulation, however the anti-parallel dimer of STAT1 is also integral to the redistribution of STAT1 after interferon signalling has terminated. In this respect, there is also a clear distinction between how the N-domain interaction between STAT1 and STAT2 behaves compared to that of a STAT1 homodimer. Mutations that disrupt the ability of STAT1 homodimers to take the anti-

parallel conformation, such as F77A, result in a hyper-phosphorylation phenotype following interferon stimulation (Meyer et al, 2004; Begitt et al, 2014). This behaviour was not observed in the STAT2 L82A mutant, which may suggest that the process by which GAF (STAT1 homodimers) and ISGF3 are inactivated by tyrosine phosphatases are not identical.

5.4. The role of STAT2 in IFN-γ dependent gene expression

Having observed the inhibition of STAT1 nuclear accumulation by STAT2, the impact of this phenomenon on the IFN-γ response was assessed. As initially observed, cells which lacked STAT2 showed a greater nuclear accumulation of STAT1. Thus it was predicted that STAT2-deficient cells would be more sensitive to IFN-γ, particularly at lower doses. A transgenic mouse line that is STAT2 deficient (S2-/-) has been available for some time but has until now primarily been used to investigate the impact of STAT2 loss on type-I interferon signalling (Park et al, 2000; Alazawi et al, 2013). Macrophages derived from these mice were characterised for their response to IFN-γ (**Figure 4.1**). Interestingly, the intrinsic expression of STAT1 in these cells was lower than in wildtype (WT) cell line (**Figure 4.1B**). This is likely to be due to a STAT2-dependent positive feedback loop involving type-II interferon signalling no longer being functional within these cells (Gough et al, 2010).

Importantly, despite a lower basal expression, the rate of STAT1 phosphorylation in response to IFN-γ was identical between WT and S2-/- cells (**Figure 4.1C**). This was not the case for STAT1 activation in response to IFN-β, which was approximately halved in the absence of STAT2. This partially supports an early model of sequential activation of first STAT2 followed by STAT1 in response to type-I interferon (Heim et al, 1995). However, in these macrophages at least, there remains a mechanism by which STAT1 can be activated by IFN-β in the absence of STAT2.

The first evidence of increased IFN-γ sensitivity in S2-/- cells was observed when both macrophage cell lines were exposed to a prolonged low dose of IFN. This resulted in an increase in the expression of STAT1 and, in WT cells, STAT2 over 48 hours, as both *STAT1*

and *STAT2* are themselves interferon stimulated genes. This process is a well-established phenomenon known as priming (Hu et al, 2002) and is important in the sensitisation of cells to cytokine signalling. Following priming with IFN-γ, the expression of STAT1 within S2-/- cells had increased to a higher level than found in similarly primed WT cells, despite a lower starting expression (**Figure 4.2**).

This example was repeated when a variety of priming concentrations were used with a dose of 0.5 U/ml of IFN-γ found to normalise the level of STAT1 between the two cell lines (**Figure 4.3**). This finding was important to the further utilisation of these cell lines within this thesis, as it facilitated a more genuine comparison of their interferon response. However this process also introduced a further variable, in that the priming of S2-/- and WT cell lines may influence STAT-independent regulators of the interferon response such as interferon receptor expression and global ubiquitination. In an attempt to account for this, initial studies into these cell lines used both un-primed and primed cells.

The expression of several key genes in response to IFN-γ was measured by RT-PCR in these macrophages. In the S2-/- cells, a number of genes showed a significantly increased sensitivity to IFN-γ such as *Cxcl10, Ido1* and *Irf1* (**Figure 4.5A**). The difference between WT and S2-/- was accentuated following priming to a 'normalise' the STAT1 concentration between the cell lines. The enhanced transcription of the *Irf1* gene is particularly notable, as the resulting protein is involved in a positive feedback loop that further enhances the IFN response (Hu et al, 2008). In this context it is also of interest that the expression of *Socs1*, a gene involved in the negative regulation of IFN, was not increased in S2-/- cells. An important caveat to these results is that they represent a small subset of genes tested as opposed the over 300 interferon stimulated genes however, taken as preliminary results, they certainly justified the further research into the biological consequence of STAT2 in IFN-γ signalling.

An alternative to the mouse macrophage model was also produced by stably reconstituting a STAT2-deficient human fibrosarcoma cell line, U6A, with STAT2 or the N-domain mutant STAT2 L82A. These cells, expressed a similar level of their respective STAT2 constructs as well as STAT1, eliminating the need for priming (**Figure 4.3**). Furthermore STAT phosphorylation in these cell lines appeared similar in response to both IFN-γ and IFN-β.

Both reconstituted lines represent incredibly useful tools for interrogating the effect of STAT2 and in particular its N-domain interaction with STAT1 on IFN-γ signalling.

As with the mouse macrophages, the expression of key IFN target genes was found to be increased in the STAT2-deficient and STAT2 L82A expressing cell lines (**Figure 4.5B**). This not only supports the results found in the macrophage cell lines but also links the increased gene expression directly to the N-domain interaction between STAT1 and STAT2. Once again, IRF1, was one of the genes that benefitted from either the complete absence of STAT2 or simply the ability of STAT2 to bind STAT1.

5.5. The biological impact of STAT2 on IFN-γ mediated response to pathogens

The establishment of two *in vitro* models of STAT2 deficiency and the subsequent enhanced induction of target gene expression by IFN-γ, warranted investigations into biological responses to this cytokine. Classic IFN-γ mediated processes, such as macrophage NO production and suppression of the protozoan parasite *T. gondii* were measured in STAT2 and STAT2-deficient conditions.

The production of NO and free radicals by macrophages in response to IFN-γ is integral to the destruction and removal of bacteria from the host. Using the murine macrophage cell lines, the ability of IFN-γ to trigger NO release was found to be significantly enhanced in cells lacking STAT2 although only after the STAT1 expression between WT and S2-/- had been normalised through priming (**Figure 4.6**). This highlighted the effect that the reduced expression of STAT1 in S2-/- cells in masking the increased ability of STAT1 to enter the nucleus and trigger gene expression. In light of this, it is conceivable that prior studies using STAT2 deficient models would not detect this increased STAT1 activity as well as explain why the phenotype of these models is often of compromised immunity.

The production of NOS in response to IFN-γ is limited to macrophages and other specialised immune cells and as such could not be investigated using the fibrosarcoma-derived reconstituted U6A cells. This does limit the impact of this observation, especially as it is only seen following priming of the macrophages which may have introduced unknown variations between the genotypes, as previously discussed.

The production of NOS is also integral to the inhibition of the intracellular parasite *T. gondii*, though all cell types are capable of IFN-γ mediated suppression of this protozoan via other mechanisms such as the depletion of cellular tryptophan or the utilisation of transmembrane proton pumps to alter the pH within the parasitic vesicle, inhibiting replication (Yarovinsky, 2014). The response of the murine macrophages was strong enough for both WT and S2-/- genotypes to almost completely inhibit *T. gondii* replication with sufficient IFN-γ stimulation (**Figure 4.8**). However, the concentration of IFN required by S2 -/- cells to prevent *T. gondii* replication was at least 500-fold less than that of the wild type. The difference between the STAT2-deficient U6A cells and their STAT2 reconstituted counterparts was less pronounced, likely due to the lack of NOS production. The inhibition of *T. gondii* growth remained significantly better in the STAT2-deficient U6A cells, and in cells expressing the STAT2 L82A mutant (**Figure 4.9**). This result provided the first direct evidence of the N-domain interaction between STAT1 and STAT2 limiting the biological effect of IFN-γ.

Taken in isolation these results focus on a new role for STAT2 as an inhibitor of several immune responses to pathogens, however, in general the opposite is the case. STAT2 as an integral part of anti-viral immunity and is the target of a wide range of viral immune evasion mechanisms (Parisien et al, 2002; Ramachandran et al, 2009; Perry et al, 2011). Recent studies have observed that the Zika virus also targets STAT2 for degradation, but not STAT1, in an effort to disrupt the anti-viral immune response (Grant et al., 2016). This prevents type-1 interferon signalling, the classic mechanism for anti-viral immunity. However, given that the work presented in this thesis shows STAT2 has an intrinsic limiting effect on STAT1 driven cytokines, the degradation of STAT2 by Zika virus could make it susceptible to IFN-γ based anti-viral immunity. In fact, a recent study by (Chaudhary et al, 2017) confirmed that cells infected with Zika were indeed sensitised to IFN-γ treatment and that this was due to enhanced nuclear translocation and target gene binding of STAT1 homodimers. The instinctive conclusion would be to consider the potential therapeutic benefits of IFN-γ in the treatment of this virus, due to the significant overlap in target genes with type-I interferon. However, the authors also observed that IFN-γ enhanced the Zika virus replication in their experiments, potentially by triggering apoptosis and subsequent virus particle release. Thus a better understanding of the role of both IFN-γ and its regulation by STAT2 in controlling

viral replication is required to further enhance our ability to generate new antiviral therapies.

5.6. Improved MHC expression in STAT2 deficient cells

Compared to type-I interferon, IFN-γ is more closely associated with mediating a wider immune response. Part of this is facilitated by activating antigen-presenting cells, which are integral to the function of cytotoxic T-cells as well as the transition from the innate to the adaptive immune response via MHC expression. The increased sensitivity of S2-/- murine macrophages to IFN-γ extended to MHC class II presentation, as they expressed almost twice as much surface MHC class II as their WT counterparts after exposure to 50 U/ml IFN-γ (**Figure 4.11**). Once again, the difference between S2-/- and WT was even more pronounced at lower IFN-γ concentrations. This result highlights that these cells are possessed of not only an increased responsiveness but also sensitivity to IFN-γ. This point is particularly important as cells will be exposed to small concentrations of a variety of cytokines *in vivo*, therefore STAT2 may play a role in setting the minimum level of STAT1 activation in order to effect changes in cell behaviour.

This effect was explored further *in vivo* using STAT2 -/- transgenic mice. These mice and their wildtype counterparts were injected with either PBS or IFN-γ prior to the isolation of peritoneal macrophages. The cell surface expression of MHC class II was compared, with the macrophages isolated from STAT2 -/- mice showing an increased expression in response to IFN-γ than those from the WT. The inherent expression of MHC class II was not significantly different between the genotypes, although the variation within the STAT2 -/- cohort was considerably greater than the WT which may hint at a lesser degree of control over MHC class II expression in these mice.

As a fibrosarcoma derived cell line, the STAT2 reconstituted U6A cells were not good candidates for investigations into MHC class II expression, which is mostly limited to professional antigen presenting cells. However, MHC class I proteins can be expressed by this cell type and were thus used to as another measure of the response to IFN-γ. Once again, the expression of the MHC complex was increased to a greater degree in the STAT2-deficient or STAT2 L82A expressing cells (**Figure 4.13**). This further highlighted that by

removing the influence of STAT2 over STAT1, either by removing it entirely or by the much more subtle effect of the L82A mutation, the responsiveness to IFN-γ can be increased.

5.7. Regulation of senescence and cell death in STAT2 deficient cells

The sensitisation of cells to IFN-γ is not a purely beneficial phenomenon; unregulated interferon signalling is involved in a wide range of diseases such as systemic lupus erythematosus and polymyositis (Meyer, 2009; Pollard et al, 2013). An initial observation made whilst culturing the S2 -/- macrophages was that they appeared more susceptible to the anti-proliferative effects of IFN-γ (Ho et al, 2016). IFN-γ signalling has recently been linked with vitiligo, a skin pigment disorder caused by the loss of pigment-producing melanocytes (Wang et al, 2014; Yang et al, 2015). These recent studies propose a model of pathogenesis whereby an increase in skin infiltrating CD8+ T cells results in high exposure to IFN-γ, which subsequently causes senescence and apoptosis. In light of this thesis, one factor of this pathogenesis to consider is the level of STAT2 in cells of vitiligo patients, which could point to a hyper-positive feedback loop caused by increased IFN-γ sensitivity.

A similar, albeit more beneficial, scenario is proposed as one of the mechanisms by which T-1-helper cells drive cancer into senescence (Braumüller et al, 2013). As performed in this study, the detection of senescence-associated heterochromatin foci was used to assess the role of STAT2 in IFN-γ induced senescence (**Figure 4.14**). The increased formation of SAHF, as measured by p-HP1γ detection, in STAT2 deficient cells suggests that not only is IFN-γ a regulator of senescence in these cells but that STAT2 acts as a barrier in the senescence process. This is further evidenced by the limited expression of p-HP1γ detected in WT cells even after exposure to a high concentration of IFN-γ. This is potentially another contributing factor in the immune-compromised nature of patients and animal models of STAT2-defieciency as the sensitivity of their immune cells to senescence is increased.

The regulation of another anti-proliferative effect of IFN-γ, namely apoptosis, was also assessed (**Figure 4.15**). Although type-I interferons are more traditionally associated with apoptosis (Carrero et al, 2004), these experiments revealed that IFN-γ exerted a weak ability to induce the expression of apoptotic markers in WT cells. Once again, the absence of STAT2 appeared to result in an increased sensitivity to IFN-γ, as apoptotic markers were detected

in a larger proportion of cells and at much lower IFN-γ concentrations. The ability of IFN-γ to induce apoptosis is not entirely surprising given the extensive overlap between type-I and type-II interferon target genes. Further work should be performed to ascertain whether the lack of STAT2 can cause sensitivity to all apoptotic signals, however the aforementioned results highlight STAT2 deficient cell lines as a powerful tool in assessing the significance of increased IFN-γ sensitivity as a compensatory mechanism in type-I interferon disorders.

5.8. Concurrent investigations and future work

The work presented in this thesis confirms an interaction between STAT1 and STAT2 that is independent of their activation, describing for the first time the role of STAT2 as a regulator of STAT1 activities. In discussing future investigations, it is important to note additional observations made by the Vinkemeier lab which augment this work. These findings are reported in Ho et al. (2016) and relate primarily to the nature of the binding between the STAT1 and STAT2 N-domains and the effect that this binding has on other STAT1 dependent cytokine signalling pathways such as IL-6 and IL-27.

Investigations utilising analytical ultracentrifugation confirmed that the N-domain interaction between STAT1 and STAT2 is exceptionally strong, 50-fold more so than the STAT1-STAT1 interaction which has previously been characterised (Wenta et al, 2008) and reconfirmed in these experiments (Ho et al, 2016). As the work within this thesis confirms that only STAT1 that is not bound to STAT2 is available for IFN-γ signalling, this provides a platform whereby the sensitivity of a cell can be fine-tuned by the balance of the STAT1:STAT2 ratio. This ratio was confirmed in concurrent work to be consistently in favour of excess STAT1 across a range of cell types, which was exacerbated following IFN exposure.

This adds a further mechanism by which priming by various cytokines can influence the sensitivity of cells to subsequent stimulation. In fact, the results in **Figure 4.2** show an example of the differential effect of priming with IFN-β or IFN-γ. Whereas IFN-β priming approximately doubles the expression of both STAT1 and STAT2 in WT macrophages, the increase in STAT1 as a result of IFN-γ priming is far more pronounced. The result of this is that the free STAT1, and thus the STAT1 available for IFN-γ signalling is increased more so by IFN-γ than IFN-β. This highlights that STAT2 expression is an important consideration when measuring the bioactivity of STAT1 in disease assessment, making the currently accepted

method of simply using STAT1 phosphorylation as a measure of IFN-γ sensitivity insufficient (Widschwendter et al, 2002).

Having established that the N-domain interaction between STAT2 and STAT1 persisted regardless of phosphorylation, the role of STAT2 as a pervasive inhibitor of STAT1-dependent cytokine signalling was assessed in Ho et al, 2016. STAT1 is involved in the signal transduction a far wider range of cytokines than STAT2, either as a homodimer or in conjunction with other STATs. IL-6 and IL-27 both activate STAT1 and STAT3, yet have distinct and sometimes antagonistic biological functions (Hirahara et al, 2015). Between these two cytokines, STAT1 is believed to play a role in determining specificity. Thus, the role of STAT2 in regulating the availability of STAT1 in IL-27 signalling was investigated. Two subsets of IL-27 target genes, identified as either STAT1-dependent or STAT1-independent were assessed in cells expressing STAT2 WT, STAT2 L82A or either deficient in STAT1 or STAT2 entirely. Within the subset of genes that were not affected by the absence of STAT1, neither the presence of STAT2 nor its ability to bind STAT1 significantly affected IL-27 induced gene expression. Conversely, the expression of some STAT1 dependent genes was found to be enhanced in cells either lacking STAT2 entirely or expressing the STAT2 L82A mutant. These preliminary results highlight how STAT2 could play a role in balancing the transcriptional activity of STAT1 with other STATs, and therefore may have a crucial influence beyond interferon signalling.

This work opens up an entirely new avenue for research, namely the innate effect of STAT2 as a STAT1 inhibitor. This has been shown in a select group of genes both in response to IFN-γ and to IL-27. However, a question over the global effect STAT2 has on the gene expression pattern remains. This could be investigated with the use of gene microarrays of cells either deficient in STAT2 or expressing the STAT2 L82A mutant in response a wide range of different cytokines. These studies could highlight other key genes and phenotypes that are negatively regulated by STAT2, which would enhance our understanding of this new role substantially.

Over the course of this work, the NES within the C terminal domain of STAT2 was mutated in line with the current literature (Frahm et al, 2006). Unfortunately, the specific mutations previously identified, LL737/741AA, did not produce the expected phenotype. The NES of

STAT2 was demonstrated to exist within the C-terminus, seen both in this work and in other literature (Banninger and Reich, 2004). In light of this observation, reassessment of the NES within STAT2 is warranted in order to isolate the key residues involved. However, this lack of clarity does not pose wider implications for STAT2 as a STAT1 inhibitor as this was demonstrated to be independent of STAT2 NES activity.

The STAT2 -/- transgenic mice have been an essential tool in dissecting the role of STAT2 in type-I interferon signalling as well as an established model of immune-comprimisation (Park et al, 2000; Hambleton et al, 2013). However in light of this work, they also represent a model of uninhibited STAT1 activity. Therefore diseases associated with unregulated STAT1, such as chronic mucocutaneous candidiasis, should be assessed in animal models of STAT2 deficiency (Toubiana et al, 2016). In fact, a loss of STAT2 could be considered as a STAT1 gain-of-function, given that mechanism of STAT1 inhibition by STAT2 is independent of cytokine signalling. The main caveat to this is the lower basal expression of STAT1 found in cells derived from the STAT2 -/- mice. This is also likely to have contributed to masking the effects of increased STAT1 transcription activity until now. This makes the discovery of the STAT2 L82A mutation all the more important, as this model allows for the interrogation of the loss of STAT2-driven inhibition of STAT1 specifically. Thus, it is clear that an animal model of STAT2 L82A will provide an essential tool in investigating the importance of this novel regulation medium *in vivo*.

The N-domain interaction between STAT1 and STAT2 may also have ramifications beyond the inhibition of STAT1 but also in the facilitation of type-I interferon signal transduction. The recruitment of STAT1 to the IFNAR1/IFNAR2 complex is believed to be dependent on STAT2 (Improta et al, 1994; Li et al, 1997). The role of the N-domain in the process of activation and receptor recruitment is poorly understood, however as an interaction that is independent of STAT activation it represents a good candidate. The STAT2 L82A mutation is also a mirror for the STAT1 F77A mutation, however it does not result in the same hyper-phosphorylation phenotype (Meyer et al, 2004). Therefore, this mutation is a better tool in further measuring the influence, if any, of STAT2 co-operative DNA binding on type-I interferon.

5.9. Conclusion

The work presented in this thesis aimed to establish the existence and influence of STAT1-STAT2 hetero-dimerisation beyond the ISGF3 transcription factor. Utilising immunofluorescence microscopy, biochemical techniques and a variety of biological assays, it was shown that STAT2 indeed binds to STAT1 in a phosphorylation independent manner with important consequences for IFN signalling. STAT2 was revealed as an innate negative regulator of STAT1 transcriptional activity, by inhibiting its translocation to the nucleus upon activation. This work adds a novel mechanism by which a STAT protein directly affects the function of another and in doing so extends its influence beyond the cytokine signalling pathway it is traditionally linked with. This thesis also highlights the importance of limiting STAT1 signalling in order to prevent a variety of hypersensitivity phenomena such as antigen presentation, senescence and apoptosis. At the same time, this work presents examples whereby immunity against pathogens can be enhanced by the removal of constitutive STAT2 inhibition of STAT1. This may explain why human cases of STAT2 deficiency have shown a surprisingly mild phenotype (Hambleton et al, 2013). In addition, the discovery of a single point mutation within the N-domain of STAT2 that dissociates it's activating and inhibitory effects on STAT1 adds an investigational tool that will allow further dissection of this mechanism and facilitate the development of new therapies.

The integral relationship between STAT1 and STAT2 has been appreciated since the very first discovery of interferon over 25 years ago. The mechanism by which these two related proteins work together as dimeric transcription factors in order to facilitate the anti-viral response is well established as shown in **Figure 1.3**. This model remains intact, however, the observations detailed in this work justify an update whereby the role of STAT2 as a STAT1 antagonist is also acknowledged and is thus represented in **Figure 5.1**.

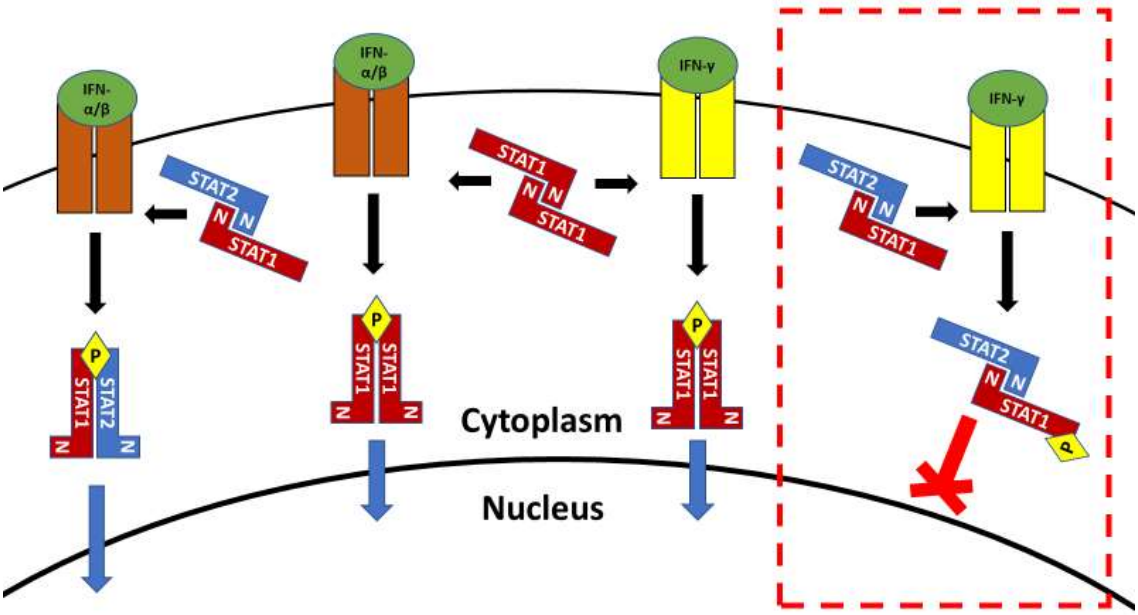

Figure 5.1: *The addition of STAT2 antagonism of STAT1 to the canonical JAK-STAT pathway in response to IFN.* The highlighted area is a simplified diagrammatic example of the formation of STAT1-STAT2 semi-phosphorylated dimers in response to type II IFN signalling. Note that the STAT1 and STAT2 proteins are represented as dimers (via N-domain interaction) prior to IFN signalling and that this determines their availability as a signal transducer to type I or type II IFN.

Reference List

AIRD, K. M. & ZHANG, R. 2013. Detection of senescence-associated heterochromatin foci (SAHF). Methods Mol Biol, 965, 185-96.

ALAZAWI, W., HEATH, H., WATERS, J. A., WOODFIN, A., O'BRIEN, A. J., SCARZELLO, A. J., MA, B., LOPEZ-OTALORA, Y., JACOBS, M., PETTS, G., GOLDIN, R. D., NOURSHARGH, S., GAMERO, A. M. & FOSTER, G. R. 2013. Stat2 loss leads to cytokine-independent, cell-mediated lethality in LPS-induced sepsis. Proc Natl Acad Sci U S A, 110, 8656-61.

AU-YEUNG, N., MANDHANA, R. & HORVATH, C. M. 2013. Transcriptional regulation by STAT1 and STAT2 in the interferon JAK-STAT pathway. JAKSTAT, 2, e23931.

BANNINGER, G. & REICH, N. C. 2004. STAT2 nuclear trafficking. J Biol Chem, 279, 39199-206.

BARTHSON, J., GERMANO, C. M., MOORE, F., MAIDA, A., DRUCKER, D. J., MARCHETTI, P., GYSEMANS, C., MATHIEU, C., NUNEZ, G., JURISICOVA, A., EIZIRIK, D. L. & GURZOV, E. N. 2011. Cytokines tumor necrosis factor-alpha and interferon-gamma induce pancreatic beta-cell apoptosis through STAT1-mediated Bim protein activation. J Biol Chem, 286, 39632-43.

BEGITT, A., DROESCHER, M., KNOBELOCH, K. P. & VINKEMEIER, U. 2011. SUMO conjugation of STAT1 protects cells from hyperresponsiveness to IFNgamma. Blood, 118, 1002-7.

BEGITT, A., DROESCHER, M., MEYER, T., SCHMID, C. D., BAKER, M., ANTUNES, F., KNOBELOCH, K. P., OWEN, M. R., NAUMANN, R., DECKER, T. & VINKEMEIER, U. 2014. STAT1-cooperative DNA binding distinguishes type 1 from type 2 interferon signaling. Nat Immunol, 15, 168-76.

BEGITT, A., MEYER, T., VAN ROSSUM, M. & VINKEMEIER, U. 2000. Nucleocytoplasmic translocation of Stat1 is regulated by a leucine-rich export signal in the coiled-coil domain. Proc Natl Acad Sci U S A, 97, 10418-23.

BILLIAU, A. 1996. Interferon-gamma: biology and role in pathogenesis. Adv Immunol., 62, 61-130.

BLADER, I. J., COLEMAN, B. I., CHEN, C. T. & GUBBELS, M. J. 2015. Lytic Cycle of Toxoplasma gondii: 15 Years Later. Annu Rev Microbiol, 69, 463-85.

BLANCHETTE, J., JARAMILLO, M. & OLIVIER, M. 2003. Signalling events involved in interferon-gamma-inducible macrophage nitric oxide generation. Immunology, 108, 513-22.

BOEHM, U., KLAMP, T., GROOT, M. & HOWARD, J. C. 1997. Cellular responses to interferon-gamma. Annu Rev Immunol., 15, 749-95.

BORDEN, E. C., SEN, G. C., UZE, G., SILVERMAN, R. H., RANSOHOFF, R. M., FOSTER, G. R. & STARK, G. R. 2007. Interferons at age 50: past, current and future impact on biomedicine. Nat Rev Drug Discov, 6, 975-90.

BOYLE, D. L., SOMA, K., HODGE, J., KAVANAUGH, A., MANDEL, D., MEASE, P., SHURMUR, R., SINGHAL, A. K., WEI, N., ROSENGREN, S., KAPLAN, I., KRISHNASWAMI, S., LUO, Z., BRADLEY, J. & FIRESTEIN, G. S. 2015. The JAK inhibitor tofacitinib suppresses synovial JAK1-STAT signalling in rheumatoid arthritis. Ann Rheum Dis, 74, 1311-6.

BRAUMULLER, H., WIEDER, T., BRENNER, E., ASSMANN, S., HAHN, M., ALKHALED, M., SCHILBACH, K., ESSMANN, F., KNEILLING, M., GRIESSINGER, C., RANTA, F., ULLRICH, S., MOCIKAT, R., BRAUNGART, K., MEHRA, T., FEHRENBACHER, B., BERDEL, J., NIESSNER, H., MEIER, F., VAN DEN BROEK, M., HARING, H. U., HANDGRETINGER, R., QUINTANILLA-MARTINEZ, L., FEND, F., PESIC, M., BAUER, J., ZENDER, L., SCHALLER, M., SCHULZE-OSTHOFF, K. & ROCKEN, M. 2013. T-helper-1-cell cytokines drive cancer into senescence. Nature, 494, 361-5.

BRAUNSTEIN, J., BRUTSAERT, S., OLSON, R. & SCHINDLER, C. 2003. STATs dimerize in the absence of phosphorylation. J Biol Chem, 278, 34133-40.

BUSCHLE, M., CAMPANA, D., CARDING, S. R., RICHARD, C., HOFFBRAND, A. V. & BRENNER, M. K. 1993. Interferon gamma inhibits apoptotic cell death in B cell chronic lymphocytic leukemia. J Exp Med, 177, 213-8.

CARRERO, J. A., CALDERON, B. & UNANUE, E. R. 2004. Type I interferon sensitizes lymphocytes to apoptosis and reduces resistance to Listeria infection. J Exp Med, 200, 535-40.

CELADA, A. & MAKI, R. A. 1991. IFN-gamma induces the expression of the genes for MHC class II I-A beta and tumor necrosis factor through a protein kinase C-independent pathway. J Immunol, 146, 114-20.

CHAN, C. W., CRAFTON, E., FAN, H. N., FLOOK, J., YOSHIMURA, K., SKARICA, M., BROCKSTEDT, D., DUBENSKY, T. W., STINS, M. F., LANIER, L. L., PARDOLL, D. M. & HOUSSEAU, F. 2006. Interferon-producing killer dendritic cells provide a link between innate and adaptive immunity. Nat Med, 12, 207-13.

CHAPGIER, A., BOISSON-DUPUIS, S., JOUANGUY, E., VOGT, G., FEINBERG, J., PROCHNICKA-CHALUFOUR, A., CASROUGE, A., YANG, K., SOUDAIS, C., FIESCHI, C., SANTOS, O. F., BUSTAMANTE, J., PICARD, C., DE BEAUCOUDREY, L., EMILE, J. F., ARKWRIGHT, P. D., SCHREIBER, R. D., ROLINCK-WERNINGHAUS, C., ROSEN-WOLFF, A., MAGDORF, K., ROESLER, J. & CASANOVA, J. L. 2006. Novel STAT1 alleles in otherwise healthy patients with mycobacterial disease. PLoS Genet, 2, e131.

CHAUDHARY, V., YUEN, K. S., CHAN, J. F., CHAN, C. P., WANG, P. H., CAI, J. P., ZHANG, S., LIANG, M., KOK, K. H., YUEN, K. Y. & JIN, D. Y. 2017. Selective Activation of Type II Interferon Signaling by Zika Virus NS5 Protein. J Virol, 91.

CHEN, J., WU, M., ZHANG, X., ZHANG, W., ZHANG, Z., CHEN, L., HE, J., ZHENG, Y., CHEN, C., WANG, F., HU, Y., ZHOU, X., WANG, C., XU, Y., LU, M. & YUAN, Z. 2013. Hepatitis B virus polymerase impairs interferon-alpha-induced STA T activation through inhibition of importin-alpha5 and protein kinase C-delta. Hepatology, 57, 470-82.

CHEN, X., BHANDARI, R., VINKEMEIER, U., VAN DEN AKKER, F., DARNELL, J. E., JR. & KURIYAN, J. 2003. A reinterpretation of the dimerization interface of the N-terminal domains of STATs. Protein Sci, 12, 361-5.

CHEN, X., VINKEMEIER, U., ZHAO, Y., JERUZALMI, D., DARNELL, J. E., JR. & KURIYAN, J. 1998. Crystal structure of a tyrosine phosphorylated STAT-1 dimer bound to DNA. Cell, 93, 827-39.

CHEON, H., HOLVEY-BATES, E. G., SCHOGGINS, J. W., FORSTER, S., HERTZOG, P., IMANAKA, N., RICE, C. M., JACKSON, M. W., JUNK, D. J. & STARK, G. R. 2013. IFNbeta-dependent

increases in STAT1, STAT2, and IRF9 mediate resistance to viruses and DNA damage. EMBO J, 32, 2751-63.

CHIN, Y. E., KITAGAWA, M., SU, W. C., YOU, Z. H., IWAMOTO, Y. & FU, X. Y. 1996. Cell growth arrest and induction of cyclin-dependent kinase inhibitor p21 WAF1/CIP1 mediated by STAT1. Science, 272, 719-22.

CHIZZOLINI, C., DAYER, J. M. & MIOSSEC, P. 2009. Cytokines in chronic rheumatic diseases: is everything lack of homeostatic balance? Arthritis Res Ther, 11, 246.

CHO, H. & KELSALL, B. L. 2014. The role of type I interferons in intestinal infection, homeostasis and inflammation. Immunol Rev. , 260(1), 145-67

DELGOFFE, G. M., MURRAY, P. J. & VIGNALI, D. A. 2011. Interpreting mixed signals: the cell's cytokine conundrum. Curr Opin Immunol, 23, 632-8.

DEUTSCHMAN, C. S. & TRACEY, K. J. 2014. Sepsis: current dogma and new perspectives. Immunity, 40, 463-75.

DIGHE, A. S., RICHARDS, E., OLD, L. J. & SCHREIBER, R. D. 1994. Enhanced in vivo growth and resistance to rejection of tumor cells expressing dominant negative IFN gamma receptors. Immunity, 1, 447-56.

DIMBERG, L. Y., DIMBERG, A., IVARSSON, K., FRYKNAS, M., RICKARDSON, L., TOBIN, G., EKMAN, S., LARSSON, R., GULLBERG, U., NILSSON, K., OBERG, F. & WIKLUND, H. J. 2012. Stat1 activation attenuates IL-6 induced Stat3 activity but does not alter apoptosis sensitivity in multiple myeloma. BMC Cancer, 12, 318.

DINARELLO, C. A. 2007. Historical insights into cytokines. Eur J Immunol, 37 Suppl 1, S34-45.

DROESCHER, M., BEGITT, A., MARG, A., ZACHARIAS, M. & VINKEMEIER, U. 2011. Cytokine-induced paracrystals prolong the activity of signal transducers and activators of transcription (STAT) and provide a model for the regulation of protein solubility by small ubiquitin-like modifier (SUMO). J Biol Chem, 286, 18731-46.

ELSHEIKHA, H. M., ROSENTHAL, B. M., MURPHY, A. J., DUNAMS, D. B., NEELIS, D. A. & MANSFIELD, L. S. 2006. Generally applicable methods to purify intracellular coccidia from

cell cultures and to quantify purification efficacy using quantitative PCR. Vet Parasitol, 135, 223-34.

FAGERLUND, R., MELEN, K., KINNUNEN, L. & JULKUNEN, I. 2002. Arginine/lysine-rich nuclear localization signals mediate interactions between dimeric STATs and importin alpha 5. J Biol Chem, 277, 30072-8.

FAHRENKROG, B., KOSER, J. & AEBI, U. 2004. The nuclear pore complex: a jack of all trades? Trends Biochem Sci, 29, 175-82.

FALSEY, A. R. & WALSH, E. E. 2006. Viral pneumonia in older adults. Clin Infect Dis., 42, 518-24.

FENSTERL, V. & SEN, G. C. 2015. Interferon-induced Ifit proteins: their role in viral pathogenesis. J Virol, 89, 2462-8.

FRAHM, T., HAUSER, H. & KOSTER, M. 2006. IFN-type-I-mediated signaling is regulated by modulation of STAT2 nuclear export. J Cell Sci, 119, 1092-104.

GOUGH, D. J., MESSINA, N. L., HII, L., GOULD, J. A., SABAPATHY, K., ROBERTSON, A. P., TRAPANI, J. A., LEVY, D. E., HERTZOG, P. J., CLARKE, C. J. & JOHNSTONE, R. W. 2010. Functional crosstalk between type I and II interferon through the regulated expression of STAT1. PLoS Biol, 8, e1000361.

GRANT, A., PONIA, S. S., TRIPATHI, S., BALASUBRAMANIAM, V., MIORIN, L., SOURISSEAU, M., SCHWARZ, M. C., SANCHEZ-SECO, M. P., EVANS, M. J., BEST, S. M. & GARCIA-SASTRE, A. 2016. Zika Virus Targets Human STAT2 to Inhibit Type I Interferon Signaling. Cell Host Microbe, 19, 882-90.

HAMBLETON, S., GOODBOURN, S., YOUNG, D. F., DICKINSON, P., MOHAMAD, S. M., VALAPPIL, M., MCGOVERN, N., CANT, A. J., HACKETT, S. J., GHAZAL, P., MORGAN, N. V. & RANDALL, R. E. 2013. STAT2 deficiency and susceptibility to viral illness in humans. Proc Natl Acad Sci U S A, 110, 3053-8.

HARVAT, B. L. & JETTEN, A. M. 1996. Gamma-interferon induces an irreversible growth arrest in mid-G1 in mammary epithelial cells which correlates with a block in hyperphosphorylation of retinoblastoma. Cell Growth Differ, 7, 289-300.

HE, J., SHI, J., XU, X., ZHANG, W., WANG, Y., CHEN, X., DU, Y., ZHU, N., ZHANG, J., WANG, Q. & YANG, J. 2012. STAT3 mutations correlated with hyper-IgE syndrome lead to blockage of IL-6/STAT3 signalling pathway. J Biosci, 37, 243-57.

HEIM, M. H., KERR, I. M., STARK, G. R. & DARNELL, J. E., JR. 1995. Contribution of STAT SH2 groups to specific interferon signaling by the Jak-STAT pathway. Science, 267, 1347-9.

HERBST, S., SCHAIBLE, U. E. & SCHNEIDER, B. E. 2011. Interferon gamma activated macrophages kill mycobacteria by nitric oxide induced apoptosis. PLoS One, 6, e19105.

HIRAHARA, K., ONODERA, A., VILLARINO, A. V., BONELLI, M., SCIUME, G., LAURENCE, A., SUN, H. W., BROOKS, S. R., VAHEDI, G., SHIH, H. Y., GUTIERREZ-CRUZ, G., IWATA, S., SUZUKI, R., MIKAMI, Y., OKAMOTO, Y., NAKAYAMA, T., HOLLAND, S. M., HUNTER, C. A., KANNO, Y. & O'SHEA, J. J. 2015. Asymmetric Action of STAT Transcription Factors Drives Transcriptional Outputs and Cytokine Specificity. Immunity, 42, 877-89.

HO, H. H. & IVASHKIV, L. B. 2006. Role of STAT3 in type I interferon responses. Negative regulation of STAT1-dependent inflammatory gene activation. J Biol Chem, 281, 14111-8.

HO, J., PELZEL, C., BEGITT, A., MEE, M., ELSHEIKHA, H. M., SCOTT, D. J. & VINKEMEIER, U. 2016. STAT2 Is a Pervasive Cytokine Regulator due to Its Inhibition of STAT1 in Multiple Signaling Pathways. PLoS Biol, 14, e2000117.

HOBEIKA, A. C., ETIENNE, W., TORRES, B. A., JOHNSON, H. M. & SUBRAMANIAM, P. S. 1999. IFN-gamma induction of p21(WAF1) is required for cell cycle inhibition and suppression of apoptosis. J Interferon Cytokine Res, 19, 1351-61.

HORVATH, C. M., WEN, Z. & DARNELL, J. E., JR. 1995. A STAT protein domain that determines DNA sequence recognition suggests a novel DNA-binding domain. Genes Dev, 9, 984-94.

HU, J., MENG, Q., ROY, S. K., RAHA, A., ZHANG, J., HASHIMOTO, K. & KALVAKOLANU, D. V. 2002. A novel transactivating factor that regulates interferon-gamma-dependent gene expression. J Biol Chem, 277, 30253-63.

HU, X., CHAKRAVARTY, S. D. & IVASHKIV, L. B. 2008. Regulation of interferon and Toll-like receptor signaling during macrophage activation by opposing feedforward and feedback inhibition mechanisms. Immunol Rev, 226, 41-56.

HUNTELMANN, B., STAAB, J., HERRMANN-LINGEN, C. & MEYER, T. 2014. A conserved motif in the linker domain of STAT1 transcription factor is required for both recognition and release from high-affinity DNA-binding sites. PLoS One, 9, e97633.

IKEDA, H., OLD, L. J. & SCHREIBER, R. D. 2002. The roles of IFN gamma in protection against tumor development and cancer immunoediting. Cytokine Growth Factor Rev, 13, 95-109.

IMPROTA, T., SCHINDLER, C., HORVATH, C. M., KERR, I. M., STARK, G. R. & DARNELL, J. E., JR. 1994. Transcription factor ISGF-3 formation requires phosphorylated Stat91 protein, but Stat113 protein is phosphorylated independently of Stat91 protein. Proc Natl Acad Sci U S A, 91, 4776-80.

ISAACS, A. & LINDENMANN, J. 1957. Virus interference. I. The interferon. Proc R Soc Lond B Biol Sci, 147, 258-67.

KAPLAN, D. H., SHANKARAN, V., DIGHE, A. S., STOCKERT, E., AGUET, M., OLD, L. J. & SCHREIBER, R. D. 1998. Demonstration of an interferon gamma-dependent tumor surveillance system in immunocompetent mice. Proc Natl Acad Sci U S A, 95, 7556-61.

KHAN, K. D., SHUAI, K., LINDWALL, G., MAHER, S. E., DARNELL, J. E., JR. & BOTHWELL, A. L. 1993. Induction of the Ly-6A/E gene by interferon alpha/beta and gamma requires a DNA element to which a tyrosine-phosphorylated 91-kDa protein binds. Proc Natl Acad Sci U S A, 90, 6806-10.

KOOPMAN, G., REUTELINGSPERGER, C. P., KUIJTEN, G. A., KEEHNEN, R. M., PALS, S. T. & VAN OERS, M. H. 1994. Annexin V for flow cytometric detection of phosphatidylserine expression on B cells undergoing apoptosis. Blood, 84, 1415-20.

LEUNG, S., QURESHI, S. A., KERR, I. M., DARNELL, J. E., JR. & STARK, G. R. 1995. Role of STAT2 in the alpha interferon signaling pathway. Mol Cell Biol, 15, 1312-7.

LEVY, D. E. & DARNELL, J. E., JR. 2002. Stats: transcriptional control and biological impact. Nat Rev Mol Cell Biol, 3, 651-62.

LEVY, D. E. & MARIE, I. J. 2012. STATus report on tetramers. Immunity, 36, 553-5.

LEVY, D. E., MARIE, I. J. & DURBIN, J. E. 2011. Induction and function of type I and III interferon in response to viral infection. Curr Opin Virol, 1, 476-86.

LI, X., LEUNG, S., KERR, I. M. & STARK, G. R. 1997. Functional subdomains of STAT2 required for preassociation with the alpha interferon receptor and for signaling. Mol Cell Biol, 17, 2048-56.

LIU, L., OKADA, S., KONG, X. F., KREINS, A. Y., CYPOWYJ, S., ABHYANKAR, A., TOUBIANA, J., ITAN, Y., AUDRY, M., NITSCHKE, P., MASSON, C., TOTH, B., FLATOT, J., MIGAUD, M., CHRABIEH, M., KOCHETKOV, T., BOLZE, A., BORGHESI, A., TOULON, A., HILLER, J., EYERICH, S., EYERICH, K., GULACSY, V., CHERNYSHOVA, L., CHERNYSHOV, V., BONDARENKO, A., GRIMALDO, R. M., BLANCAS-GALICIA, L., BEAS, I. M., ROESLER, J., MAGDORF, K., ENGELHARD, D., THUMERELLE, C., BURGEL, P. R., HOERNES, M., DREXEL, B., SEGER, R., KUSUMA, T., JANSSON, A. F., SAWALLE-BELOHRADSKY, J., BELOHRADSKY, B., JOUANGUY, E., BUSTAMANTE, J., BUE, M., KARIN, N., WILDBAUM, G., BODEMER, C., LORTHOLARY, O., FISCHER, A., BLANCHE, S., AL-MUHSEN, S., REICHENBACH, J., KOBAYASHI, M., ROSALES, F. E., LOZANO, C. T., KILIC, S. S., OLEASTRO, M., ETZIONI, A., TRAIDL-HOFFMANN, C., RENNER, E. D., ABEL, L., PICARD, C., MARODI, L., BOISSON-DUPUIS, S., PUEL, A. & CASANOVA, J. L. 2011. Gain-of-function human STAT1 mutations impair IL-17 immunity and underlie chronic mucocutaneous candidiasis. J Exp Med, 208, 1635-48.

LORSBACH, R. B., MURPHY, W. J., LOWENSTEIN, C. J., SNYDER, S. H. & RUSSELL, S. W. 1993. Expression of the nitric oxide synthase gene in mouse macrophages activated for tumor cell killing. Molecular basis for the synergy between interferon-gamma and lipopolysaccharide. J Biol Chem, 268, 1908-13.

LOU, Y. J., PAN, X. R., JIA, P. M., LI, D., XIAO, S., ZHANG, Z. L., CHEN, S. J., CHEN, Z. & TONG, J. H. 2009. IRF-9/STAT2 [corrected] functional interaction drives retinoic acid-induced gene G expression independently of STAT1. Cancer Res, 69, 3673-80.

MAARIFI, G., MAROUI, M. A., DUTRIEUX, J., DIANOUX, L., NISOLE, S. & CHELBI-ALIX, M. K. 2015. Small Ubiquitin-like Modifier Alters IFN Response. J Immunol, 195, 2312-24.

MAJOROS, A., PLATANITIS, E., SZAPPANOS, D., CHEON, H., VOGL, C., SHUKLA, P., STARK, G. R., SEXL, V., SCHREIBER, R., SCHINDLER, C., MULLER, M. & DECKER, T. 2016. Response to interferons and antibacterial innate immunity in the absence of tyrosine-phosphorylated STAT1. EMBO Rep, 17, 367-82.

MALAKHOV, M. P., MALAKHOVA, O. A., KIM, K. I., RITCHIE, K. J. & ZHANG, D. E. 2002. UBP43 (USP18) specifically removes ISG15 from conjugated proteins. J Biol Chem, 277, 9976-81.

MALAKHOVA, O. A., YAN, M., MALAKHOV, M. P., YUAN, Y., RITCHIE, K. J., KIM, K. I., PETERSON, L. F., SHUAI, K. & ZHANG, D. E. 2003. Protein ISGylation modulates the JAK-STAT signaling pathway. Genes Dev, 17, 455-60.

MAO, X., REN, Z., PARKER, G. N., SONDERMANN, H., PASTORELLO, M. A., WANG, W., MCMURRAY, J. S., DEMELER, B., DARNELL, J. E., JR. & CHEN, X. 2005. Structural bases of unphosphorylated STAT1 association and receptor binding. Mol Cell, 17, 761-71.

MARG, A., SHAN, Y., MEYER, T., MEISSNER, T., BRANDENBURG, M. & VINKEMEIER, U. 2004. Nucleocytoplasmic shuttling by nucleoporins Nup153 and Nup214 and CRM1-dependent nuclear export control the subcellular distribution of latent Stat1. J Cell Biol, 165, 823-33.

MARTIN, S. J. & GREEN, D. R. 1995. Protease activation during apoptosis: death by a thousand cuts? Cell, 82, 349-52.

MARTINEZ-MARTINEZ, L., MARTINEZ-SAAVEDRA, M. T., FUENTES-PRIOR, P., BARNADAS, M., RUBIALES, M. V., NODA, J., BADELL, I., RODRIGUEZ-GALLEGO, C. & DE LA CALLE-MARTIN, O. 2015. A novel gain-of-function STAT1 mutation resulting in basal phosphorylation of STAT1 and increased distal IFN-gamma-mediated responses in chronic mucocutaneous candidiasis. Mol Immunol, 68, 597-605.

MATJUSAITIS, M., CHIN, G., SARNOSKI, E. A. & STOLZING, A. 2016. Biomarkers to identify and isolate senescent cells. Ageing Res Rev, 29, 1-12.

MCKENDRY, R., JOHN, J., FLAVELL, D., MULLER, M., KERR, I. M. & STARK, G. R. 1991. High-frequency mutagenesis of human cells and characterization of a mutant unresponsive to both alpha and gamma interferons. Proc Natl Acad Sci U S A, 88, 11455-9.

MCLEOD, R. & REMINGTON, J. S. 1977. A new method for evaluation of intracellular inhibition of multiplication or killing by mononuclear phagocytes. J Immunol, 119, 1894-7.

MEISSNER, T., KRAUSE, E. & VINKEMEIER, U. 2004. Ratjadone and leptomycin B block CRM1-dependent nuclear export by identical mechanisms. FEBS Lett, 576, 27-30.

MELEN, K., FAGERLUND, R., FRANKE, J., KOHLER, M., KINNUNEN, L. & JULKUNEN, I. 2003. Importin alpha nuclear localization signal binding sites for STAT1, STAT2, and influenza A virus nucleoprotein. J Biol Chem, 278, 28193-200.

MELEN, K., KINNUNEN, L. & JULKUNEN, I. 2001. Arginine/lysine-rich structural element is involved in interferon-induced nuclear import of STATs. J Biol Chem, 276, 16447-55.

MERAZ, M. A., WHITE, J. M., SHEEHAN, K. C., BACH, E. A., RODIG, S. J., DIGHE, A. S., KAPLAN, D. H., RILEY, J. K., GREENLUND, A. C., CAMPBELL, D., CARVER-MOORE, K., DUBOIS, R. N., CLARK, R., AGUET, M. & SCHREIBER, R. D. 1996. Targeted disruption of the Stat1 gene in mice reveals unexpected physiologic specificity in the JAK-STAT signaling pathway. Cell, 84, 431-42.

MERTENS, C., ZHONG, M., KRISHNARAJ, R., ZOU, W., CHEN, X. & DARNELL, J. E., JR. 2006. Dephosphorylation of phosphotyrosine on STAT1 dimers requires extensive spatial reorientation of the monomers facilitated by the N-terminal domain. Genes Dev, 20, 3372-81.

MEYER, O. 2009. Interferons and autoimmune disorders. Joint Bone Spine, 76, 464-73.

MEYER, T., GAVENIS, K. & VINKEMEIER, U. 2002. Cell type-specific and tyrosine phosphorylation-independent nuclear presence of STAT1 and STAT3. Exp Cell Res, 272, 45-55.

MEYER, T., HENDRY, L., BEGITT, A., JOHN, S. & VINKEMEIER, U. 2004. A single residue modulates tyrosine dephosphorylation, oligomerization, and nuclear accumulation of stat transcription factors. J Biol Chem, 279, 18998-9007.

MEYER, T., MARG, A., LEMKE, P., WIESNER, B. & VINKEMEIER, U. 2003. DNA binding controls inactivation and nuclear accumulation of the transcription factor Stat1. Genes Dev, 17, 1992-2005.

MINEGISHI, Y., SAITO, M., TSUCHIYA, S., TSUGE, I., TAKADA, H., HARA, T., KAWAMURA, N., ARIGA, T., PASIC, S., STOJKOVIC, O., METIN, A. & KARASUYAMA, H. 2007. Dominant-negative mutations in the DNA-binding domain of STAT3 cause hyper-IgE syndrome. Nature, 448, 1058-62.

MURPHY, T. L., GEISSAL, E. D., FARRAR, J. D. & MURPHY, K. M. 2000. Role of the Stat4 N domain in receptor proximal tyrosine phosphorylation. Mol Cell Biol, 20, 7121-31.

NARDOZZI, J., WENTA, N., YASUHARA, N., VINKEMEIER, U. & CINGOLANI, G. 2010. Molecular basis for the recognition of phosphorylated STAT1 by importin alpha5. J Mol Biol, 402, 83-100.

OKABAYASHI, T., KOJIMA, T., MASAKI, T., YOKOTA, S., IMAIZUMI, T., TSUTSUMI, H., HIMI, T., FUJII, N. & SAWADA, N. 2011. Type-III interferon, not type-I, is the predominant interferon induced by respiratory viruses in nasal epithelial cells. Virus Res, 160, 360-6.

OTA, N., BRETT, T. J., MURPHY, T. L., FREMONT, D. H. & MURPHY, K. M. 2004. N-domain-dependent nonphosphorylated STAT4 dimers required for cytokine-driven activation. Nat Immunol, 5, 208-15.

PARISIEN, J. P., LAU, J. F., RODRIGUEZ, J. J., ULANE, C. M. & HORVATH, C. M. 2002. Selective STAT protein degradation induced by paramyxoviruses requires both STAT1 and STAT2 but is independent of alpha/beta interferon signal transduction. J Virol, 76, 4190-8.

PARK, C., LI, S., CHA, E. & SCHINDLER, C. 2000. Immune response in Stat2 knockout mice. Immunity, 13, 795-804.

PAWLOWSKA, J., SMOLENSKA, Z., DACA, A., WOTKOWSKI, J. M. & BRYL, E. 2010. Older age of rheumatoid arthritis onset is associated with higher activation status of peripheral blood CD4+ T cells and disease activity. Clin. Experiment. Immunol, 163 (2).

PERRY, S. T., BUCK, M. D., LADA, S. M., SCHINDLER, C. & SHRESTA, S. 2011. STAT2 mediates innate immunity to Dengue virus in the absence of STAT1 via the type I interferon receptor. PLoS Pathog, 7, e1001297.

PESTKA, S., KRAUSE, C. D. & WALTER, M. R. 2004. Interferons, interferon-like cytokines, and their receptors. Immunol Rev., 202, 8-32

POLLARD, K. M., CAUVI, D. M., TOOMEY, C. B., MORRIS, K. V. & KONO, D. H. 2013. Interferon-gamma and systemic autoimmunity. Discov Med, 16, 123-31.

QURESHI, S. A., SALDITT-GEORGIEFF, M. & DARNELL, J. E., JR. 1995. Tyrosine-phosphorylated Stat1 and Stat2 plus a 48-kDa protein all contact DNA in forming interferon-stimulated-gene factor 3. Proc Natl Acad Sci U S A, 92, 3829-33.

RACKOV, G., SHOKRI, R., ALVAREZ DE MON, M., MARTINEZ-A, C. & BALOMENOS, D. 2017. The Role of IFN-β during the Course of Sepsis Progression and Its Therapeutic Potential. Front Immunol, 8, 493.

RAMACHANDRAN, A. & HORVATH, C. M. 2009. Paramyxovirus disruption of interferon signal transduction: STATus report. J Interferon Cytokine Res, 29, 531-7.

RANDALL, R. E. & GOODBOURN, S. 2008. Interferons and viruses: an interplay between induction, signalling, antiviral responses and virus countermeasures. J Gen Virol, 89, 1-47.

RAY, A. & DITTEL, B. N. 2010. Isolation of mouse peritoneal cavity cells. J Vis Exp.

REDER, A. T. & FENG, X. 2013. Aberrant Type I Interferon Regulation in Autoimmunity: Opposite Directions in MS and SLE, Shaped by Evolution and Body Ecology. Front Immunol, 4, 281.

RHEE, S. H., JONES, B. W., TOSHCHAKOV, V., VOGEL, S. N. & FENTON, M. J. 2003. Toll-like receptors 2 and 4 activate STAT1 serine phosphorylation by distinct mechanisms in macrophages. J Biol Chem, 278, 22506-12.

SANDA, C., WEITZEL, P., TSUKAHARA, T., SCHALEY, J., EDENBERG, H. J., STEPHENS, M. A., MCCLINTICK, J. N., BLATT, L. M., LI, L., BRODSKY, L. & TAYLOR, M. W. 2006. Differential gene induction by type I and type II interferons and their combination. J Interferon Cytokine Res, 26, 462-72.

SCHANZER, D. L., LANGLEY, J. M. & TAM, T. W. 2008. Co-morbidities associated with influenza-attributed mortality, 1994-2000, Canada. Vaccine, 26, 4697-703.

SCHINDLER, C., SHUAI, K., PREZIOSO, V. R. & DARNELL, J. E., JR. 1992. Interferon-dependent tyrosine phosphorylation of a latent cytoplasmic transcription factor. Science, 257, 809-13.

SCHRODER, K., HERTZOG, P. J., RAVASI, T. & HUME, D. A. 2004. Interferon-gamma: an overview of signals, mechanisms and functions. J Leukoc Biol, 75, 163-89.

SHEN, Y. & DARNELL, J. E., JR. 2001. Antiviral response in cells containing Stat1 with heterologous transactivation domains. J Virol, 75, 2627-33.

SHUAI, K., HORVATH, C. M., HUANG, L. H., QURESHI, S. A., COWBURN, D. & DARNELL, J. E., JR. 1994. Interferon activation of the transcription factor Stat91 involves dimerization through SH2-phosphotyrosyl peptide interactions. Cell, 76, 821-8.

SHUAI, K. & LIU, B. 2005. Regulation of gene-activation pathways by PIAS proteins in the immune system. Nat Rev Immunol, 5, 593-605.

SHUAI, K., STARK, G. R., KERR, I. M. & DARNELL, J. E., JR. 1993. A single phosphotyrosine residue of Stat91 required for gene activation by interferon-gamma. Science, 261, 1744-6.

STANCATO, L. F., DAVID, M., CARTER-SU, C., LARNER, A. C. & PRATT, W. B. 1996. Preassociation of STAT1 with STAT2 and STAT3 in separate signalling complexes prior to cytokine stimulation. J Biol Chem, 271, 4134-7.

STARK, G. R. & DARNELL, J. E., JR. 2012. The JAK-STAT pathway at twenty. Immunity, 36, 503-14.

STEEN, H. C. & GAMERO, A. M. 2013. STAT2 phosphorylation and signaling. JAKSTAT, 2, e25790.

STEEN, H. C., NOGUSA, S., THAPA, R. J., BASAGOUDANAVAR, S. H., GILL, A. L., MERALI, S., BARRERO, C. A., BALACHANDRAN, S. & GAMERO, A. M. 2013. Identification of STAT2 serine 287 as a novel regulatory phosphorylation site in type I interferon-induced cellular responses. J Biol Chem, 288, 747-58.

STREHLOW, I. & SCHINDLER, C. 1998. Amino-terminal signal transducer and activator of transcription (STAT) domains regulate nuclear translocation and STAT deactivation. J Biol Chem, 273, 28049-56.

SUZUKI, Y., ORELLANA, M. A., SCHREIBER, R. D. & REMINGTON, J. S. 1988. Interferon-gamma: the major mediator of resistance against Toxoplasma gondii. Science, 240, 516-8.

SZABO, A., MAGYARICS, Z., PAZMANDI, K., GOPCSA, L., RAJNAVOLGYI, E. & BACSI, A. 2014. TLR ligands upregulate RIG-I expression in human plasmacytoid dendritic cells in a type I IFN-independent manner. Immunol Cell Biol, 92, 671-8.

TAM, J. C. H. & JACQUES, D. A. 2014. Intracellular immunity: finding the enemy within—how cells recognize and respond to intracellular pathogens

TEN HOEVE, J., DE JESUS IBARRA-SANCHEZ, M., FU, Y., ZHU, W., TREMBLAY, M., DAVID, M. & SHUAI, K. 2002. Identification of a nuclear Stat1 protein tyrosine phosphatase. Mol Cell Biol, 22, 5662-8.

THOMPSON, A. J. & LOCARNINI, S. A. 2007. Toll-like receptors, RIG-I-like RNA helicases and the antiviral innate immune response. Immunol Cell Biol, 85, 435-45.

TOUBIANA, J., OKADA, S., HILLER, J., OLEASTRO, M., LAGOS GOMEZ, M., ALDAVE BECERRA, J. C., OUACHEE-CHARDIN, M., FOUYSSAC, F., GIRISHA, K. M., ETZIONI, A., VAN MONTFRANS, J., CAMCIOGLU, Y., KERNS, L. A., BELOHRADSKY, B., BLANCHE, S., BOUSFIHA, A., RODRIGUEZ-GALLEGO, C., MEYTS, I., KISAND, K., REICHENBACH, J., RENNER, E. D., ROSENZWEIG, S., GRIMBACHER, B., VAN DE VEERDONK, F. L., TRAIDL-HOFFMANN, C., PICARD, C., MARODI, L., MORIO, T., KOBAYASHI, M., LILIC, D., MILNER, J. D., HOLLAND, S., CASANOVA, J. L. & PUEL, A. 2016. Heterozygous STAT1 gain-of-function mutations underlie an unexpectedly broad clinical phenotype. Blood, 127, 3154-64.

UEMATSU, S. & AKIRA, S. 2007. Toll-like receptors and Type I interferons. J Biol Chem, 282, 15319-23.

VINKEMEIER, U. 2004. Getting the message across, STAT! Design principles of a molecular signaling circuit. J Cell Biol, 167, 197-201.

VUONG, B. Q., ARENZANA, T. L., SHOWALTER, B. M., LOSMAN, J., CHEN, X. P., MOSTECKI, J., BANKS, A. S., LIMNANDER, A., FERNANDEZ, N. & ROTHMAN, P. B. 2004. SOCS-1 localizes to the microtubule organizing complex-associated 20S proteasome. Mol Cell Biol, 24, 9092-101.

WANG, S., ZHOU, M., LIN, F., LIU, D., HONG, W., LU, L., ZHU, Y. & XU, A. 2014. Interferon-gamma induces senescence in normal human melanocytes. PLoS One, 9, e93232.

WEINBAUER, M. G. 2004 Ecology of prokaryotic viruses. FEMS Microbiol Rev., 2, 127-81

WENTA, N., STRAUSS, H., MEYER, S. & VINKEMEIER, U. 2008. Tyrosine phosphorylation regulates the partitioning of STAT1 between different dimer conformations. Proc Natl Acad Sci U S A, 105, 9238-43.

WIDSCHWENDTER, A., TONKO-GEYMAYER, S., WELTE, T., DAXENBICHLER, G., MARTH, C. & DOPPLER, W. 2002. Prognostic significance of signal transducer and activator of transcription 1 activation in breast cancer. Clin Cancer Res, 8, 3065-74.

WU, D., SANIN, D. E., EVERTS, B., CHEN, Q., BUCK, M. D., PATTERSON, A., SMITH, A. M., CHANG, C. H., LIU, Z., ARTYOMOV, M. N., PEARCE, E. L., CELLA, M. & PEARCE, E. J. 2016. Type 1 Interferons induce Changes in Core Metabolism that Are Critical for Immune Function. Immunity, 44 (6), 1325-36.

XU, W., EDWARDS, M. R., BOREK, D. M., FEAGINS, A. R., MITTAL, A., ALINGER, J. B., BERRY, K. N., YEN, B., HAMILTON, J., BRETT, T. J., PAPPU, R. V., LEUNG, D. W., BASLER, C. F. & AMARASINGHE, G. K. 2014. Ebola virus VP24 targets a unique NLS binding site on karyopherin alpha 5 to selectively compete with nuclear import of phosphorylated STAT1. Cell Host Microbe, 16, 187-200.

XU, X., SUN, Y. L. & HOEY, T. 1996. Cooperative DNA binding and sequence-selective recognition conferred by the STAT amino-terminal domain. Science, 273, 794-7.

YANG, L., WEI, Y., SUN, Y., SHI, W., YANG, J., ZHU, L. & LI, M. 2015. Interferon-gamma Inhibits Melanogenesis and Induces Apoptosis in Melanocytes: A Pivotal Role of CD8+ Cytotoxic T Lymphocytes in Vitiligo. Acta Derm Venereol, 95, 664-70.

YAO, Y., WANG, J. B., XIN, M. M., LI, H., LIU, B., WANG, L. L., WANG, L. Q. & ZHAO, L. 2016. Balance between inflammatory and regulatory cytokines in systemic lupus erythematosus. Genet Mol Res, 15.

YAROVINSKY, F. 2014. Innate immunity to Toxoplasma gondii infection. Nat Rev Immunol, 14, 109-21.

YASUKAWA, H., MISAWA, H., SAKAMOTO, H., MASUHARA, M., SASAKI, A., WAKIOKA, T., OHTSUKA, S., IMAIZUMI, T., MATSUDA, T., IHLE, J. N. & YOSHIMURA, A. 1999. The JAK-binding protein JAB inhibits Janus tyrosine kinase activity through binding in the activation loop. EMBO J, 18, 1309-20.

YOO, C. H., YEOM, J. H., HEO, J. J., SONG, E. K., LEE, S. I. & HAN, M. K. 2014. Interferon β protects against lethal endotoxic and septic shock through SIRT1 upregulation. Scientific Reports, 4220.

YOSHIMURA, A., NAKA, T. & KUBO, M. 2007. SOCS proteins, cytokine signalling and immune regulation. Nat Rev Immunol, 7, 454-65.

YU, Q., KATLINSKAYA, Y. V., CARBONE, C. J., ZHOA, B., KATLINSKI, K. V., ZHENG, H., GUHA, M., LI, N., CHEN, Q., YANG, T., LENGNER, C. J., GREENBERG, R. A., JOHNSON, F. B. & FUCHS, S. Y. 2015 DNA-damage-induced type I interferon promotes senescence and inhibits stem cell function. Cell Rep. 11, 785-797

ZHANG, D. & ZHANG, D. E. 2011. Interferon-stimulated gene 15 and the protein ISGylation system. J Interferon Cytokine Res, 31, 119-30.

ZHANG, S. Y., BOISSON-DUPUIS, S., CHAPGIER, A., YANG, K., BUSTAMANTE, J., PUEL, A., PICARD, C., ABEL, L., JOUANGUY, E. & CASANOVA, J. L. 2008. Inborn errors of interferon

(IFN)-mediated immunity in humans: insights into the respective roles of IFN-alpha/beta, IFN-gamma, and IFN-lambda in host defense. Immunol Rev, 226, 29-40.

ZHOU, Z., HAMMING, O. J., ANK, N., PALUDAN, S. R., NIELSEN, A. L. & HARTMANN, R. 2007. Type III interferon (IFN) induces a type I IFN-like response in a restricted subset of cells through signaling pathways involving both the Jak-STAT pathway and the mitogen-activated protein kinases. J Virol, 81, 7749-58